STUDIES ON TWILIGHT AND ATMOSPHERIC OZONE

Presented by

J.V.DAVE,M.Sc.

for the degree of

DOCTOR OF PHILOSOPHY

of

THE GUJARAT UNIVERSITY

September 1957

Physical Research Laboratory,
Ahmedabad-9.

PREFACE

The problem of the scattering of sunlight by the earth's atmosphere and the allied problem of determining the vertical distribution of ozone in the atmosphere have been engaging the attention of workers in the Physical Research Laboratory, Ahmedabad, working under the guidance of Professor K.R.Ramanathan. The author has been associated with this work for the last several years and the results reported in this thesis, form part of the work done by him. The thesis contains the following sections:

Section I — Studies on twilight

The study of the scattering of sunlight by the earth's atmosphere during twilight is one of great interest because as the sun goes down, the lower layers of the atmosphere are gradually removed out of direct illumination by the sun and there is possibility of detecting and measuring phenomena characteristic of the higher layers of the atmosphere. Twilight emission of Sodium is well-known. Considering the scattering of the continuous part of the solar spectrum during twilight, the question arises as to the relative importance of the light primarily scattered by the upper part of the atmosphere directly lit by the sun's rays, and the

secondary and multiple scattering from the denser lower layers not directly illuminated by the sun. Observations of the zenith sky intensity and polarisation taken during twilight at Mt. Abu with a photomultiplier and narrow-band filters revealed the following features:

1. The intensity of the zenith scattered light followed the curve of the pressure at the base of illuminated layer for solar depressions upto 6^{o}. For higher depressions of the sun, the measured intensity were found to be several times greater than what would be expected from primary scattering alone.

2. Observed zenith sky polarisation curve during twilight showed remarkable discontinuities at 6^{o}, 8^{o}, 12^{o} and 16^{o} solar depressions.

Both these features were also revealed in the observations taken by independent workers in different parts of the world. This showed the necessity of calculating the amount of primary and secondary scattered radiations received by an observer from the zenith at different stages during twilight. For this purpose, the theory developed by Chapman and Hammad for a plane-parallel atmosphere was modified so as to suit the twilight problem.

Calculations were made of the intensity and polarisation of the light received from the zenith sky for different values of solar depression from 0^{o} to 17^{o} and for a radiation for which the optical thickness of the atmosphere

is 0.2. The following results were obtained:

For 0° to 5° solar depression, the primary scattered radiation is predominant; as the angle increases, the secondary scattered light becomes more and more important and when the sun's depression is 6° to 12°, it is the principal contributing factor. Afterwards, the night air-glow becomes comparable in intensity and when the solar depression is 17° to 18°, only the air-glow radiation remains. The discontinuities in the polarisation curve can be explained from this. The results were published in the Proceedings of the Indian Academy of Sciences (Vol. 43, 1956 A, pp.336-358). A reprint of this paper is given in this section.

The section ends with the tables of equivalent optical path for different heights in the atmosphere and when solar zenith angle is greater than 90°. These were prepared from the formula given in the above paper and were used in the calculations of twilight intensities. The values of the equivalent optical paths for solar angles below horizon, are generally not available in the current literature for sufficiently small intervals of solar zenith distance (Z).

Section II Vertical distribution of ozone

This section deals with the determination of the vertical distribution of ozone from the umkehr curves obtained with Dobson Spectrophotometer. After reviewing in brief the present status of the problem, a pre-print of the paper "The calculation of the vertical distribution of ozone by the Götz

umkehr-effect Method (B)" by K.R.Ramanathan and J.V.Dave, is presented. The method described in this paper will be in use at different ozone stations over the world during the International Geophysical Year whenever a complete umkehr curve is available. It has been shown with solved examples, that with the help of this modified Method B, it is possible to follow the day-to-day changes in the vertical distribution of ozone in the entire atmosphere. A small sub-section is added on the effect of second and higher orders of scattering on the observed umkehr curve.

Section III Measurement of surface ozone

In this section, the results of surface ozone measurements made at Ahmedabad by the author during June 1954 to May 1955 are presented. The daily and seasonal variations have been analysed. This work is important as it proves the existence of measurable quantities of surface ozone in low latitudes. The work though not directly related to the scattering problem, is a problem allied to the vertical distribution of ozone.

Section IV A review of work on scattering of light by the earth's atmosphere

In this section, theoretical contributions made to problem of scattering of sunlight in the earth's atmosphere, by Rayleigh, King, Chapman & Hammad, and Chandrasekhar have been reviewed in brief.

A part of the first paper, presented in Section I (article 1.1) was submitted by the author for his M.Sc. thesis to the University of Bombay in 1952. It has been given here for ready reference and continuity and not as a part of the work submitted for Ph.D. thesis. The remaining work is original and has not been submitted previously for any degree. References to work done by others in the field of this subject have been given at the appropriate places in the text.

The computational work involved in obtaining the results of Sections I and II was carried out by the author using a desk calculator with the help of a computational assistant for part of the work.

The author was the recipient of a Senior Research Assistantship from the Council of Scientific and Industrial Research, Government of India, when this work was in progress. I wish to acknowledge my sincere thanks to the Council for the help given by them.

In the end, I wish to express my grateful thanks to Professor K.A.Ramanathan without whose valuable guidance and keen interest, this work would not have materialised.

Date: August 19, 1957.

K.A.Ramanathan
(K.A.Ramanathan)

J.V.Dave
(J.V.Dave)

CONTENTS

SECTION III

Measurement of surface ozone

SECTION IV

A review of work on scattering of light by the earth's atmosphere

ooo00000ooo

SECTION I

STUDIES ON TWILIGHT

1.1 "On the intensity and polarisation of the light from the sky during twilight". This was published as a paper by J.V.Dave and K.R.Ramanathan in the Proceedings of the Indian Academy of Sciences. Vol. 43 A, 1956. pp. 67-78.

Reprinted from the "Proceedings of the Indian Academy of Sciences," Vol. XLIII, 1956

ON THE INTENSITY AND POLARISATION OF THE LIGHT FROM THE SKY DURING TWILIGHT

By

J. V. Dave and K. R. Ramanathan

Reprinted from "The Proceedings of the Indian Academy of Sciences", Vol. XLIII, No. 2, Sec. A, 1956

ON THE INTENSITY AND POLARISATION OF THE LIGHT FROM THE SKY DURING TWILIGHT

By J. V. Dave and K. R. Ramanathan, F.A.Sc.

Received December 24, 1955

1. Introduction

The object of this paper is to present the results of some new homogeneous measurements of the brightness of the clear zenith sky taken at Mt. Abu (24° 26′ N; 72° 43′ E) with a photon multiplier and six narrow band filters for different values of solar depression from 0° to 20° together with some measurements of polarisation, discuss the results in the light of our present knowledge of the upper atmosphere and attempt on broad lines an explanation of the optical phenomena observed during the transition between day and night.

2. Experimental Arrangements

An R.C.A. photomultiplier 931–A, selected for small dark current, was used with an A.C. operated D.C. power-supply stabilised by a degenerative type of electronic regulation. The photomultiplier output current was amplified by a balanced-bridge stabilised D.C. amplifier. The sensitivity of the amplifier could be changed successively by factors of about 10 by introducing different resistances varying from 10^3 to 10^8 ohms in its grid circuit. The exact scaling factor from one stage to the next was determined by illuminating the photocathode by a beam of constant intensity and noting the reading in each successive stage. No attempt was made to measure the absolute values of the intensities; only relative intensities were determined. For values of output current less than 400 microamperes, the current was found to be proportional to the intensity of light falling on the photocathode. For higher outputs, the correction due to the non-linearity of the variation of output against input voltage was measured and applied. The effect of varying the orientation of the plane of polarisation of the incident beam on the sensitivity of the photomultiplier was tested and found to be negligible.

Suitable optical filters were used to transmit different parts of the spectrum. The components and characteristics of the filters are shown in Table I. The figures take into account the spectral sensitivity of the photomultiplier. It will be noted that with the green, yellow and red filters, the effective transmissions are about 200 A centred approximately at the respective lines of the airglow spectrum.

TABLE I

Components and effective transmissions of optical filters when used with RCA Photomultiplier 931 A

Brief name for filter	Components	Half band-width of transmission	Maximum transmission
U	Chance OX 1	3300–3850	3700–32%
V	Chance OV 1	3640–4050	3850–44%
B	Chance OY 18 and OB 10 ..	4350–4800	4600–9½%
G	I.F. *plus* ON 16 *plus* Plastic Yellow	5530–5750	5600–3½%
Y	I.F. *plus* Chance OY 1	5800–6000	5870–2%
R	I.F. *plus* Plastic Red	6150–6400	6300–1%
J	Polaroid	4000–5500	4600–40%

I. F. stands for interference filter obtained from Messrs. Barr and Stroud.

For the measurement of polarisation, a polaroid of type J was placed in the path of the radiation so as to measure (1) the intensity I_R of the component perpendicular to the sun's meridian and (2) the intensity I_L of the component parallel to it. Both the intensities were measured within a time interval of 5 seconds. The percentage polarisation was calculated from the formula,

$$P = \frac{I_R - I_L}{I_R + I_L} \times 100.$$

3. RESULTS

(*a*) *Intensity*.—Observations were made only on cloudless clear skies. Only one narrow-band filter was used on any particular morning or evening. Meter readings were noted at regular intervals of half a minute except during late twilight when the rate of change of intensity was very small. Frequent check was made on the zero reading and photomultiplier voltage. After applying linearity and zero shift corrections, the corrected meter readings were multiplied by appropriate scaling factors so that the final values were proportional to the intensity of the light falling on the photocathode.

The readings taken on different *clear* days with the same filter were found to agree well when the photomultiplier voltage was kept very steady.

The actual readings for the same solar depression were found to differ in certain ranges on some days. This might have been due to small changes in photomultiplier voltage, changes in the scattering and absorption of light by dust and haze in the atmosphere and changes in the emission of the air-

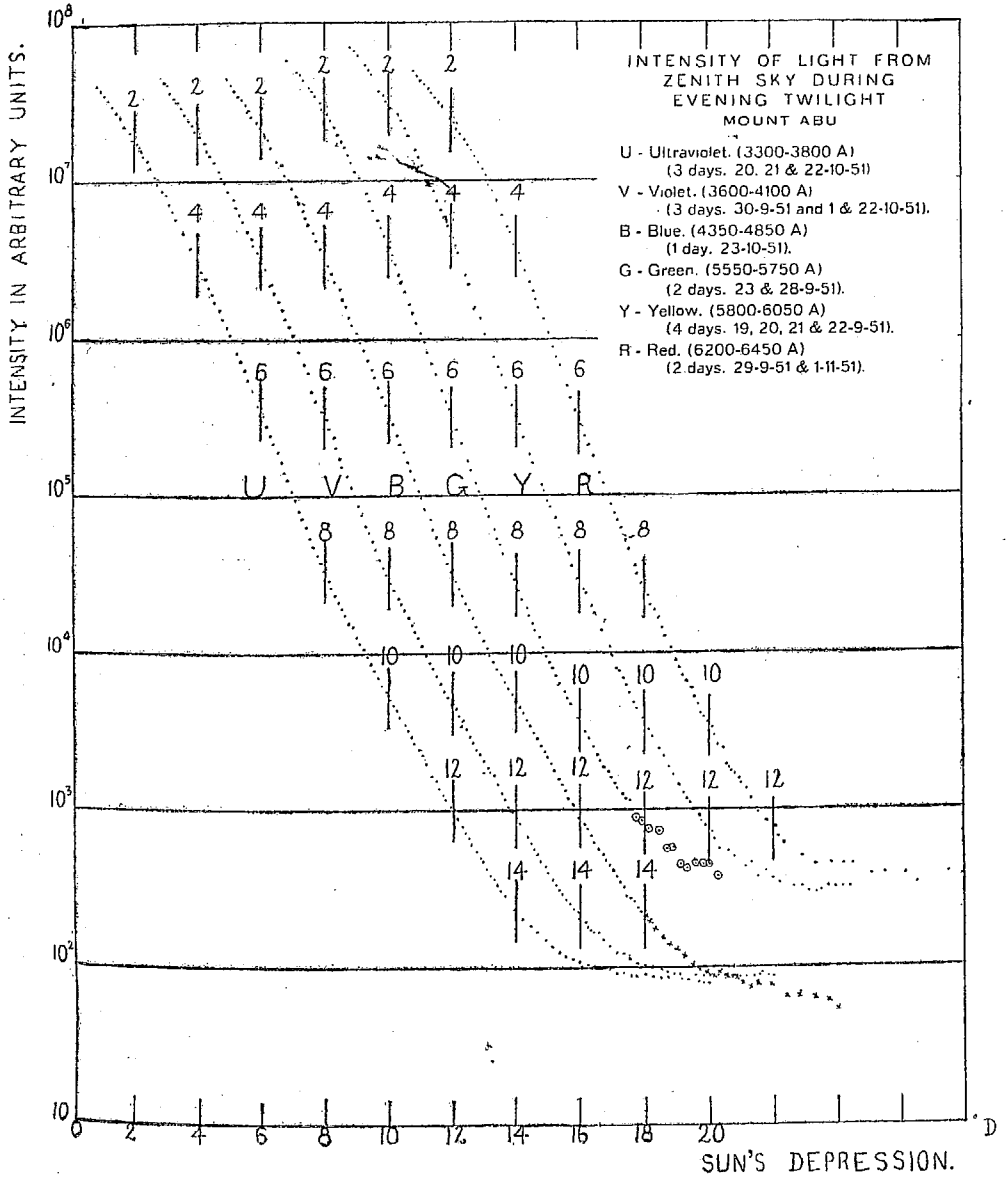

FIG. 1. Intensity of the light from the zenith sky in evening twilight in defined regions of the spectrum.

glow lines. For comparing the course of the variation on different days and in different wave-lengths, the readings were reduced to a common standard by multiplying the values on a particular morning or evening by a factor which would make the readings on all the occasions have the same value at a solar depression of 5°. The means of the intensities observed on different days with the same filter and for the same solar depressions, were calculated.

The average values of the observed intensities of the zenith sky in arbitrary units during evening twilight in different portions of the spectrum are plotted against solar depression in Fig. 1. The intensity scale is logarithmic. The following are the main features of zenith sky brightness during twilight:

(1) The curves for the different wave-lengths from the near ultra-violet to red are *generally* similar from D = 0 to D = 12°, but in the shorter wave-lengths, the rate of decrease of intensity with increasing solar depression becomes markedly less when D is about 8°.

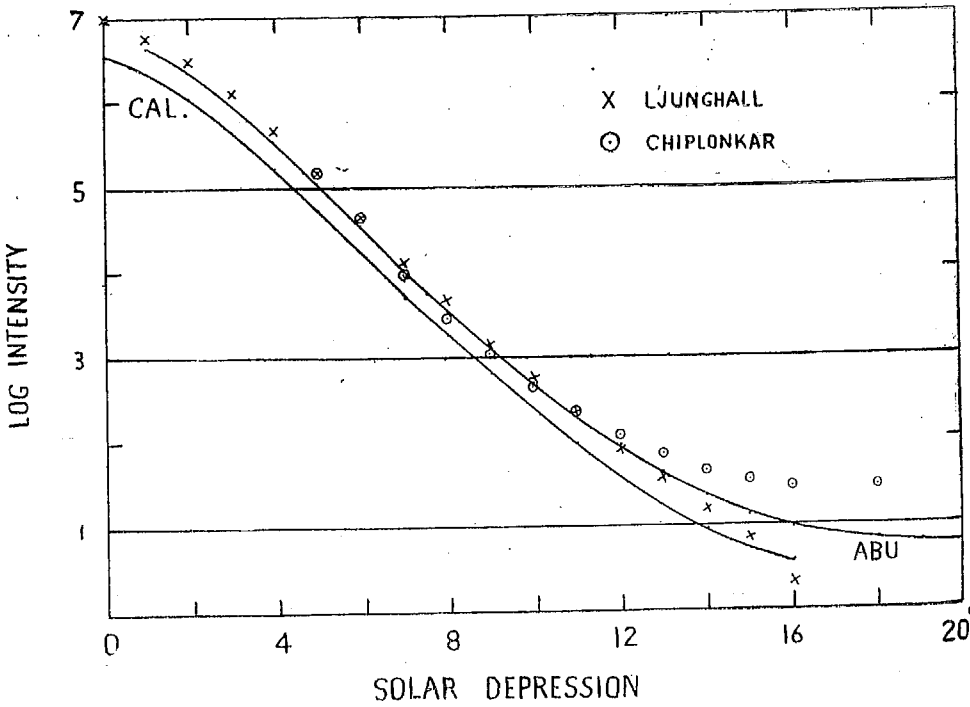

FIG. 2. Comparison of twilight zenith sky intensities as measured in different places.
ABU 4600 A.
CAL. 4400 A. Ashburn (Cactus Peak, California).
× Composite. Ljunghall (Helwan and other places).
⊙ Visual including green. Chiplonkar and Ranade (Sinhagad, Poona).

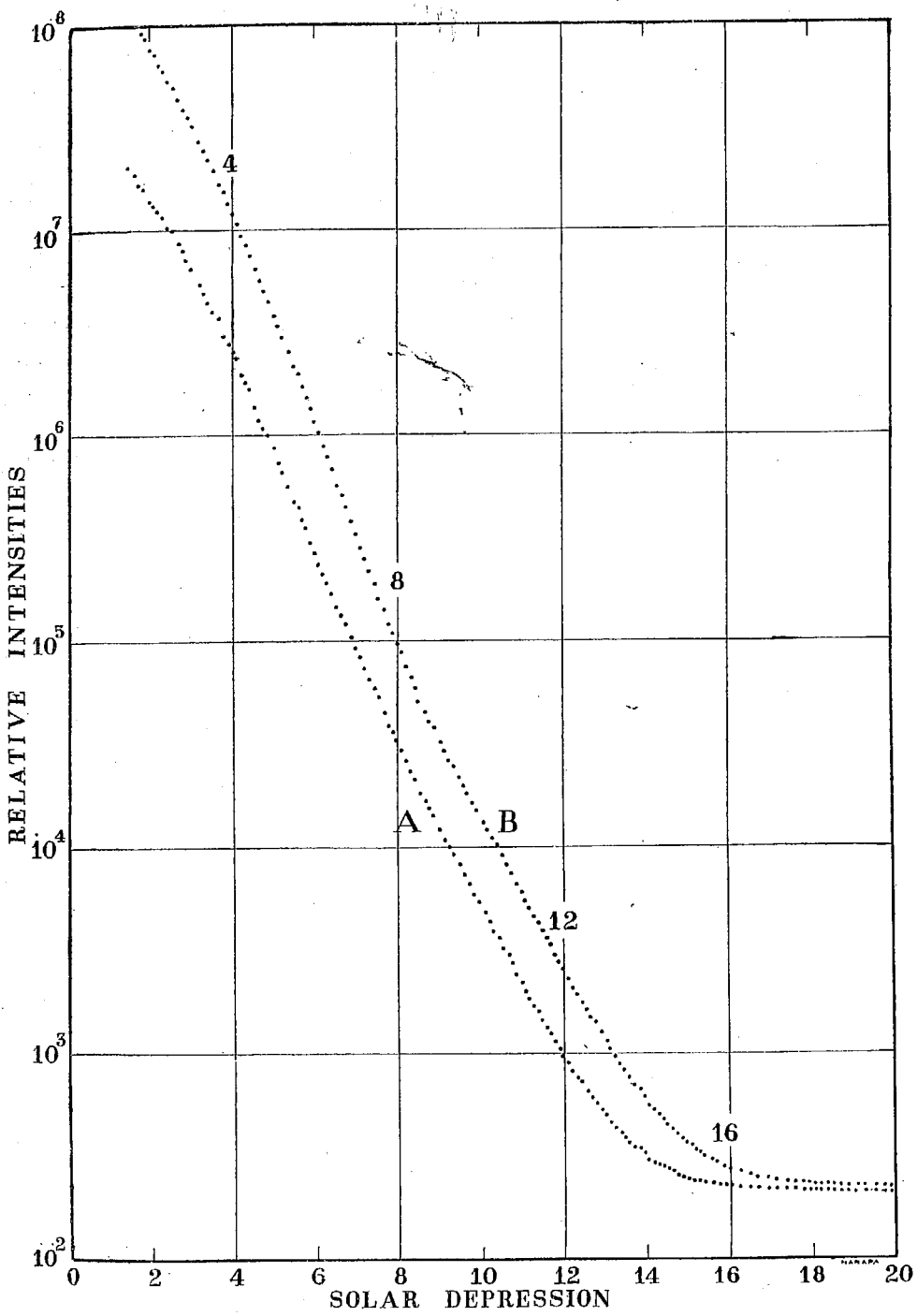

FIG. 3. Intensity of parallel and perpendicular components of zenith sky light during morning twilight (4000–5700 A).

A, Parallel component, B, Perpendicular component.

(2) While the intensities of the ultraviolet, violet and blue flatten out when the sun's depression is 16° to 18°, the intensities of the green, yellow and red which include bright lines in the night airglow flatten out when D is 13° to 14° at a higher level of relative intensity.

(3) In the green and the red, there were observed on many days a reduction in the rate of fall of intensity when D was about 12° suggesting a temporary brightening near the boundary of earth's shadow. This requires further examination.

For comparison, the values of zenith sky intensities observed during twilight by other observers are plotted side by side with the Abu values. Ashburn's measurements[1] in California were made with a phototube and filters and come closest to Abu values. The observations of Chiplonkar and Ranade[2] were made at Sinhagad near Poona with a visual photometer including the oxygen green line. Ljunghall's[3] curve is composite being made up of his own observations at Helwan with a photocell and filter and of the old visual observations of Dufay and others.

(*b*) *Polarisation.*—Observations of I_L and I_R for studying the polarisation of the sky were taken on a number of mornings and evenings: (1) with the polaroid alone (which transmits the violet, the blue and the green including an appreciable fraction of the green line 5577 A) and (2) with polaroid and blue filter.

In Fig. 3 are plotted the values of I_L and I_R for different solar depressions during morning twilight with polaroid alone. The corresponding curves for evening twilight taken with polaroid and blue filter for the spectral region 4350–4850 A, are essentially similar.

The values of the percentage polarisation as calculated from the values of I_L and I_R are plotted in Fig. 4. Curves B and C represent the values obtained in the effective spectral region 4350–4850 A for evening and morning twilight respectively, while the curves D and E are for the spectral region 4000–5700 A.

The curves showing zenith sky polarisation against solar depression are in general agreement with those obtained by Robley[4] visually at Pic du Midi. His observations extended to 16° and are also shown in Fig. 4, curve A. From Fig. 4, the following points are clear. When observations were taken with a blue filter, the zenith sky polarisation remained more or less steady at about 70% till D was 5°, and then showed a pronounced fall till D was $8\frac{1}{2}$°. Between $8\frac{1}{2}$° and 12° solar depression, the polarisation again showed a plateau at 45% to 50%, after which it declined rapidly so that when D was greater than 18°, the zenith sky was practically unpolarised.

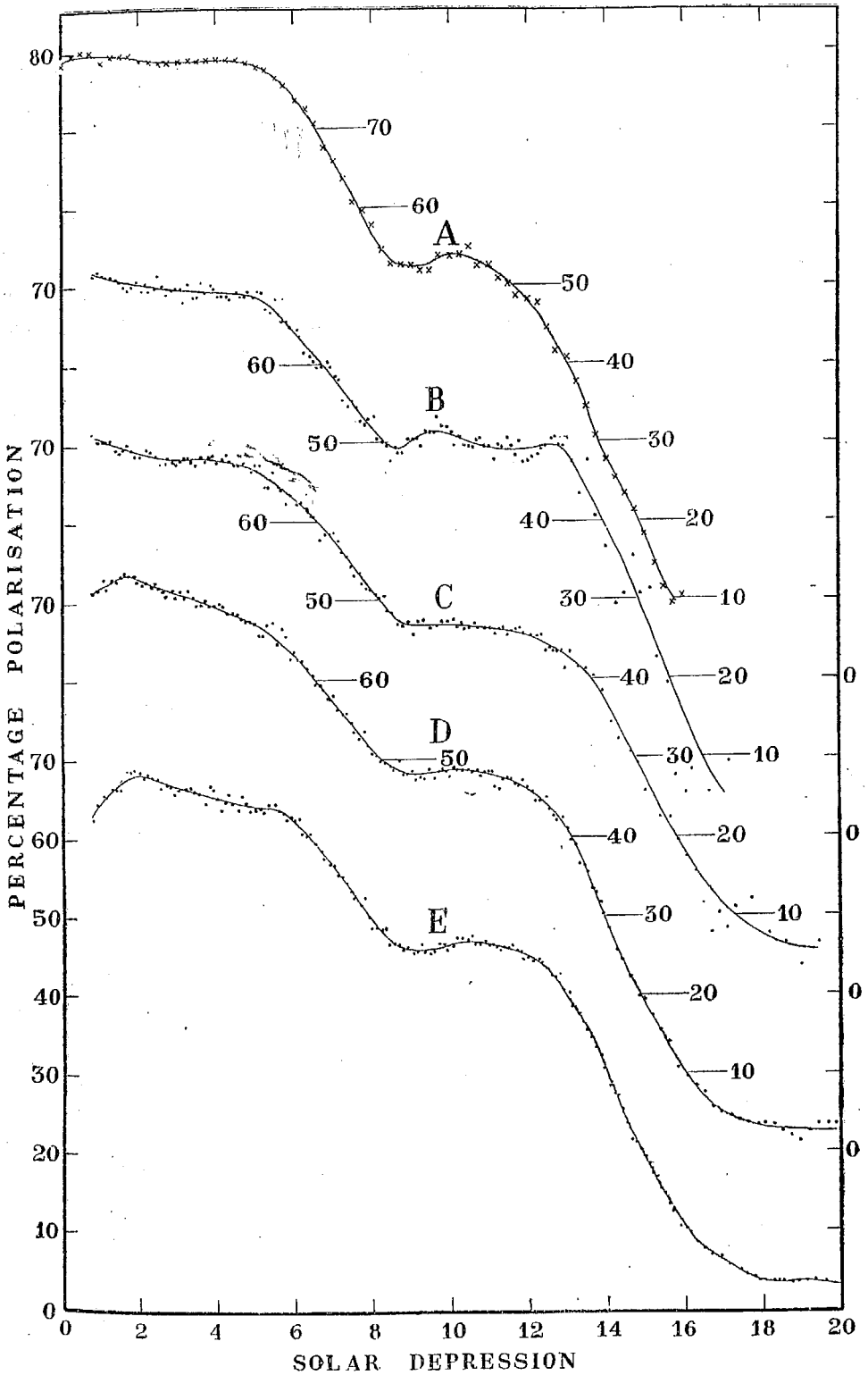

FIG. 4. Percentage polarisation of the light from the zenith sky during twilight.
A. Robley, Visual. Pic du Midi (1950) B. 4350–4850 Evening. Mt. Abu.
C. 4350–4850 Morning. Mt. Abu. D. 4000–5700 Evening. Mt. Abu.
E. 4000–5700 Morning. Mt. Abu.

Robley's curve shows similar variations, but the initial polarisation at low values of solar depression is higher, due no doubt to the clearer skies over Pic du Midi.

The curves obtained with the polaroid alone without the blue filter show similar features but the changes of polarisation are less sharp.

The polarisations at points 30° from the zenith in the vertical plane through the sun were measured both towards the sun and away from the sun

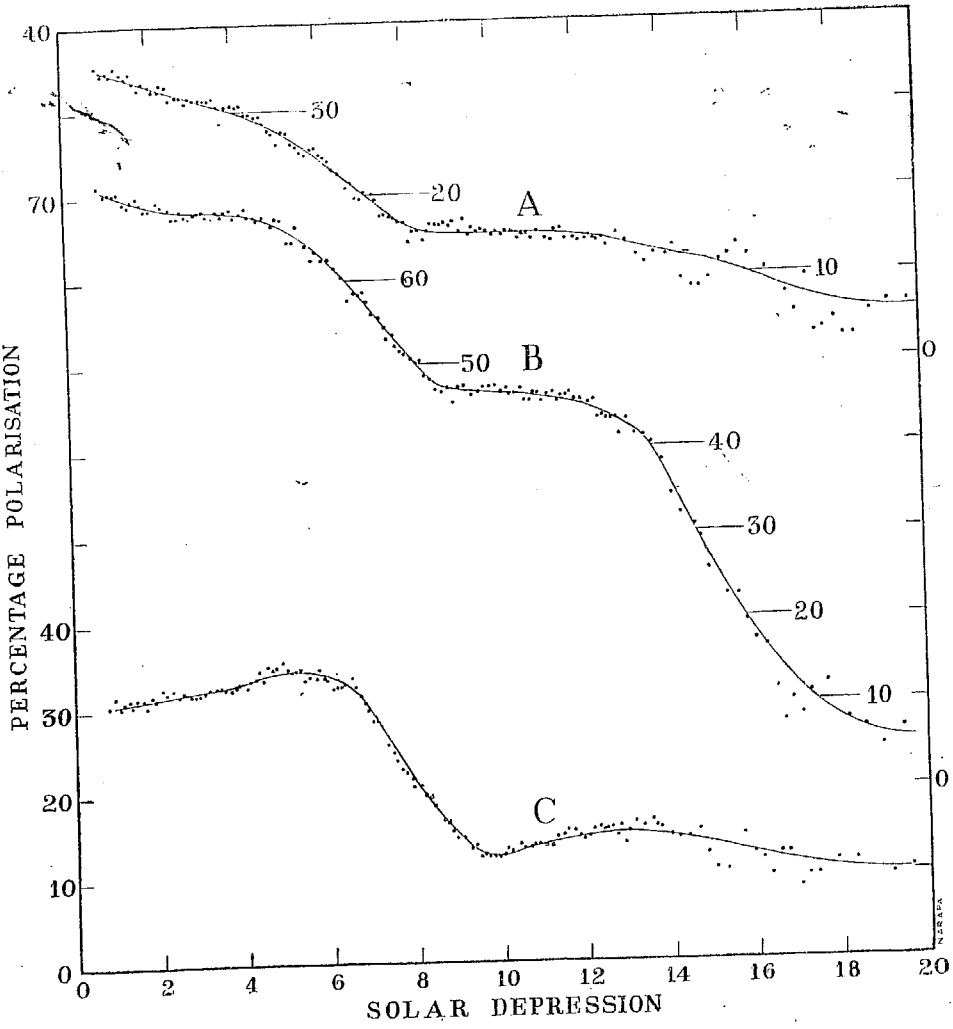

FIG. 5. Percentage polarisation of skylight in morning twilight (4350–4850).
A. 30° from the zenith away from the sun.
B. At zenith.
C. 30° from the zenith towards the sun.

on different days during morning twilight. The values of the polarisation calculated from the observed values of I_L and I_R are plotted in Fig. 5. Curves B, A and C represent the variations of polarisation with solar depression at zenith, 30° from the zenith towards the sun and at 30° from the zenith on the anti-sunside respectively.

It will be observed that the changes in sky polarisation 30° away from the zenith but towards the sun are sharper than those at the same angular distance from the zenith on the anti-sunside. The corresponding changes occur as may be expected, first on the anti-sunside, then at the zenith, and lastly on the sunside; the flattening out of the polarisation curve occurs at 9·5° on the sunside, at 9° at the zenith and at 8·5° on the anti-sunside.

To explain the humps in the polarisation curves requires further analysis of secondary scattered light.

4. Discussion

When the sun is a few degrees below the horizon, the upper part of the atmosphere is directly illuminated by the sun's rays, while the lower part lies in the shadow of the earth. The shadow region is however illuminated by scattered radiation from the sky all round, particularly from the hemisphere towards the sun. The light from the zenith sky is therefore made up of the primary scattered light from the upper part of the atmosphere and secondary (and multiple) scattered light. Owing to the greater air density in the lower part of the atmosphere, however, the main secondary scattered light would come from layers lower down in the atmosphere than the primary scattered light. As a consequence, as the sun goes down, the primary scattered light would decrease at a much faster rate than the secondary scattered light.

The observed variation of the brightness of the zenith sky with the depression D of the sun below the horizon agrees with the view that the sky illumination during twilight is only in part due to primary scattered light P. If it were due mainly to P, the variation of the sky brightness with D would be similar to the variation of the amount of air above the lower boundary of the directly illuminated upper atmosphere, that is, of the pressure at the shadow boundary. In Fig. 6 are drawn the curves of brightness RR and BB, of the zenith sky observed at Abu in the red (6300 A) and the blue (4600 A) and also the curve of pressure PP at the shadow limit. The height of the earth's shadow above the ground (for 4500 A) corresponding to different values of D are taken from Ljunghall's paper. Ljunghall assumes that above 6 km., the attenuation of light in the atmosphere is due only to molecular scattering while at lower levels, the coefficient increases, becoming at ground

level 2–2·5 times the value for molecular scattering. The refraction due to the atmosphere has been neglected. It will be seen from Fig. 6 that while the curves of BB and RR follow approximately the curve of PP down to a

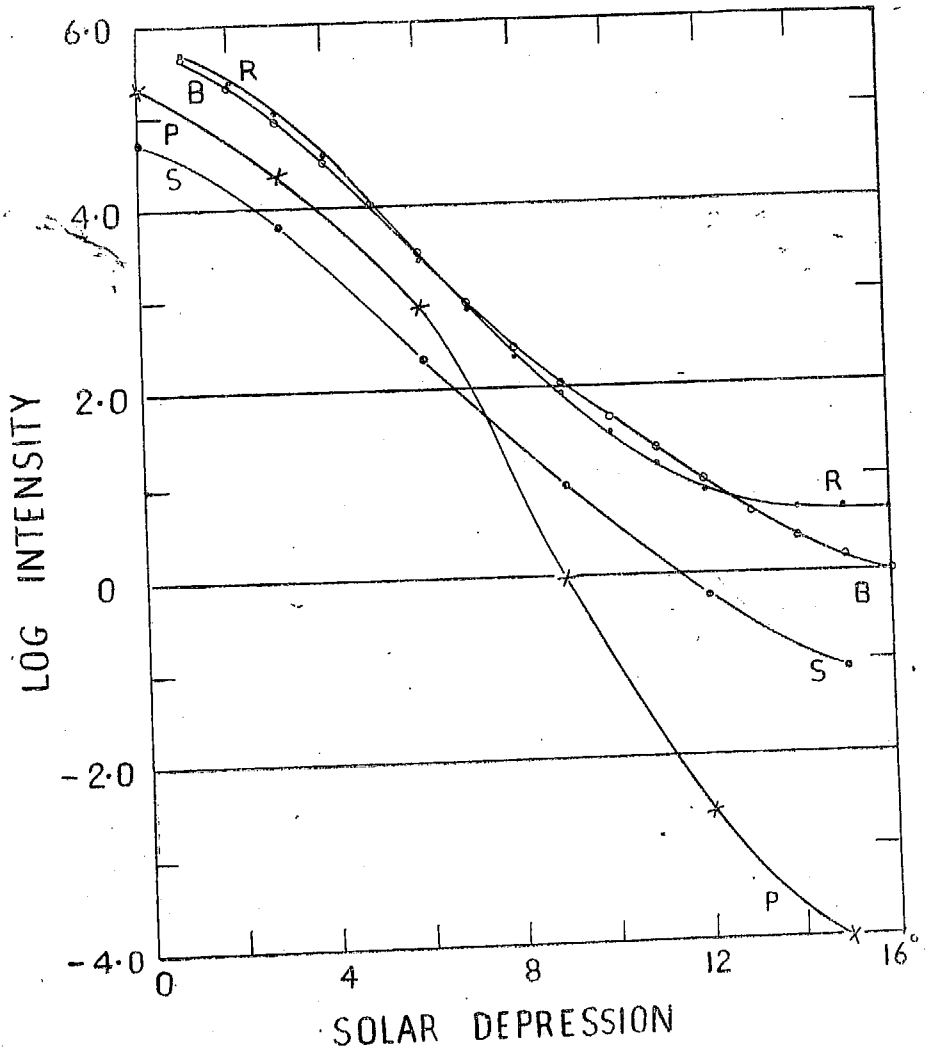

FIG. 6. Comparison of the observed zenith sky intensity with pressure at the base of the illuminated layer.

RR Observed intensity at 6300 A.
BB Observed intensity at 4600 A.
PP Pressure at the base of illuminated layer.
Height of base as given by Ljunghall.
SS Integrated illumination at ground level due to scattered light from the whole sky during twilight.

solar depression of about 6°, they deviate more and more from it at greater values of D.

At solar depressions of 12° and 15°, the values of BB are more than a thousand times greater. Many years ago, it was suggested by Hulburt[5] that secondary scattering plays an important part in twilight illumination. He showed that when the solar depression exceeds 8°, the light scattered from the zenith sky from the lower part of the atmosphere lying within the shadow of the earth but illuminated secondarily by the twilight glow is comparable in amount to the light scattered by the upper part of the atmosphere directly lit by the sun's rays. We now find that the discrepancy is enormous; can all this be explained by multiple scattering? From observations now available, it is possible to make an estimate of the relative contributions of primary and multiply scattered light to the brightness of the zenith sky during twilight.

Koomen[6] and others have given values of sky brightness measured in different azimuths and altitudes at Sacramento Peak in New Mexico (2800 m. above sea-level) for different values of sun's depression down to 15° below horizon. From these measurements, one can by numerical integration estimate the illumination due to scattered light from the whole sky at the point of observation on the earth's surface. This has been done and the following are the results.

Sun's depression below horizon	Illumination due to skylight at ground
0°	180 candles/ft.^{2}
3°	22·6
6°	0·76
9°	0·031
12°	0·0017
15°	0·00027

The values in column 2 are plotted in Fig. 6 as curve SS.

We may assume as a *first approximation* that the scattered light incident after sunset or before sunrise on a vertical column of the atmosphere above the observer will vary similarly to the integrated illumination at ground as

given in column 2 above. PP and SS will then represent respectively the relative variations of primary and secondary scattered light from the atmosphere during twilight. It is known that when the sun is on the horizon, *i.e.*, at D = 0, the secondary scattered light from the zenith for 4500 A is nearly 0·25 of the primary scattered light, but we do not know how this ratio will change when D increases. In what proportions the primary and secondary should be combined at different times after sunset is a matter for investigation.

5. Polarisation of Light from Zenith Sky during Twilight

The view that secondary scattering is the main factor responsible for extending the twilight period is borne out by the measurements of polarisation of the sky during twilight. Robley first showed from his observations at Pic du Midi that the polarisation of the clear zenith sky during twilight fell rapidly when D increased to more than 6° but that it later attained a steady value of 50% to 55% when the sun's depression was between 9° and 12°. These observations have been corroborated by our Abu observations (Fig. 4). When the secondary scattering also becomes insignificant, the light from the zenith sky is only scattered starlight and light from the airglow and is practically unpolarised. This happens when D is 16° to 18° for blue light. Robley found that with red light for which the secondary scattering would be much smaller, the first dip in polarisation and the plateau between D = 9° and D = 12° were inconspicuous. It may be observed that the sky illumination during evening twilight, especially in its later half, is markedly anisotropic, the light coming from the direction of the sun being much greater than from other directions. This light, when secondarily scattered downward by the atmosphere above the observer, will naturally have a large polarisation.

Quantitative checking of these ideas with observation requires the calculation of the intensity and polarisation of secondary scattered light by the spherical atmosphere when the sun is below the horizon. The calculations have been made and will be the subject of communication of Part II.

References

1. Ashburn, E. V. .. *Jour. Geophy. Res.*, 1952, **57**, 85.
2. Chiplonkar, M. W. and Ranade, J. D. .. *Proc. Ind. Acad. Sci.*, 1953, **18 A**, 121.
3. Ljunghall Arvid .. *The Intensity of the Twilight and Its Connection with the Density of the Atmosphere*, Meddelande fran Lunds Astronomiska Observatorium, Ser. II, Nr. 125, 1949.
4. Robley, R. .. *Annale de Geophysique*, 1950, **6**, 191.
5. Hulburt, E. O. .. *Journ. Opt. Soc. America*, 1938, **28**, 227.
6. Koomen, Lock, Packer Scolnik, Tousey and Hulburt .. *Ibid.*, 1952, **42**, 353.


BANGALORE
PRESS
LAKE VIEW
MYSORE P.O.
BANGALORE
CITY

1.2 "On the intensity and polarisation of the light from the sky during twilight - Part II". This was published as a paper by J.V.Dave in the Proceedings of the Indian Academy of Sciences. Vol. 43 A, 1956. pp. 336-358.

Reprinted from the "Proceedings of the Indian Academy of Sciences," Vol. XLIII, 1956

ON THE INTENSITY AND POLARISATION OF THE LIGHT FROM THE SKY DURING TWILIGHT—PART II

By

J. V. Dave

Reprinted from "The Proceedings of the Indian Academy of Sciences", Vol. XLIII, No. 6, Sec. A, 1956

ON THE INTENSITY AND POLARISATION OF THE LIGHT FROM THE SKY DURING TWILIGHT—PART II

BY J. V. DAVE

(*Physical Research Laboratory, Ahmedabad-9*)

Received April 12, 1956

(Communicated by Professor K. R. Ramanathan, F.A.SC.)

I. INTRODUCTION

IN a recent paper,[1] observations of the intensity and polarisation of the light from the sky during twilight taken at Mount Abu during 1951 were presented and briefly discussed. It was shown that for depressions of the sun exceeding 7° or 8°, the zenith sky was much brighter than would be expected if primary scattering alone were responsible for the light and that in the treatment of twilight problems, due account should be taken of the contributions from secondary scattering, as has been shown by Hulburt.[2] Marked discontinuities in the polarisation of the light from the zenith sky at solar depressions of 5°, 8°, 12° and 17° support the presence in twilight of other contributions in addition to primary scattered light.

1.1. *Summary of previous work*

Robley[3] has recently given a method of calculating the intensity and polarisation of the secondary (multiply) scattered light during twilight. His work is based on the work of Dr. S. Chandrasekhar[4] for an infinite plane-parallel atmosphere of defined optical thickness. To compute the secondary scattered radiation for the zenith sky for a solar depression D, Robley extends the atmospheric path traversed by the solar rays to a vertical plane in the atmosphere passing through the centre of the earth and making an angle D/2 with the observer's vertical. He then calculates the scattered light emanating from this plane in a direction parallel to the observer's horizon, with certain simplifying assumptions which lead to a constant value of 50% for the polarisation of the secondary scattered light from the zenith sky throughout the period of twilight. *Prima facie*, this does not appear to be correct, because observation shows that with increasing values of solar depression, the brightness of the sky becomes more and more concentrated towards the horizon in the sun's meridian plane.

1.2. *General outline of the method adopted in this paper*

The method adopted in this paper for the calculation of secondary scattering is based on the work of Chapman and Hammad.[5,6] The following assumptions were made:—

(1) The earth was taken to be a uniform sphere of radius 6370 km., surrounded by an exponential atmosphere of equivalent scale height 7 km.

(2) The atmosphere was arbitrarily divided into a number of concentric shells of 4 km. thickness, for computing the intensities of primary and secondary scattered radiations.

(3) The solar radiation falling on the top of the atmosphere was assumed to be unpolarised and its intensity taken to be unity.

(4) The depolarisation factor d of air due to molecular anisotropy was taken to be 0·04.

(5) Higher orders of scattering than secondary were neglected.

(6) No correction was made for the absorption or scattering of light by dust or haze.

(7) Atmospheric refraction was neglected.

(8) No correction was made for reflection by the ground.

II. Theory

In Fig. 1, ABC represents a section of the earth; O is its centre and a its radius. R_0 is the position of the observer on the surface of the earth. OR_0 represents the direction of the observer's zenith. Q is a point in the atmosphere in the direction of observation R_0Q. The Z-axis is chosen to lie along the observer's zenith OR_0. The X-axis lies in the plane of the paper such that the XOZ plane is parallel to the incident solar radiation. The Y-axis is perpendicular to the plane of paper passing through O. The polar co-ordinates (θ, ϕ) of a given direction are such that θ is the angle which the direction makes with the Z-axis, and ϕ is the azimuth with XOZ as the reference plane. With this convention, the polar co-ordinates of the incident solar radiation SP are (Z_0, O). If the direction of observation is the zenith or R_0Q, its θ, ϕ are (O, O). PQ the direction of primary scattered radiation is given by (θ', ϕ'). The unit vectors along SP, QR_0 and PQ are denoted respectively by s, k and k'.

2.1. *Intensity of primary scattered radiation*

Consider a solar beam of intensity I_∞ travelling along SP. I_∞ denotes the intensity of solar radiation outside the earth's atmosphere in a specified narrow wave band, being the energy received per unit time on unit area normal to the vector s. Let σ denote the mass coefficient of scattering and ρ the density of air at a distance s from P along PS.

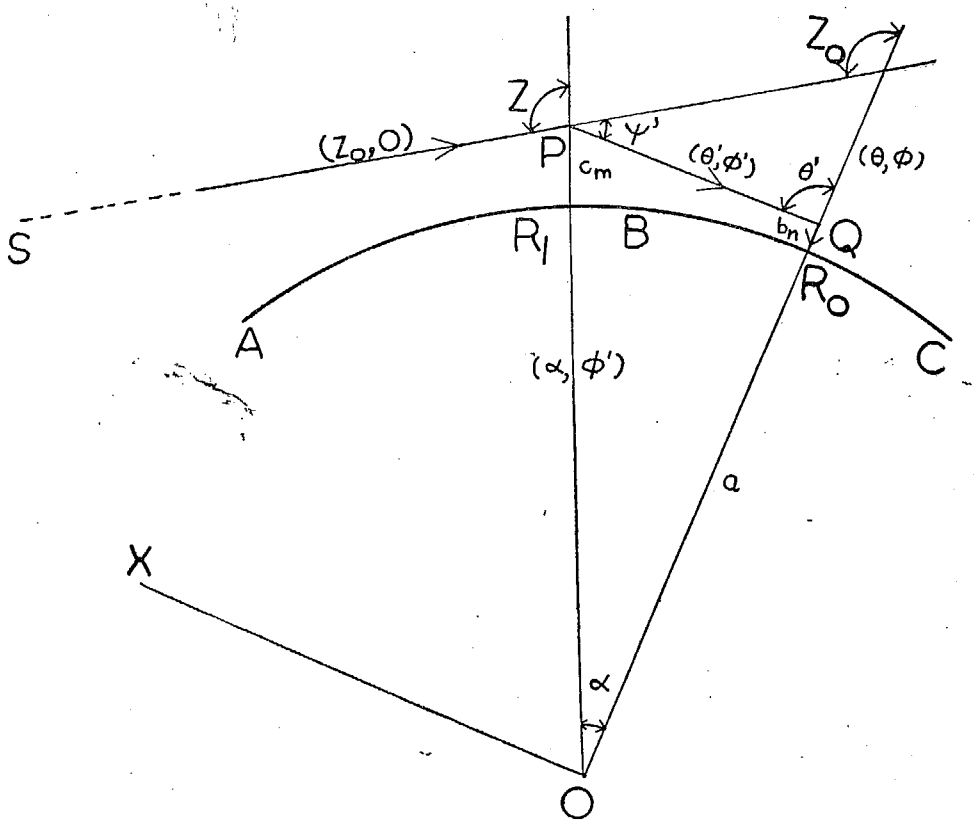

FIG. 1. The incident light is primarily scattered at P (where the local zenith angle of the sun is Z, and the height $R_1P = c_m$). The direction PQ is defined by (θ', ϕ'). The direction of observation towards the observer's zenith is defined by $\theta = 0$, $\phi = 0$. The primary scattered light travelling along PQ gets rescattered at Q along QR_0 towards the observer. $QR_0 = b_n$.

Then

$$\int_{\infty}^{P} \sigma . \rho . ds = \tau_{SP} \tag{1}$$

is the equivalent optical path which the solar radiation has to travel in the earth's atmosphere before reaching P. It will be shown later that τ_{SP} is a function of the vertical height c_m of P above the surface of the earth and of the local zenith angle (Z) of the sun at P. The intensity of the solar radiation at P is then given by

$$I = I_{\infty} e^{-\tau_{SP}} \tag{2}$$

Let PQ (θ', ϕ') be a direction along which the incident solar radiation s scattered from P according to the Rayleigh law of scattering. The energy

scattered from P in a cone of small solid angle dk' with apex at P is given by

$$E_1\,dk' = \frac{3\sigma I_\infty}{16\pi\,(1+\frac{1}{2}d)}\,e^{-\tau_{SP}}\,(1+\cos^2\psi'+d\sin^2\psi')\,dk' \qquad (3)$$

where d is the depolarisation factor due to molecular anisotropy and ψ' the angle between s and k' given by

$$\cos\psi' = \cos Z_0\cos\theta' + \sin Z_0\sin\theta'\cos\phi' \qquad (4)$$

This scattered radiation is polarised and can be resolved into two beams of plane polarised light at right angles to each other. If $E_{1n'}$ represents the primary scattered emission from P in the direction of k' with its electric vibration along the vector n' perpendicular to the plane sk' at P, and $E_{1t'}$, the intensity of the radiation with its electric vector along t' perpendicular to n', we have

$$E_{1n'} = \frac{3\sigma I_\infty}{16\pi\,(1+\frac{1}{2}d)}\,e^{-\tau_{SP}} \qquad (5)$$

and

$$E_{1t'} = KE_{1n'} \qquad (6)$$

where

$$K = d + (1-d)\cos^2\psi' \qquad (7)$$

Consider a small surface area dS at Q perpendicular to PQ. The amount of primary scattered radiation from P passing through dS per second is given by

$$E_{1n'}\,(1+K)\,e^{-\tau_{PQ}} \times \frac{dS}{s^2}$$

where dS/s^2 is the solid angle subtended by dS at P and τ_{PQ} the equivalent optical path from P to Q. It will be later shown that τ_{PQ} which is given by

$$\tau_{PQ} = \int_P^Q \sigma\cdot\rho\cdot ds$$

is a function of θ', c_m and b_n. If dV is a small volume element surrounding P and subtending a small solid angle dk' at dS, and if ρ' is the density at P, then the amount of primary scattered radiation passing through dS per second from a mass element $\rho'.dV$ surrounding P is given by

$$E_{1n'}\,(1+K)\,e^{-\tau_{PQ}}\frac{dS}{s^2}\,\rho'.dV$$

and the intensities $R_{1n'}$ and $R_{1t'}$ of the normal and transverse components of primary scattered radiation passing normally through unit area at Q through unit solid angle along k' is given by

$$R_{1n'} = \int_{Q}^{\infty} E_{1n'}\, e^{-\tau_{PQ}} \frac{dS}{s^2} \times \frac{\rho' \cdot dV}{dS \cdot dk'}$$

and

$$R_{1t'} = K R_{1n'}$$

the integration extending from ∞ to Q when the whole path is illuminated by solar rays, or upto the shadow limit when a part of PQ lies in the shadow region of the earth.

Substituting the values of $E_{1n'}$ and of $dV = s^2 . ds . dk'$ in $R_{1n'}$, we have

$$R_{1n'} = \frac{3\sigma I_{\infty}}{16\pi (1 + \frac{1}{2}d)} \int_{Q}^{\infty} e^{-\tau_{SP}} e^{-\tau_{PQ}} \rho' . ds \tag{8}$$

and

$$R_{1t'} = K R_{1n'} \tag{9}$$

It must be noted that unlike the plane-parallel atmosphere, cos Z on the actual earth changes along QP and also with ϕ'. Hence τ_{SP} is not independent of ϕ'. Thus the integration formulæ developed by Chapman and Hammad for $R_{1n'}$ are not applicable in this and we have adopted numerical integration.

2.2. *Intensity of secondary scattered radiation*

Having obtained the values of $R_{1n'}$ and $R_{1t'}$ for different values of θ' and ϕ' at Q, the next problem is to consider the effective contribution by the volume element at Q towards the secondary scattered radiation travelling along QR_0. Let n be the unit vector perpendicular to the $k'k$ plane at Q. If E_{2n} and E_{2t} are defined as the energy of the secondary emission for normal and transverse components emitted at Q respectively, then as shown by Hammad, we have

$$E_{2n} = \frac{3\sigma}{16\pi (1 + \frac{1}{2}d)} \int \{A_1 + K A_2\} R_{1n'}\, dk'$$

and

$$E_{2t} = \frac{3\sigma}{16\pi (1 + \frac{1}{2}d)} \int \{B_1 + K B_2\} R_{1n'}\, dk'$$

where

$$\left.\begin{aligned} A_1 &= d + 2(1-d)\cos^2 \chi_{nn'} \\ A_2 &= d + 2(1-d)\cos^2 \chi_{nt'} \\ B_1 &= d + 2(1-d)\cos^2 \chi_{tn'} \\ B_2 &= d + 2(1-d)\cos^2 \chi_{tt'} \end{aligned}\right\} \quad (10)$$

$\chi_{nn'}$, $\chi_{nt'}$, $\chi_{tn'}$ and $\chi_{tt'}$ are respectively the angles between the vectors n and n', n and t', t and n' and t and t' and the formulæ for obtaining their values are as given by Hammad.

$$\cos \chi_{nn'} = \cos(\xi - \xi') \quad (11)$$

$$\cos \chi_{nt'} = \cos \psi' \sin(\xi - \xi') \quad (12)$$

$$\cos \chi_{tn'} = \cos \psi \sin(\xi' - \xi) \quad (13)$$

$$\cos \chi_{tt'} = \sin \psi \sin \psi' + \cos \psi \cos \psi' \cos(\xi' - \xi) \quad (14)$$

where ψ, ψ', ξ and ξ' are defined by the equations

$$\cos \psi = \cos Z_0 \cos \theta + \sin Z_0 \sin \theta \cos \phi \quad (15)$$

and

$$\sin \xi = \frac{\sin \theta \sin \phi}{\sin \psi} \quad (16)$$

Since $dk' = \sin \theta' . d\theta' . d\phi'$, the equations for E_{2n} and E_{2t} can be re-written as

$$E_{2n} = \frac{3\sigma}{16\pi(1 + \frac{1}{2}d)} \iint \{A_1 + KA_2\} R_{1n'} \sin \theta' . d\theta' . d\phi' \quad (17)$$

and

$$E_{2t} = \frac{3\sigma}{16\pi(1 + \frac{1}{2}d)} \iint \{B_1 + KB_2\} R_{1n'} \sin \theta' . d\theta' . d\phi' \quad (18)$$

Knowing E_{2n} and E_{2t} for a number of points along QR_0, the tota secondary scattered radiation received at R_0 along QR_0, can be integrated. Its normal and transverse components R_{2n} and R_{2t} are given by

$$R_{2n} = \int_{R_0}^{\infty} E_{2n} e^{-\tau_{QR_0}} \rho . ds \quad (19)$$

and

$$R_{2t} = \int_{R_0}^{\infty} E_{2t} e^{-\tau_{QR_0}} \rho . ds \quad (20)$$

where ρ is the density of air at Q and τ_{QR_0} is the equivalent optical path from Q to R_0. It is a function of b_n as well as of θ.

III. TABLES FOR COMPUTING THE SECONDARY SCATTERED RADIATION

The quantities required for computing $R_{1n'}$ by the summation method such as s, Δs, τ_{SP}, have been tabulated by many workers such as Sekera,[7] Chapman[8,9] and others. However, their tabulation could not easily fit into our system, and all the quantities required for this work were therefore tabulated from the formulæ given below.

As already mentioned in 1.2, the atmosphere is arbitrarily divided into a number of concentric layers of 4 km. thickness. The base of the nth layer is at a height of $4(n-1)$ km. while its centre is at $(4n-2)$ km. The positions of Q are selected at the base of the different layers, and of P at the centres of the successive layers. On replacing the integral of Equation (8) by a sum, we have

$$R_{1n'} = \frac{3\sigma\rho_0 I_\infty}{16\pi(1+\frac{1}{2}d)} \sum e^{-\tau_{SP}} e^{-\tau_{PQ}} e^{-c_m/H} \Delta s \qquad (21)$$

$\rho' = \rho_0 e^{-c_m/H}$ for an exponential atmosphere and H the equivalent scale height is assumed to have a uniform value of 7 km.

If the values of τ_{SP}, τ_{PQ} at the centres of the different layers and also of Δs the thickness of the layers for any θ' are known, $R_{1n'}$ can be calculated. Since τ_{SP} is a function of Z and c_m, we have to calculate for a given position of Q and a fixed value of Z_0, the local zenith angle Z of the sun at the centres of the successive layers along QP. For this, it is necessary to tabulate a shown in Fig. 1 for different values of c_m.

3.1. s, *the distance of the centre of the layer from the base of another layer in any direction*

From Fig. 1, we have

$$(a+c_m)^2 = s^2 + (a+b_n)^2 + 2s(a+b_n)\cos\theta'$$

On neglecting c_m^2 and b_n^2 in comparison with the other terms,

$$s^2 + 2s(a+b_n)\cos\theta' - 2a(c_m - b_n) = 0 \qquad (22)$$

With the help of Equation (22), the values of s were tabulated for different values of c_m and $\theta' = 0°$, 15°, 30°, 45°, 60°, 75°, 80°, 85°, 88° and 90° when the position of Q is at b_1, the ground level. From this table, it is easy to obtain the values of s corresponding to any b_n and θ' between 0° and 90° with sufficient accuracy. For positions of Q above the ground, when θ' can take values greater than 90°, QP can intercept some of the lower layers twice. This was appropriately allowed for in computing the path lengths for θ' between 90° and 180° at similar intervals. It is expected that the

tabulated values of s are correct within 1 km. when s is small and within 2 km. when it is large.

3.2. Δs, *thickness of the layer in any direction*

Equation (22) was used to calculate the distance Δs between the bases of two consecutive layers for all the above-mentioned values of θ'. $\text{Log}_e \Delta s$ was tabulated for all values of c_m, b_n and θ' required in the calculation.

3.3. Z, *the local zenith distance of the sun for any position of P for a given* Z_0

In Fig. 1, the vertical through P (PR_1O) makes an angle α with the Z-axis. It can be represented by (α, ϕ') and Z is given by

$$\cos Z = \cos Z_0 \cos \alpha + \sin Z_0 \sin \alpha \cos \phi' \tag{23}$$

α can be determined from the relation

$$\sin \alpha = \frac{s}{a + c_m} \sin \theta' \tag{24}$$

The values of $\sin \alpha$ and $\cos \alpha$ were tabulated for all the positions mentioned in 3.1 and used for the other similar positions as necessary.

When Z is greater than 90°, there is a limit below which P would not be illuminated by direct sunlight. Limiting values of $\cos Z$ for different values of c_m can be obtained from

$$\sin Z_s = \frac{a}{a + c_m} \tag{25}$$

With the help of Equation (24) tables of $\cos Z$ were prepared for Z_0 corresponding to 90°, 94°, 98°, 102° and 106° for all the values of θ' and b_n and at intervals of 15° for ϕ'.

3.4. τ_{SP}, *the equivalent optical path from outside the atmosphere to the point P which is at a height* c_m *above ground and for different values of cos Z*

Consider a point P situated at a height c_m in its vertical above the surface of the earth. Let the incident solar radiation make an angle Z with OP (Fig. 2). Let P′ be any point in SP, at a distance s from P and at a vertical height h from the ground. The density at P′ is given by

$$\rho = \rho_0 e^{-h/H}$$

and the equivalent optical path $\tau_{SP}(\cos Z, c_m)$ as defined by (1) is given by

$$\tau_{SP}(\cos Z, c_m) = \sigma\rho_0 \int_{\infty}^{P} e^{-h/H}\, ds \tag{26}$$

$$\sigma\rho_0 = \frac{8\pi^3}{3\lambda^4} \times \frac{(n_0^2 - 1)^2}{N_0} \times \frac{6(1 + d)}{6 - 7d} \tag{27}$$

where

λ = wave-length of the incident radiation

n_0 = refractive index of the air

N_0 = number of molecules per c.c. at the ground

ρ_0 = density of the air in gm. per c.c. at the ground.

From Fig. 2, we have,

$$(a + h)^2 = s^2 + (a + c_m)^2 + 2s\,(a + c_m)\cos Z$$

and neglecting c_m^2 and h^2 compared to the other terms, we have,

$$h = \frac{s^2}{2a} + \frac{(a + c_m)\cos Z}{a}\,s + c_m$$

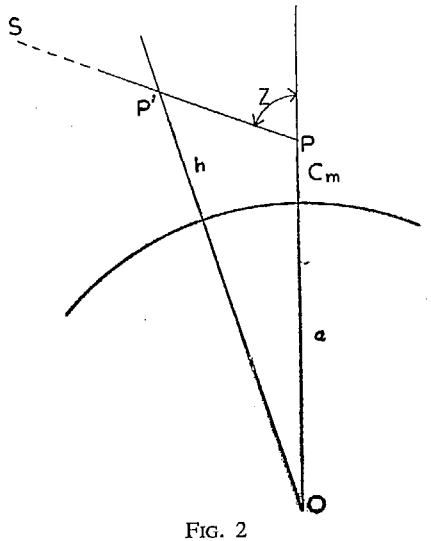

FIG. 2

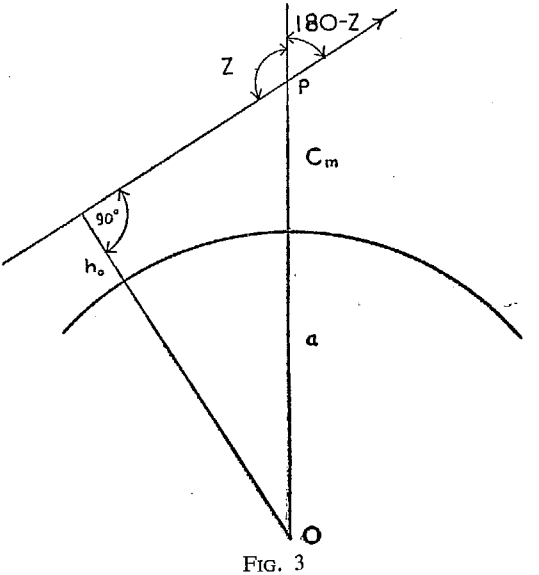

FIG. 3

On substituting this in Equation (26) and carrying out the integration, we have

$$\tau_{SP}(\cos Z, c_m) = \sigma\rho_0 \sqrt{\frac{\pi a\mathrm{H}}{2}} e^{-c_m/\mathrm{H}} \times e^{\frac{(a+c_m)^2 \cos^2 Z}{2a\mathrm{H}}} \left[1 - \mathrm{E}rf\left\{\frac{(a + c_m)\cos Z}{\sqrt{2a\mathrm{H}}}\right\}\right] \qquad (28)$$

The function $\mathrm{E}rf(y)$ is tabulated in books of *Mathematical Tables* at regular intervals between 0 and 3 while for $y > 3$, we can use the standard expansion formula. It can be shown that for $\cos Z = 1$ and $c_m = 0$, Equation (28) reduces to

$$\tau_{SP}(1, 0) = \sigma\rho_0 H = \tau_1$$
$$= \text{the vertical optical path} \qquad (29)$$

After substituting $\sigma\rho_0$ by τ_1/H in Equation (28), the equation was used to tabulate $\tau_{SP}(\cos Z, O)/\tau_1$ for a number of intervals of cos Z between 0 and 1. From this, we can calculate τ_{SP} for any wave-length by selecting τ_1. The intervals are sufficiently numerous to obtain τ_{SP}/τ_1 for any cos Z within the accuracy required. For positive values of cos Z and c_m, $e^{-c_m/H}$ is the most important factor and

$$\tau_{SP}(\cos Z, c_m)/\tau_1 = \tau_{SP}(\cos Z, O)\, e^{-c_m/H}/\tau_1 \qquad (30)$$

For negative values of cos Z, the following method is used. From Fig. 3,

$$\frac{a + h_0}{a + c_m} = \sin Z$$

from which h_0 can be calculated for a given Z and c_m. Then

$$\frac{\tau_{SP}(\cos Z, c_m)}{\tau_1} = \frac{2\tau_{SP}(O, O)}{\tau_1} e^{-h/H} - \frac{\tau_{SP}\{\cos(180 - Z), c_m\}}{\tau_1} \qquad (31)$$

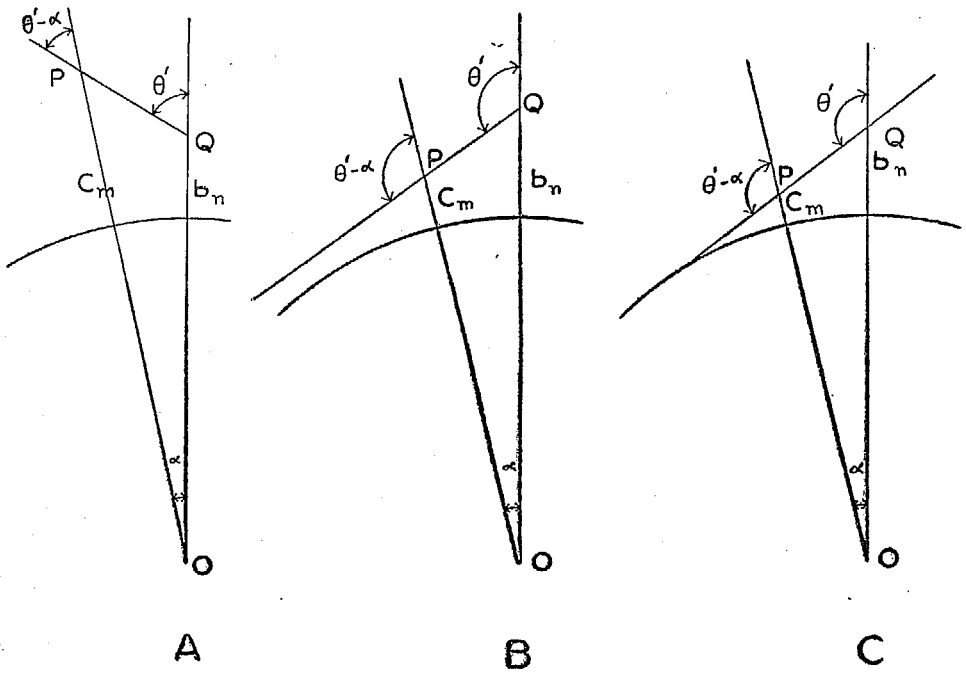

FIG. 4

Using Equation (31), $\tau_{SP}(\cos Z, c_m)/\tau_1$ were tabulated at regular intervals from zero to the shadow limit for different values of c_m from c_1 to c_{18}. For higher values of c_m the calculations were carried out whenever necessary.

3.5. τ_{PQ}, *equivalent optical path between any two points in the atmosphere*

From Figs. 4 A and B, we can write

$$\frac{\tau_{PQ}(\cos\theta', c_m \text{ to } b_n)}{\tau_1} = \frac{\tau_{SP}(\cos\theta', b_n)}{\tau_1} - \frac{\tau_{SP}\{\cos(\theta' - \alpha), c_m\}}{\tau_1} \quad (32)$$

For negative values of θ', for which PQ intersects the surface of the earth, the calculation of τ_{PQ} is similar to that indicated in Fig. 4 C.

IV. Intensity and Polarisation of the Zenith Sky

In this section the results of the computation of the intensity and polarisation of the primary and secondary radiations from the zenith sky during twilight for $\tau_1 = 0{\cdot}2$ corresponding to $\lambda = 4350$ A are given. The effect of adding a fixed intensity of night air-glow radiation with a polarisation of 4% as obtained from twilight observations is then discussed.

4.1. $R_{1n'}$, *primary scattered radiation received from any direction for different values of* Z_0

$R_{1n'}$ was calculated with the help of Equation (21). The summation extends over all the layers which lie in the sunlit part of the atmosphere. I_∞ was taken to be equal to unity, and $\sigma\rho_0 = \tau_1/H$ from Equation (29). Equation (21) shows that the part $e^{-\tau_{PQ}} e^{-c_m/H} \Delta s$ is independent of ϕ' and Z_0. An auxiliary table of $\{-\tau_{PQ} - c_m/H + \text{Log}_e \Delta s\}$ for different values of b_n and $\tau_1 = 0{\cdot}2$ was prepared to reduce the work of computation.

When $R_{1n'}$ was computed for different values of θ' and ϕ', for $Z_0 = 90°$ and $b_n = b_1$ or b_2, it was noticed that for a fixed θ', the graph of $R_{1n'}$ against $\cos\phi'$ was nearly a straight line for values of θ' between 0° to 75° and between 100° to 180° (Fig. 5). It was slightly curved when θ' lay between 75° and 95°. Therefore, $R_{1n'}$ was obtained by linear interpolation after computing its value for $\cos\phi' = 1{\cdot}0, 0{\cdot}5, 0{\cdot}0, -0{\cdot}5$ and $-1{\cdot}0$ for a given b_n. This procedure was adopted when Z_0 was 90° and 94° and the whole sky more or less illuminated by direct solar radiation. For higher values of Z_0, $R_{1n'}$ was calculated individually for each ϕ' and θ' as only a small portion of the sky could then get direct sunshine.

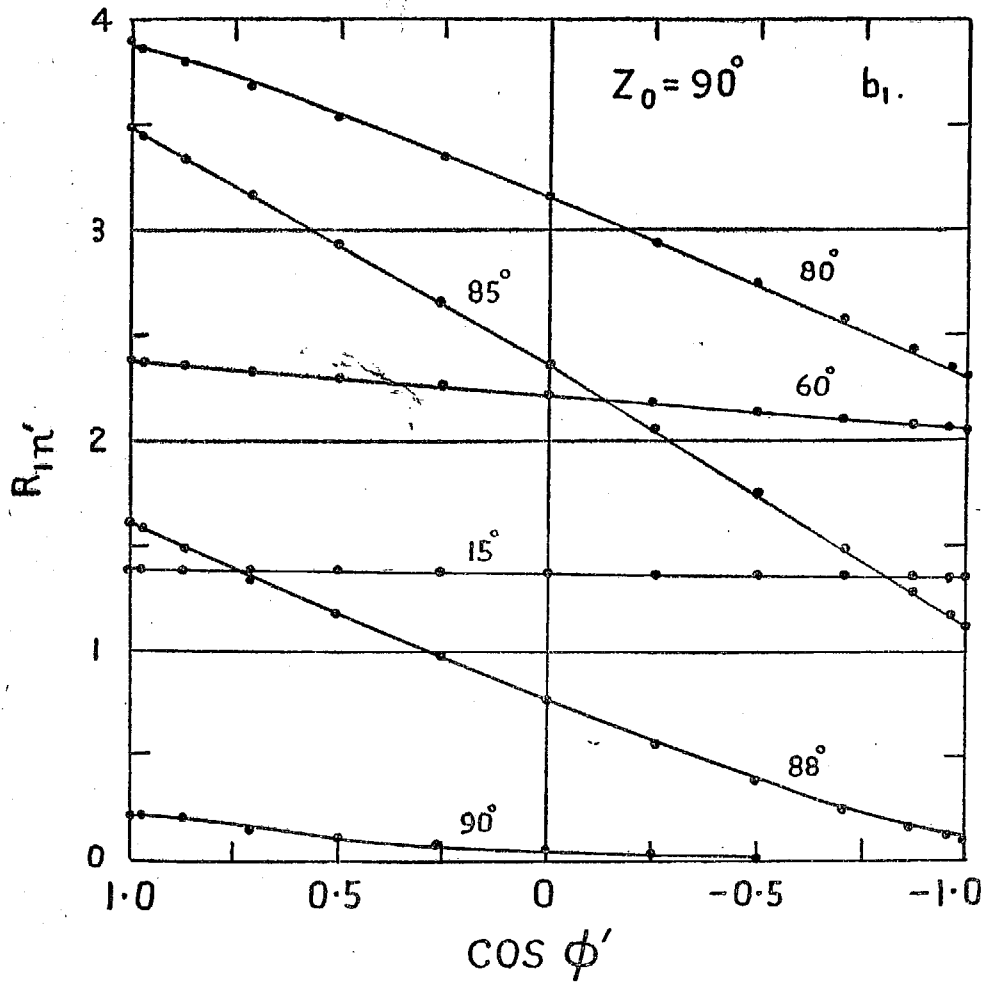

FIG. 5. Variation of the normal component of primary scattered light ($R_{1n'}$) with solar azimuth (cos ϕ') for different zenith angles of the sky from 15° to 90° as seen by an observer at ground level ($b_1 = 0$ km.). The sun is assumed to be on the observer's horizon ($Z_0 = 90°$).

The variation of the normal component of primary scattered radiation as received by the observer at the ground from different parts of the sky for Z_0 from 90° to 102° is shown in Fig. 6.

4.2. *E_{2n} and E_{2t}: Secondary emission from any point in the direction of observation*

Equation (17) can be rewritten as

$$\rho_0 E_{2n} = \frac{3\sigma\rho_0}{16\pi(1+\frac{1}{2}d)} \sum\sum [\{A_1 + KA_2\} R_{1n'} d\phi'] \sin\theta' . d\theta'$$

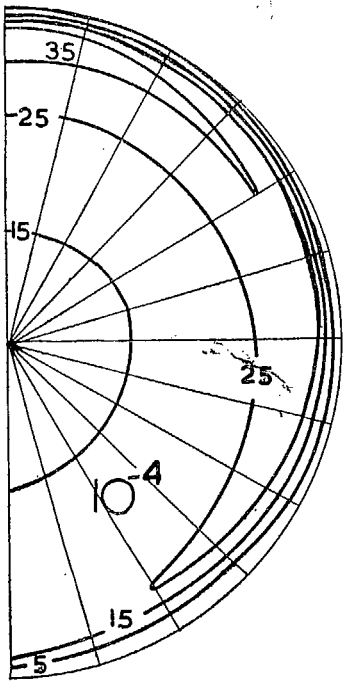

90°

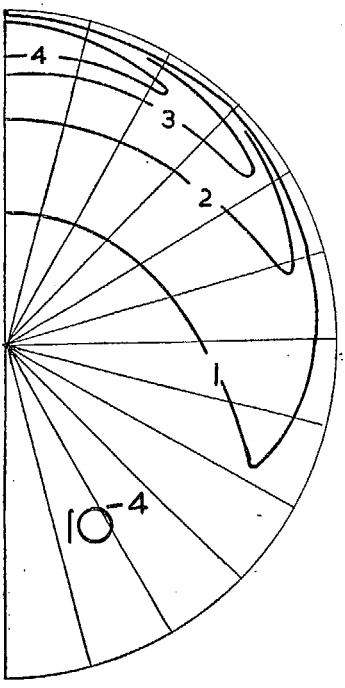

94°

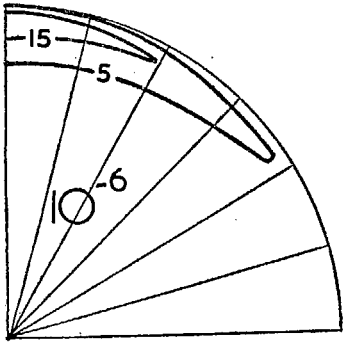

98°

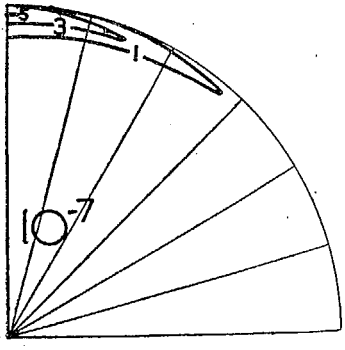

102°

FIG. 6. Distribution of the normal component of primary scattered radiation received at the ground from different parts of the sky.

Knowing the values of $\{A_1 + KA_2\}$ and $R_{1n'}$ at definite intervals of θ' and ϕ' for different values of b_n and Z_0, further calculation was carried out in the following manner:

First, summation was carried out over ϕ', keeping θ' constant. $R_{1n'}$ was multiplied by the corresponding $\{A_1 + KA_2\}$, the arithmetic means of the consecutive products were then added and the sum multiplied by $d\phi' = 0{\cdot}5237$ radians corresponding to 30° interval. Symmetry about the principal plane gives the value for 30° from the tabulated values for 15° intervals.

For summation over θ', $\Sigma[\{A_1 + KA_2\} R_{1n'} d\phi']$ was multiplied by the corresponding value of sin θ', and the arithmetic means of consecutive terms were taken. $R_{1n'}$ includes the exponential $\exp(-\tau_{SP} - \tau_{PQ})$. These were then multiplied by corresponding intervals of $d\theta'$ in radians. The summation of the product multiplied by $3\sigma\rho_0/16\pi(1 + \frac{1}{2}d)$ gave the value of $\rho_0 E_{2n}$ for the particular level b_n and Z_0 under consideration. The values of $\rho_0 E_{2n}$ and $\rho_0 E_{2t}$ so obtained are given in Table I for different values of b_n and Z_0.

TABLE I

$\rho_0 E_{2n}$ for the observer's zenith for different values of b_n and Z_0

b_n \ Z_0	90°	94°	98°	102°	106°
b_1	$0{\cdot}245\times10^{-4}$	$0{\cdot}143\times10^{-5}$	$0{\cdot}015\times10^{-6}$	$0{\cdot}013\times10^{-8}$	$0{\cdot}000\times10^{-10}$
b_2	0·339	0·199	0·032	0·051	0·025
b_3	0·445	0·262	0·062	0·133	0·117
b_4	0·535	0·326	0·101	0·287	0·383
b_5	0·584	0·406	0·162	0·605	1·037
b_6	0·587	0·491	0·237	1·040	1·994
b_7			0·295	1·389	2·769
b_8			0·311	1·507	3·048

$\rho_0 E_{2t}$ for the observer's zenith for different values of b_n and Z_0

b_1	$0{\cdot}077\times10^{-4}$	$0{\cdot}044\times10^{-5}$	$0{\cdot}004\times10^{-6}$	$0{\cdot}002\times10^{-8}$	$0{\cdot}000\times10^{-10}$
b_2	0·113	0·062	0·008	0·008	0·003
b_3	0·156	0·082	0·014	0·021	0·013
b_4	0·193	0·105	0·022	0·046	0·045
b_5	0·214	0·132	0·036	0·096	0·125
b_6	0·216	0·162	0·053	0·167	0·244
b_7			0·066	0·225	0·340
b_8			0·071	0·247	0·383

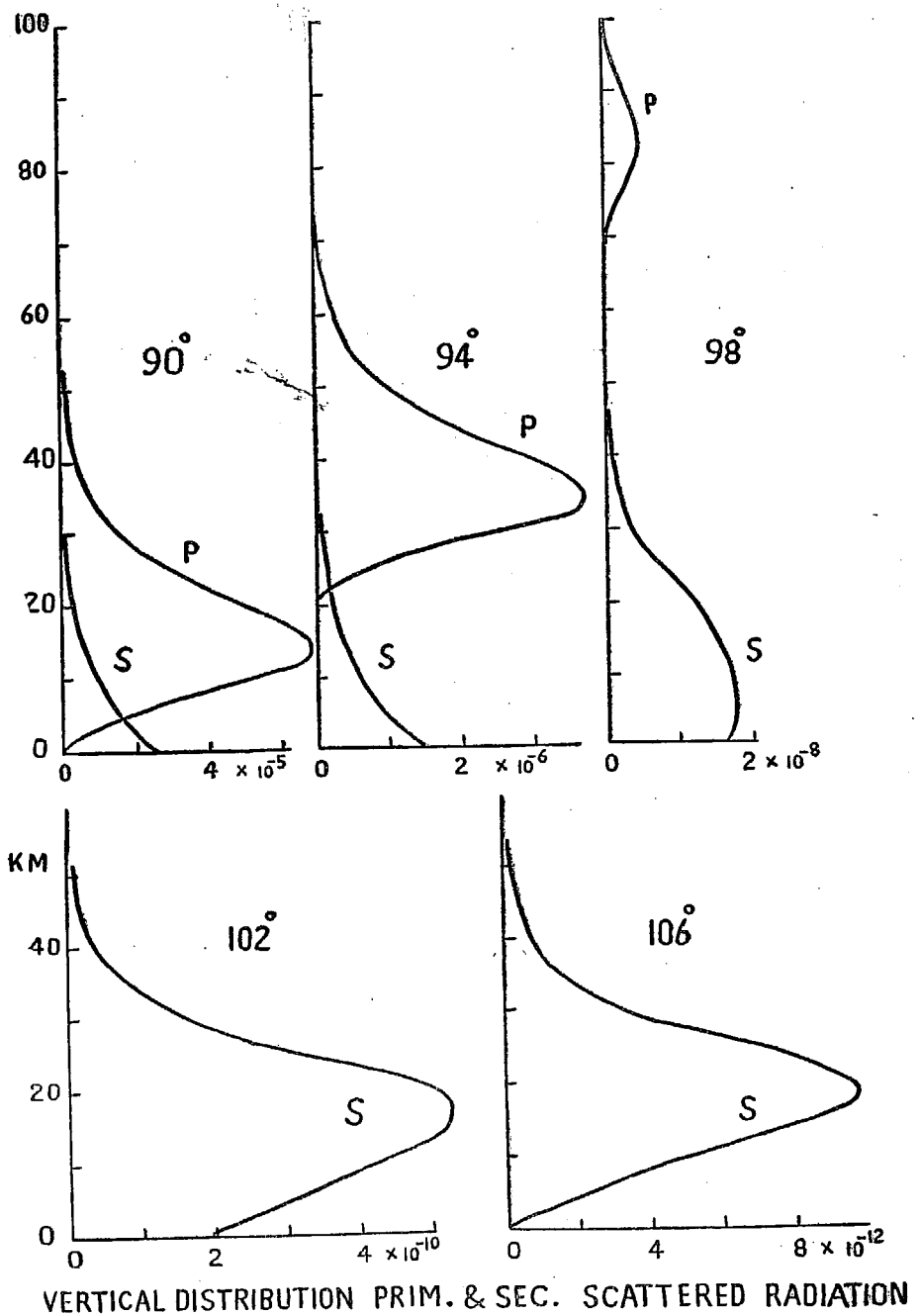

FIG. 7. Vertical distribution of primary and secondary scattered light from the zenith sky during twilight for solar zenith angles from 90° to 106°.

It will be seen from Table I that the computation has been stopped at b_6 for 90° and 94°. For heights greater than b_6, the value corresponding to b_6 has been used. A similar remark applies to heights greater than b_8 for 98°, 102° and 106°. This is justifiable because at these heights, the density becomes relatively small and the effective contribution to the light received by the observer becomes negligible (see Fig. 7).

4.3. *R_{2n} and R_{2t}: Normal and transverse components of the total secondary scattered light as received by the observer at the ground from his zenith*

Equation (19) can be rewritten as

$$R_{2n} = \Sigma \rho_0 E_{2n} e^{-\tau_{QR_0}} e^{-c_m/H} \Delta s \tag{33}$$

the summation extending over all the layers above the point of observation. $\Delta s = 4$ km. for $\theta = 0°$, $\phi = 0°$. τ_{QR_0} is the same as τ_{PQ} for $\theta' = 0°$ and $b_n = b_1$ when the observer is situated at ground level and the direction of observation is along his zenith. The value of $\rho_0 E_{2n}$ is the arithmetic mean of two successive values of b_n given in Table I. The vertical distribution of primary and secondary scattered radiation from the zenith sky for different solar angles are plotted in Fig. 7.

The values of R_{2n} and R_{2t} are given in Table II along with R_{1n}, R_{1t}, P_1 and P_2 where P_1, P_2 are the percentage polarisations of primary and secondary scattered light. P is defined by

$$P = \frac{R_n - R_t}{R_n + R_t} \times 100 \tag{34}$$

TABLE II

Intensity and polarisation of the primary and secondary scattered radiations from the zenith sky

Z_0	R_{1n}	R_{1t}	P_1 %	R_{2n}	R_{2t}	P_2 %
90	$1{\cdot}30\times10^{-3}$	$0{\cdot}052\times10^{-3}$	92·3	$2{\cdot}43\times10^{-4}$	$0{\cdot}84\times10^{-4}$	49
94	$6{\cdot}93\times10^{-5}$	$0{\cdot}31\times10^{-5}$	91·4	$1{\cdot}52\times10^{-5}$	$0{\cdot}48\times10^{-5}$	52
98	$9{\cdot}0\times10^{-8}$	$0{\cdot}5\times10^{-8}$	89	$4{\cdot}13\times10^{-7}$	$0{\cdot}94\times10^{-7}$	63
102	..	..	..	$1{\cdot}26\times10^{-8}$	$0{\cdot}20\times10^{-8}$	72
106	..	..	..	$1{\cdot}95\times10^{-10}$	$0{\cdot}24\times10^{-10}$	78

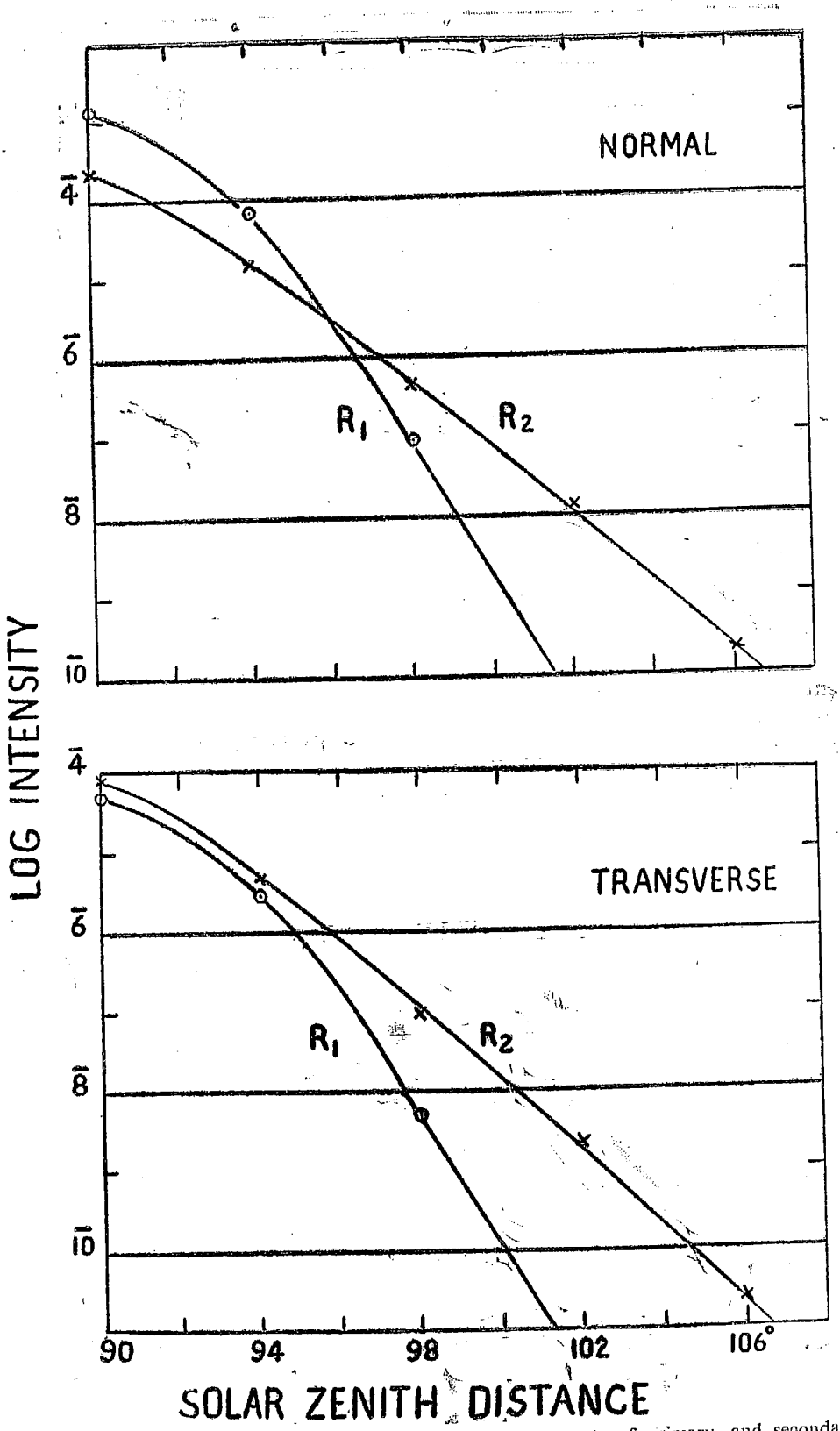

FIG. 8. Variation of the normal and transverse components of primary and secondary scattered light from the zenith sky during twilight.

4.4. *Variation of the intensity and polarisation of the zenith sky during twilight*

Figure 8 gives the variation of R_{1n}, R_{1t}, R_{2n} and R_{2t} with Z_0. Smooth curves were drawn from the values given in Table II and from them, the values were read out at each 1° interval to calculate the intensities and polarisations of the zenith sky at different zenith angles of the sun.

Figure 9 shows the variation with Z_0, of (*a*) the primary scattered radiation R_1, (*b*) the primary and secondary scattered radiations together, $R_1 + R_2$, (*c*) $R_1 + R_2 + R_0$ when R_0 is the background night air-glow radiation assumed to be constant at $1{\cdot}92 \times 10^{-9}$ and (*d*) the observed intensity

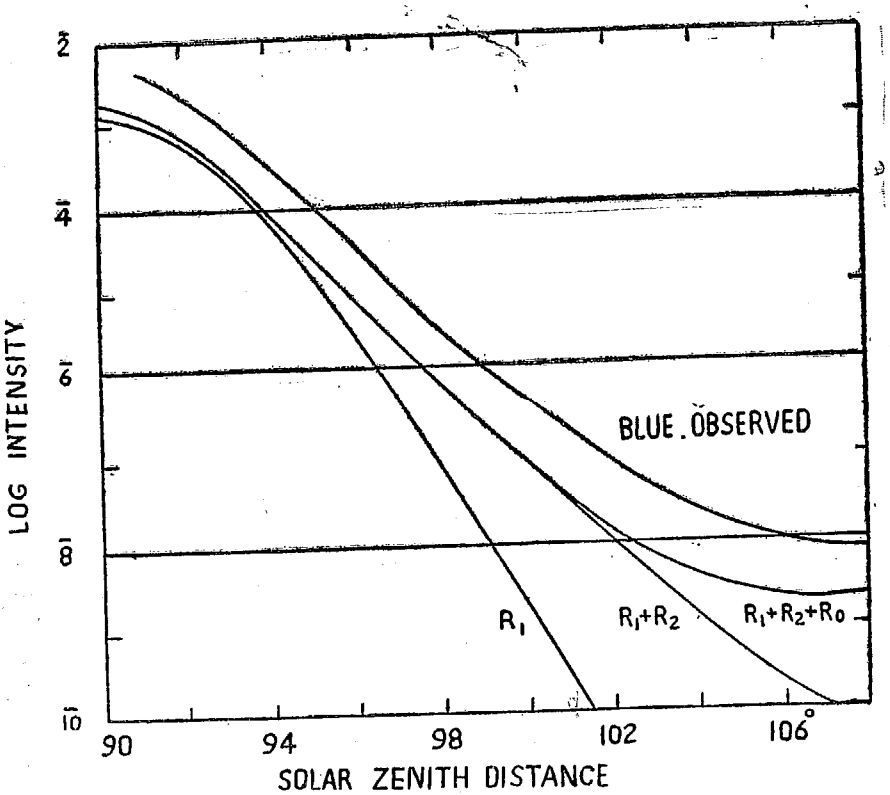

FIG. 9. Variation of the intensity of the zenith sky during twilight.

R_1 .. Primary scattering alone.

$R_1 + R_2$ .. Primary *plus* secondary scattering.

$R_1 + R_2 + R_0$.. $R_1 + R_2$ *plus* background night air-glow of constant intensity.

of the zenith sky for $\lambda = 4{,}500$ A during evening twilight as observed at Mount Abu. The magnitude of R_0 was fixed from observations of the zenith sky when the sun was more than 18° below the horizon.

It can be seen from the figure that the secondary scattered radiation becomes more and more important after 95°. Between 98° and 102°, the light received by the observer is mainly secondary scattered radiation. Afterwards, the night air-glow becomes comparable in intensity to secondary scattered light, and by 106°, practically only night sky emission remains as the factor contributing to the zenith sky intensity.

In Fig. 10 are given the curves of polarisation of the zenith sky when the different contributions are considered singly or jointly. The curve giving the polarisation of the primary scattered light shows that it is 92% at sunset and decreases to 88% at 100°. On the contrary, S representing the polarisation of the secondary scattered light shows an increase from 48% at sunset to 79% at 106°. Adding the normal and transverse components of the two radiations from the zenith sky and calculating the effective polarisation, the polarisation gets reduced to 84% at sunset. After 94°, the secondary scattered radiation becomes relatively more important and the polarisation shows a rapid fall; after 98°, P becomes unimportant and P + S follows S.

If night sky radiation of intensities $R_{0n} = 1{\cdot}00 \times 10^{-9}$ and $R_{0t} = 0{\cdot}92 \times 10^{-9}$ be added to $R_{1n} + R_{2n}$ and $R_{1t} + R_{2t}$ respectively, and the polarisation recalculated (Curve P + S + N), the curve gradually changes its course when the zenith distance of the sun increases beyond 99°, and the change becomes rapid after 102°. When Z is greater than 108°, night conditions get fully established.

When the calculated polarisation curve is compared with that obtained by observation, it is seen that while there is agreement in general features, there are some important differences. The observed values of polarisation are markedly smaller. The transitions are sharper in the observed curve than in the calculated one.*

This is probably due to the following causes:—

(1) The effect of dust in the atmosphere and of tertiary and higher orders of scattering have been neglected. Inclusion of these in the calculation will decrease the polarisation.

(2) The density of the atmosphere has been assumed to decrease exponentially with height with a scale height of 7 km. Actually, there are well marked stratifications in the atmosphere and the decrease of density with height is not a simple exponential. The difference

* Recent observations of polarisation at Mount Abu with a better type of polaroid have shown 80% polarisation at sunset and 55 to 60% between 8 and 12° solar depression.

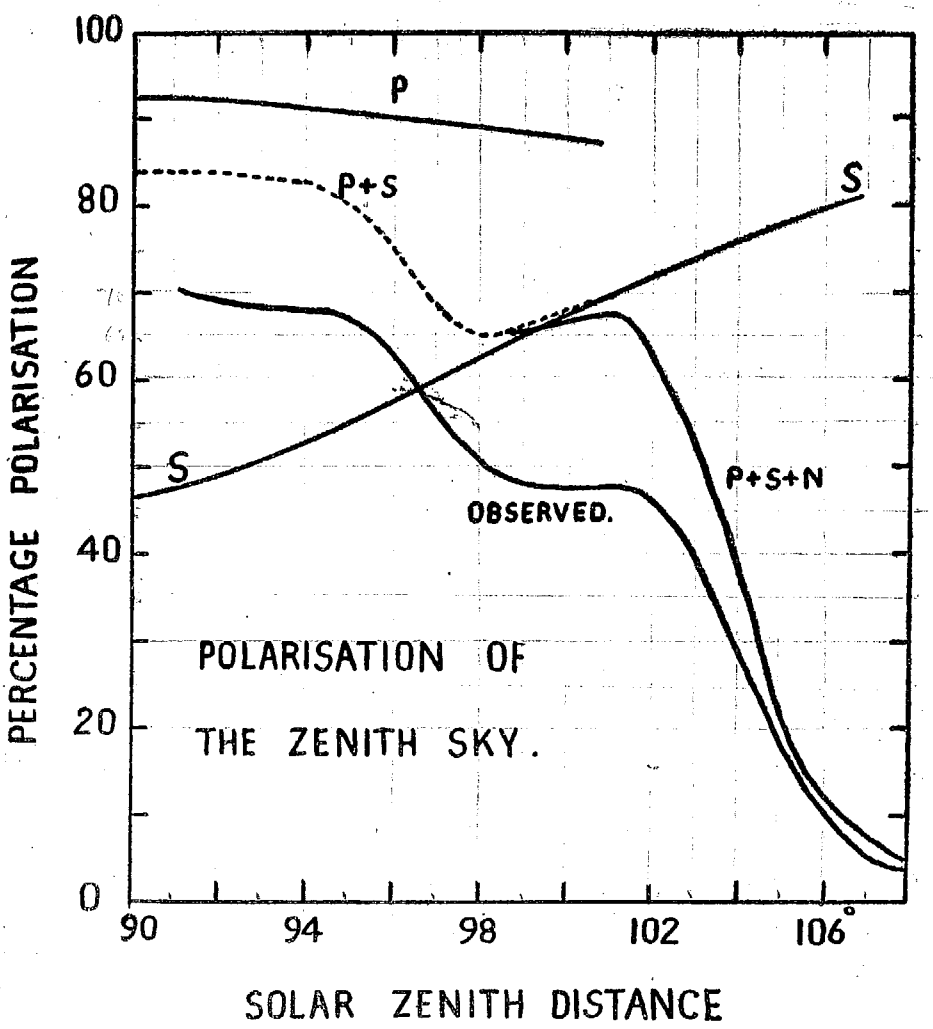

FIG. 10. Polarisation of the zenith sky during twilight for different zenith distances of the sun.

P	..	Percentage polarisation of primary scattered light.
S	..	Percentage polarisation of secondary scattered light.
P + S	..	Effective percentage polarisation of primary *plus* secondary scattered light.
P + S + N	..	Total effective polarisation when night air-glow of constant intensity and 4% polarisation is added to primary *plus* secondary scattered light.
Observed	..	Observed zenith sky polarisation at Mount Abu.

between the courses of the observed and calculated curves between 94° and 98° can be related to the existence of the warm ozone layer between 30 and 60 km. An attempt is being made to remedy these defects in the theory.

V. POLARISATION OF THE SKY AT POINTS 30° FROM THE ZENITH AND IN THE PRINCIPAL PLANE OF THE SUN

In Part I, we also presented the observations of polarisation during twilight from two directions in the sky other than zenith, (1) at 30° from the zenith on the sunside $\theta = 30°$, $\phi = 0°$ and (2) at 30° from the zenith on the anti-sunside, $\theta = 30°$, $\phi = 180°$. These curves while showing the general features of the zenith polarisation curve, show some differences. In order to understand this, calculations have also been made of the polarisation in these two directions. They are plotted in Fig. 11.

The polarisation curves for the sunside show that the polarisation of primary scattered light (P) increases with Z_0 and so also the polarisation of secondary scattered light (S). However, the secondary scattered radiation is polarised to a much smaller extent than the primary and hence the resultant polarisation P + S, increases with Z_0 in the beginning when the primary scattered radiation is prominent and decreases afterwards when $Z_0 = 94{\cdot}5°$. For $Z_0 = 100°$, the primary scattered radiation is negligible and P + S practically coincides with S. On adding the night sky radiation, the P + S curve deviates from the S curve at 100°, and by 102° a sharp fall occurs.

On the anti-sun side, the polarisation of P shows a fall with Z_0 and the rate of increase of S is much smaller than on the side of the sun. This causes a slight fall of polarisation in the beginning and a comparative flat region between 98° and 102°.

VI. SUMMARY

The formulæ for the intensity of the secondary scattered light from the sky as developed by Chapman and Hammad for a plane-parallel infinite atmosphere of defined optical thickness have been modified so as to deal with the twilight problem in which the curvature of the atmosphere is of fundamental importance. Calculations have been made of the intensity and polarisation of the light received from the zenith sky for different values of the sun's zenith distance from 90° to 107° and for a radiation for which the optical thickness of the atmosphere is 0·2. For 0° to 5° solar depression, the primary scattering is predominant; as the angle increases, the secondary scattered light becomes more and more important and when the sun's depression is 8° to 12°, it is the principal contributing factor. Afterwards, the night air-glow becomes comparable in intensity and when the solar depression is 17° to 18°, only the air-glow radiation remains. The calculated values of intensity and polarisation are compared with the observational data collected at Mount Abu.

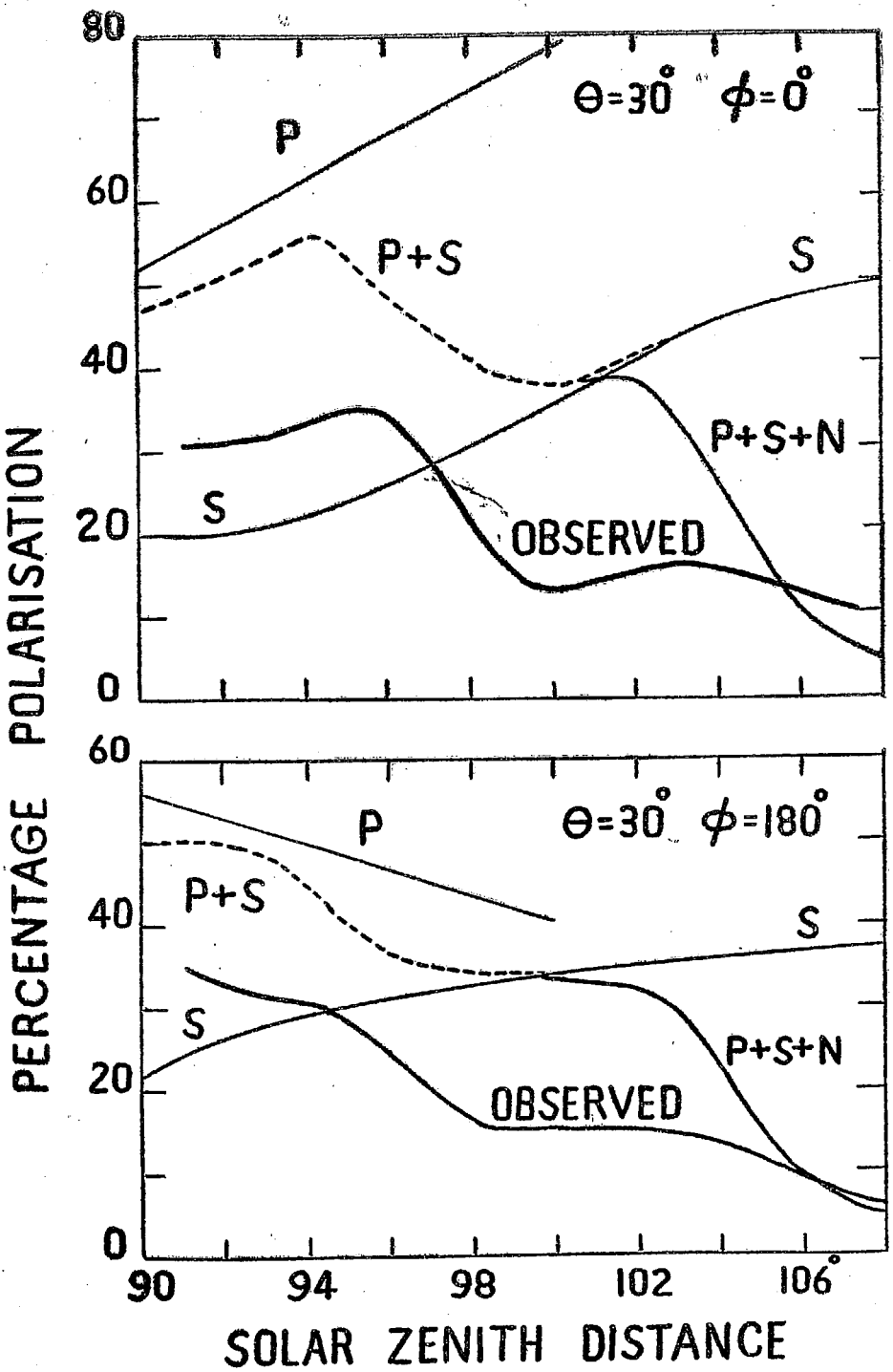

FIG. 11. Polarisation of the sky at points 30° from the zenith in the principal plane of the sun.

P	..	Percentage polarisation of primary scattered light.
S	..	Percentage polarisation of secondary scattered light.
P + S	..	Effective percentage polarisation of primary *plus* secondary scattered light.
P + S + N	..	Total effective percentage polarisation when night air-glow of constant intensity and 4% polarisation is added to primary *plus* secondary scattered light.
Observed	..	Observed sky polarisation at Mount Abu.

The author is grateful to the Council of Scientific and Industrial Research for the award of a Research Assistantship during the course of this study. He acknowledges with pleasure the help given by Shri V. L. Bhatt, M.Sc., in preparing some of the diagrams. Finally, the author takes this opportunity to express his indebtedness to Prof. K. R. Ramanathan, for suggesting the problem and valuable guidance.

REFERENCES

1. Dave, J. V. and Ramanathan, K. R. — *Proc. Ind. Acad. Sci.*, 1956, **43 A**, 67.
2. Hulburt, E. O. .. *Journ. Opt. Soc. America*, 1938, **28**, 227.
3. Robley, R. .. *Annales de Geophysique*, 1952, **8**, 1.
4. Chandrasekhar, S. .. *Radiative Transfer*, The International Series of Monographs on Physics, Clarendon Press, Oxford, 1950.
5. Hammad, A. and Chapman, S. .. *Phil. Mag.*, 1939, **28**, 99.
6. Hammad, A. .. *Astrophys. Journ.*, 1948, **108**, 338.
7. Link, F. and Sekera, Z. .. *Publ. Obs. Nat., Prague*, 1940, **14**, 1.
8. Chapman, S. .. *Proc. Phys. Soc.*, 1931, **43**, 483.
9. ———— .. *Ibid.*, 1953, **66 B**, 710.


BANGALORE
PRESS
BANGALORE

1.3 Tables of the equivalent optical path from the sun to a point P in the observer's zenith for values of zenith angle of the sun greater than 90°.

Values of τ_{sp} (cos Z, C_m)/ τ_1 are calculated for different negative values of Cos Z for a point P situated at different heights in the observer's zenith. Corresponding t a given height C_m, there is a limiting value of Z beyond whi the ray will intersect the earth. The computation of τ_{sp} is carried up to that limiting value of Z. τ_1 is the vertic equivalent optical path.

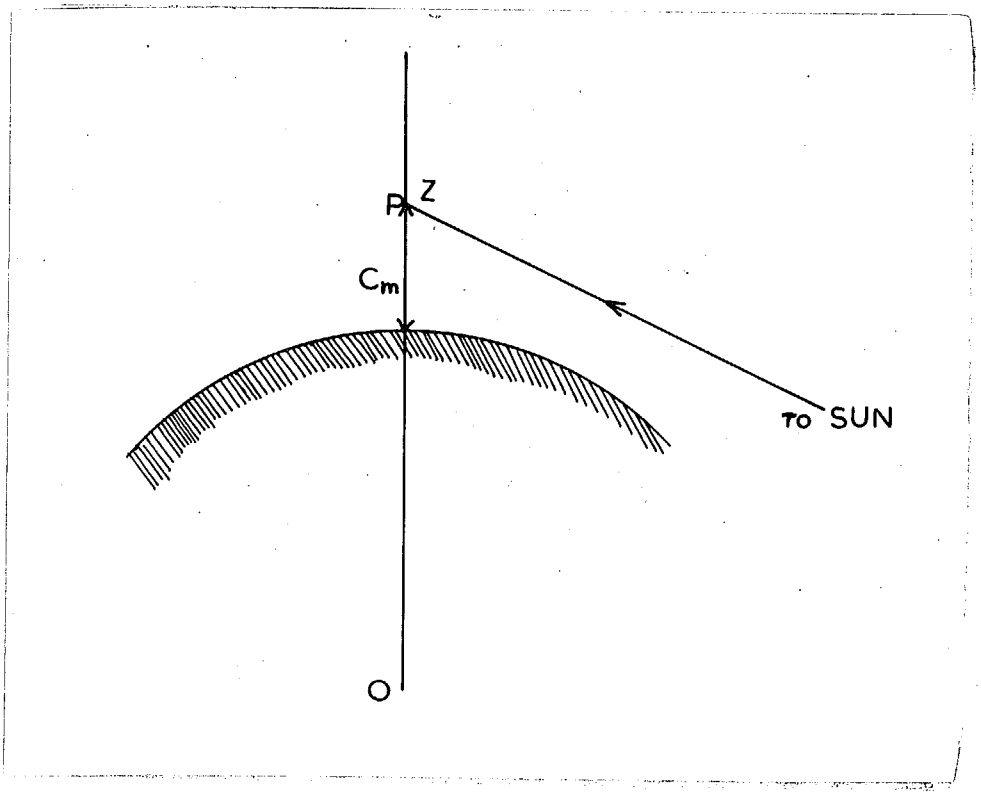

H_1 = 2 Km

Cos Z	τ_{SP}/τ_1	Cos Z	τ_{SP}/τ_1	Cos Z	τ_{SP}/τ_1	Cos Z	τ_{SP}/τ_1	Cos Z	τ_{SP}/τ_1
-0.001	29.10	-0.006	33.04	-0.011	37.84	-0.016	43.77	-0.021	51.18
-0.002	29.83	-0.007	33.91	-0.012	38.92	-0.017	45.12	-0.022	52.89
-0.003	30.59	-0.008	34.84	-0.013	40.05	-0.018	46.54	-0.023	54.67
-0.004	31.37	-0.009	35.79	-0.014	41.24	-0.019	48.00	-0.024	56.55
-0.005	32.19	-0.010	36.79	-0.015	42.47	-0.020	49.56	-0.025	58.52

H_2 = 6 Km

-0.001	16.44	-0.010	20.78	-0.019	27.11	-0.028	36.74	-0.037	51.96
-0.002	16.85	-0.011	21.37	-0.020	27.99	-0.029	38.09	-0.038	54.17
-0.003	17.27	-0.012	21.97	-0.021	28.91	-0.030	39.53	-0.039	56.49
-0.004	17.71	-0.013	22.62	-0.022	29.87	-0.031	41.03	-0.040	58.95
-0.005	18.18	-0.014	23.29	-0.023	30.88	-0.032	42.61	-0.041	61.56
-0.006	18.65	-0.015	23.99	-0.024	31.94	-0.033	44.29	-0.042	64.32
-0.007	19.14	-0.016	24.71	-0.025	33.05	-0.034	46.05	-0.043	67.26
-0.008	19.67	-0.017	25.48	-0.026	34.22	-0.035	47.91		
-0.009	20.22	-0.018	26.27	-0.027	35.44	-0.036	49.89		

C_3 = 10 Km

Cos Z	τ_{SP}/τ_1	Cos Z	τ_{SP}/τ_1	Cos Z	τ_{SP}/τ_1	Cos Z	τ_{SP}/τ_1	Cos Z	τ_{SP}/τ_1
-0.001	9.28	-0.013	12.77	-0.025	18.67	-0.037	29.37	-0.049	50.40
-0.002	9.52	-0.014	13.15	-0.026	19.33	-0.038	30.63	-0.050	52.97
-0.003	9.76	-0.015	13.55	-0.027	20.02	-0.039	31.93	-0.051	55.66
-0.004	10.00	-0.016	13.96	-0.028	20.74	-0.040	33.34	-0.052	58.58
-0.005	10.27	-0.017	14.40	-0.029	21.53	-0.041	34.80	-0.053	61.65
-0.006	10.53	-0.018	14.85	-0.030	22.32	-0.042	36.34	-0.054	64.99
-0.007	10.81	-0.019	15.31	-0.031	23.19	-0.043	38.01	-0.055	68.50
-0.008	11.11	-0.020	15.81	-0.032	24.07	-0.044	39.81	-0.056	72.18
-0.009	11.41	-0.021	16.33	-0.033	25.04	-0.045	41.65		
-0.010	11.74	-0.022	16.88	-0.034	26.01	-0.046	43.66		
-0.011	12.07	-0.023	17.44	-0.035	27.08	-0.047	45.75		
-0.012	12.41	-0.024	18.04	-0.036	28.18	-0.048	48.02		

T.3

z_4 = 14 Km

Cos Z	τ_{SP}/τ_1	Cos Z	τ_{SP}/τ_1	Cos Z	τ_{SP}/τ_1	Cos Z	τ_{SP}/τ_1	Cos Z	τ_{SP}/τ_1
-0.001	5.24	-0.015	7.65	-0.029	12.16	-0.043	21.48	-0.057	43.18
-0.002	5.37	-0.016	7.88	-0.030	12.61	-0.044	22.49	-0.058	45.65
-0.003	5.51	-0.017	8.13	-0.031	13.10	-0.045	23.53	-0.059	48.27
-0.004	5.65	-0.018	8.39	-0.032	13.60	-0.046	24.67	-0.060	51.10
-0.005	5.80	-0.019	8.65	-0.033	14.14	-0.047	25.86	-0.061	54.10
-0.006	5.95	-0.020	8.93	-0.034	14.70	-0.048	27.15	-0.062	57.38
-0.007	6.11	-0.021	9.23	-0.035	15.30	-0.049	28.47	-0.063	60.84
-0.008	6.28	-0.022	9.53	-0.036	15.92	-0.050	29.93	-0.064	64.63
-0.009	6.45	-0.023	9.85	-0.037	16.60	-0.051	31.46	-0.065	68.69
-0.010	6.62	-0.024	10.19	-0.038	17.31	-0.052	33.12	-0.066	73.02
-0.011	6.81	-0.025	10.54	-0.039	18.04	-0.053	34.85		
-0.012	7.01	-0.026	10.92	-0.040	18.84	-0.054	36.74		
-0.013	7.21	-0.027	11.31	-0.041	19.66	-0.055	38.71		
-0.014	7.43	-0.028	11.72	-0.042	20.54	-0.056	40.91		

H_5 = 18 Km

Cos Z	τ_{SP}/τ_1	Cos Z	τ_{SP}/τ_1	Cos Z	τ_{SP}/τ_1	Cos Z	τ_{SP}/τ_1	Cos Z	τ_{SP}/τ_1
-0.001	2.96	-0.016	4.46	-0.031	7.40	-0.046	13.94	-0.061	30.59
-0.002	3.03	-0.017	4.59	-0.032	7.68	-0.047	14.61	-0.062	32.44
-0.003	3.11	-0.018	4.73	-0.033	7.98	-0.048	15.34	-0.063	34.40
-0.004	3.19	-0.019	4.88	-0.034	8.30	-0.049	16.10	-0.064	36.54
-0.005	3.28	-0.020	5.05	-0.035	8.64	-0.050	16.91	-0.065	38.84
-0.006	3.35	-0.021	5.21	-0.036	8.99	-0.051	17.78	-0.066	41.29
-0.007	3.45	-0.022	5.38	-0.037	9.38	-0.052	18.72	-0.067	44.01
-0.008	3.54	-0.023	5.57	-0.038	9.78	-0.053	19.70	-0.068	46.86
-0.009	3.64	-0.024	5.76	-0.039	10.19	-0.054	20.76	-0.069	49.97
-0.010	3.74	-0.025	5.96	-0.040	10.65	-0.055	21.89	-0.070	53.29
-0.011	3.85	-0.026	6.17	-0.041	11.11	-0.056	23.12	-0.071	56.94
-0.012	3.96	-0.027	6.39	-0.042	11.61	-0.057	24.41	-0.072	60.82
-0.013	4.07	-0.028	6.63	-0.043	12.15	-0.058	25.81	-0.073	65.08
-0.014	4.19	-0.029	6.86	-0.044	12.70	-0.059	27.28	-0.074	69.64
-0.015	4.32	-0.030	7.13	-0.045	13.30	-0.060	28.88	-0.075	74.72

z_0 = 22 Km

Cos Z	τ_{SP}/τ_1	Cos Z	τ_{SP}/τ_1	Cos Z	τ_{SP}/τ_1	Cos Z	τ_{SP}/τ_1	Cos Z	τ_{SP}/τ_1
-0.001	1.68	-0.028	3.74	-0.042	6.55	-0.056	13.07	-0.070	30.13
-0.003	1.76	-0.029	3.88	-0.043	6.86	-0.057	13.80	-0.071	32.20
-0.005	1.85	-0.030	4.02	-0.044	7.18	-0.058	14.59	-0.072	34.39
-0.007	1.95	-0.031	4.18	-0.045	7.51	-0.059	15.42	-0.073	36.81
-0.009	2.06	-0.032	4.34	-0.046	7.88	-0.060	16.33	-0.074	39.39
-0.011	2.17	-0.033	4.51	-0.047	8.25	-0.061	17.30	-0.075	42.26
-0.013	2.31	-0.034	4.69	-0.048	8.66	-0.062	18.34	-0.076	45.30
-0.015	2.44	-0.035	4.88	-0.049	9.09	-0.063	19.45	-0.077	48.59
-0.017	2.59	-0.036	5.08	-0.050	9.56	-0.064	20.66	-0.078	52.27
-0.019	2.76	-0.037	5.30	-0.051	10.05	-0.065	21.96	-0.079	56.17
-0.021	2.94	-0.038	5.53	-0.052	10.58	-0.066	23.35	-0.080	60.46
-0.023	3.15	-0.039	5.76	-0.053	11.14	-0.067	24.89	-0.081	65.15
-0.025	3.36	-0.040	6.01	-0.054	11.73	-0.068	26.49	-0.082	70.26
-0.027	3.61	-0.041	6.28	-0.055	12.37	-0.069	28.26		

z_7 = 26 Km

Cos Z	τ_{SP}/τ_1	Cos Z	τ_{SP}/τ_1	Cos Z	τ_{SP}/τ_1	Cos Z	τ_{SP}/τ_1	Cos Z	τ_{SP}/τ_1
-0.001	0.94	-0.030	2.27	-0.045	4.25	-0.060	9.24	-0.075	23.90
-0.003	0.99	-0.031	2.36	-0.046	4.45	-0.061	9.78	-0.076	25.62
-0.005	1.04	-0.032	2.45	-0.047	4.67	-0.062	10.36	-0.077	27.48
-0.007	1.10	-0.033	2.55	-0.048	4.90	-0.063	11.00	-0.078	29.57
-0.009	1.16	-0.034	2.65	-0.049	5.14	-0.064	11.68	-0.079	31.78
-0.011	1.23	-0.035	2.76	-0.050	5.40	-0.065	12.42	-0.080	34.21
-0.013	1.30	-0.036	2.87	-0.051	5.68	-0.066	13.20	-0.081	36.87
-0.015	1.38	-0.037	3.00	-0.052	5.98	-0.067	14.07	-0.082	39.76
-0.017	1.46	-0.038	3.12	-0.053	6.30	-0.068	14.99	-0.083	42.91
-0.019	1.55	-0.039	3.25	-0.054	6.63	-0.069	15.98	-0.084	46.35
-0.021	1.66	-0.040	3.40	-0.055	7.00	-0.070	17.04	-0.085	50.09
-0.023	1.78	-0.041	3.55	-0.056	7.39	-0.071	18.21	-0.086	54.20
-0.025	1.90	-0.042	3.71	-0.057	7.80	-0.072	19.45	-0.087	58.70
-0.027	2.04	-0.043	3.87	-0.058	8.25	-0.073	20.82	-0.088	63.64
-0.029	2.19	-0.044	4.06	-0.059	8.72	-0.074	22.28	-0.089	69.00
								-0.090	75.00

z_s = 30 km

Cos Z	τ_{SP}/τ_1	Cos Z	τ_{SP}/τ_1	Cos Z	τ_{SP}/τ_1	Cos Z	τ_{SP}/τ_1	Cos Z	τ_{SP}/τ_1
0.000	0.52	-0.040	1.92	-0.055	3.95	-0.069	9.04	-0.083	24.26
-0.005	0.59	-0.042	2.09	-0.056	4.17	-0.070	9.64	-0.084	26.23
-0.010	0.67	-0.043	2.19	-0.057	4.40	-0.071	10.30	-0.085	28.33
-0.015	0.77	-0.044	2.29	-0.058	4.66	-0.072	11.01	-0.086	30.68
-0.020	0.91	-0.045	2.40	-0.059	4.93	-0.073	11.78	-0.087	33.23
-0.022	0.97	-0.046	2.51	-0.060	5.22	-0.074	12.60	-0.088	36.02
-0.024	1.03	-0.047	2.64	-0.061	5.52	-0.075	13.52	-0.089	39.05
-0.026	1.11	-0.048	2.77	-0.062	5.87	-0.076	14.49	-0.090	42.45
-0.028	1.19	-0.049	2.90	-0.063	6.22	-0.077	15.55	-0.091	46.11
-0.030	1.28	-0.050	3.06	-0.064	6.60	-0.078	16.73	-0.092	50.21
-0.032	1.38	-0.051	3.21	-0.065	7.02	-0.079	17.98	-0.093	54.64
-0.034	1.50	-0.052	3.38	-0.066	7.46	-0.080	19.36	-0.094	59.56
-0.036	1.62	-0.053	3.55	-0.067	7.96	-0.081	20.86	-0.095	64.98
-0.038	1.77	-0.054	3.75	-0.068	8.47	-0.082	22.49	-0.096	70.88

z_g = 34 Km

Cos Z	τ_{SP}/τ_1	Cos Z	τ_{SP}/τ_1	Cos Z	τ_{SP}/τ_1	Cos Z	τ_{SP}/τ_1	Cos Z	τ_{SP}/τ_1
0.000	0.29	-0.046	1.42	-0.061	3.12	-0.076	8.20	-0.091	26.10
-0.005	0.33	-0.047	1.49	-0.062	3.32	-0.077	8.79	-0.092	28.42
-0.010	0.39	-0.048	1.57	-0.063	3.52	-0.078	9.46	-0.093	30.93
-0.015	0.44	-0.049	1.64	-0.064	3.74	-0.079	10.17	-0.094	33.72
-0.020	0.52	-0.050	1.73	-0.065	3.97	-0.080	10.95	-0.095	36.79
-0.025	0.60	-0.051	1.81	-0.066	4.22	-0.081	11.81	-0.096	40.14
-0.030	0.73	-0.052	1.91	-0.067	4.50	-0.082	12.73	-0.097	43.91
-0.032	0.78	-0.053	2.01	-0.068	4.79	-0.083	13.74	-0.098	47.99
-0.034	0.85	-0.054	2.12	-0.069	5.11	-0.084	14.85	-0.099	52.60
-0.036	0.91	-0.055	2.24	-0.070	5.46	-0.085	16.04	-0.100	57.59
-0.038	1.00	-0.056	2.36	-0.071	5.83	-0.086	17.36	-0.101	63.23
-0.040	1.08	-0.057	2.49	-0.072	6.23	-0.087	18.80	-0.102	69.36
-0.042	1.19	-0.058	2.63	-0.073	6.66	-0.088	20.39		
-0.044	1.30	-0.059	2.78	-0.074	7.13	-0.089	22.10		
-0.045	1.35	-0.060	2.95	-0.075	7.65	-0.090	24.03		

z_{10} = 38 Km

Cos Z	τ_{SP}/τ_1	Cos Z	τ_{SP}/τ_1	Cos Z	τ_{SP}/τ_1	Cos Z	τ_{SP}/τ_1	Cos Z	τ_{SP}/τ_1
0.000	0.17	-0.034	1.20	-0.068	2.71	-0.082	7.20	-0.096	22.73
-0.010	0.22	-0.035	1.27	-0.069	2.89	-0.083	7.77	-0.097	24.86
-0.020	0.29	-0.056	1.34	-0.070	3.09	-0.084	8.40	-0.098	27.18
-0.030	0.41	-0.057	1.41	-0.071	3.30	-0.085	9.07	-0.099	29.78
-0.035	0.50	-0.058	1.49	-0.072	3.52	-0.086	9.82	-0.100	32.62
-0.040	0.61	-0.059	1.58	-0.073	3.77	-0.087	10.65	-0.101	35.81
-0.042	0.66	-0.060	1.67	-0.074	4.03	-0.088	11.54	-0.102	39.28
-0.044	0.74	-0.061	1.77	-0.075	4.33	-0.089	12.52	-0.103	43.21
-0.046	0.80	-0.062	1.87	-0.076	4.64	-0.090	13.61	-0.104	47.49
-0.048	0.88	-0.063	1.98	-0.077	4.98	-0.091	14.78	-0.105	52.33
-0.050	0.97	-0.064	2.11	-0.078	5.35	-0.092	16.10	-0.106	57.67
-0.051	1.02	-0.065	2.24	-0.079	5.75	-0.093	17.51	-0.107	63.61
-0.052	1.08	-0.066	2.38	-0.080	6.19	-0.094	19.09	-0.108	70.23
-0.053	1.13	-0.067	2.54	-0.081	6.67	-0.095	20.83		

a_{11} = 42 Å

Cos Z	τ_{sp}/τ_1	Cos Z	τ_{sp}/τ_1	Cos Z	τ_{sp}/τ_1	Cos Z	τ_{sp}/τ_1	Cos Z	τ_{sp}/τ_1
0.000	0.09	-0.063	1.13	-0.077	2.81	-0.091	8.37	-0.105	29.65
-0.010	0.13	-0.064	1.20	-0.078	3.03	-0.092	9.11	-0.106	32.68
-0.020	0.17	-0.065	1.27	-0.079	3.25	-0.093	9.92	-0.107	36.04
-0.030	0.23	-0.066	1.35	-0.080	3.50	-0.094	10.81	-0.108	39.80
-0.040	0.35	-0.067	1.44	-0.081	3.77	-0.095	11.80	-0.109	43.98
-0.045	0.43	-0.068	1.53	-0.082	4.07	-0.096	12.87	-0.110	48.64
-0.050	0.53	-0.069	1.64	-0.083	4.39	-0.097	14.08	-0.111	53.90
-0.052	0.61	-0.070	1.74	-0.084	4.75	-0.098	15.39	-0.112	59.67
-0.054	0.67	-0.071	1.86	-0.085	5.13	-0.099	16.87	-0.113	66.24
-0.056	0.75	-0.072	1.99	-0.086	5.55	-0.100	18.47	-0.114	73.53
-0.058	0.85	-0.073	2.13	-0.087	6.02	-0.101	20.25		
-0.060	0.95	-0.074	2.28	-0.088	6.53	-0.102	22.25		
-0.061	1.00	-0.075	2.45	-0.089	7.08	-0.103	24.48		
-0.062	1.06	-0.076	2.62	-0.090	7.70	-0.104	26.90		

z_{12} = 46 Km

Cos Z	τ_{SP}/τ_1	Cos Z	τ_{SP}/τ_1	Cos Z	τ_{SP}/τ_1	Cos Z	τ_{SP}/τ_1	Cos Z	τ_{SP}/τ_1
0.000	0.05	-0.071	1.05	-0.084	2.69	-0.097	7.98	-0.110	27.56
-0.010	0.07	-0.072	1.12	-0.085	2.91	-0.098	8.72	-0.111	30.55
-0.020	0.10	-0.073	1.20	-0.086	3.15	-0.099	9.56	-0.112	33.82
-0.030	0.13	-0.074	1.29	-0.087	3.41	-0.100	10.46	-0.113	37.55
-0.040	0.20	-0.075	1.38	-0.088	3.70	-0.101	11.49	-0.114	41.68
-0.050	0.31	-0.076	1.48	-0.089	4.01	-0.102	12.61	-0.115	46.36
-0.055	0.40	-0.077	1.59	-0.090	4.36	-0.103	13.87	-0.116	51.56
-0.060	0.53	-0.078	1.71	-0.091	4.74	-0.104	15.24	-0.117	57.35
-0.062	0.60	-0.079	1.84	-0.092	5.16	-0.105	16.80	-0.118	63.96
-0.064	0.67	-0.080	1.98	-0.093	5.62	-0.106	18.51	-0.119	71.40
-0.066	0.76	-0.081	2.13	-0.094	6.12	-0.107	20.42		
-0.068	0.86	-0.082	2.30	-0.095	6.68	-0.108	22.55		
-0.070	0.98	-0.083	2.49	-0.096	7.29	-0.109	24.92		

C_{13} = 50 Km

Cos Z	τ_{SP}/τ_1	Cos Z	τ_{SP}/τ_1	Cos Z	τ_{SP}/τ_1	Cos Z	τ_{SP}/τ_1	Cos Z	τ_{SP}/τ_1
0.000	0.03	-0.076	0.84	-0.094	3.46	-0.105	9.51	-0.116	29.23
-0.010	0.04	-0.078	0.97	-0.095	3.78	-0.106	10.48	-0.117	32.51
-0.020	0.05	-0.080	1.12	-0.096	4.12	-0.107	11.57	-0.118	36.26
-0.030	0.07	-0.082	1.30	-0.097	4.51	-0.108	12.77	-0.119	40.48
-0.040	0.11	-0.084	1.52	-0.098	4.93	-0.109	14.12	-0.120	45.24
-0.050	0.18	-0.086	1.78	-0.099	5.41	-0.110	15.62	-0.121	50.55
-0.060	0.30	-0.088	2.09	-0.100	5.92	-0.111	17.31	-0.122	56.53
-0.065	0.38	-0.090	2.46	-0.101	6.50	-0.112	19.16	-0.123	63.22
-0.070	0.56	-0.091	2.68	-0.102	7.14	-0.113	21.28	-0.124	70.97
-0.072	0.64	-0.092	2.92	-0.103	7.85	-0.114	23.62		
-0.074	0.73	-0.093	3.18	-0.104	8.63	-0.115	26.28		

z_{14} = 54 Km

Cos Z	τ_{sp}/τ_1	Cos Z	τ_{sp}/τ_1	Cos Z	τ_{sp}/τ_1	Cos Z	τ_{sp}/τ_1	Cos Z	τ_{sp}/τ_1
0.000	0.02	-0.075	0.44	-0.096	2.34	-0.112	10.87	-0.121	28.67
-0.010	0.02	-0.080	0.64	-0.098	2.80	-0.113	12.07	-0.122	32.07
-0.020	0.03	-0.082	0.74	-0.100	3.36	-0.114	13.40	-0.123	35.87
-0.030	0.04	-0.084	0.87	-0.102	4.05	-0.115	14.90	-0.124	40.26
-0.040	0.06	-0.086	1.01	-0.104	4.89	-0.116	16.57	-0.125	45.15
-0.050	0.10	-0.088	1.19	-0.106	5.95	-0.117	18.44	-0.126	50.74
-0.060	0.17	-0.090	1.40	-0.108	7.24	-0.118	20.57	-0.127	57.07
-0.065	0.21	-0.092	1.66	-0.110	8.86	-0.119	22.96	-0.128	64.18
-0.070	0.31	-0.094	1.97	-0.111	9.81	-0.120	25.65	-0.129	72.25

z_{15} = 58 Km

Cos Z	τ_{SP}/τ_1	Cos Z	τ_{SP}/τ_1	Cos Z	τ_{SP}/τ_1	Cos Z	τ_{SP}/τ_1	Cos Z	τ_{SP}/τ_1
0.000	0.01	-0.084	0.49	-0.104	2.77	-0.117	10.45	-0.127	32.37
-0.010	0.01	-0.086	0.57	-0.106	3.37	-0.118	11.66	-0.128	36.42
-0.020	0.01	-0.088	0.67	-0.108	4.10	-0.119	13.02	-0.129	40.99
-0.030	0.02	-0.090	0.79	-0.110	5.02	-0.120	14.55	-0.130	46.23
-0.040	0.04	-0.092	0.94	-0.111	5.56	-0.121	16.26	-0.131	52.15
-0.050	0.06	-0.094	1.11	-0.112	6.16	-0.122	18.19	-0.132	58.98
-0.060	0.10	-0.096	1.32	-0.113	6.84	-0.123	20.34	-0.133	66.64
-0.070	0.16	-0.098	1.56	-0.114	7.59	-0.124	22.84	-0.134	75.44
-0.080	0.26	-0.100	1.90	-0.115	8.45	-0.125	25.62		
-0.082	0.42	-0.102	2.29	-0.116	9.40	-0.126	28.78		

c_{16} = 62 Km

Cos Z	τ_{SP}/τ_1	Cos Z	τ_{SP}/τ_1	Cos Z	τ_{SP}/τ_1	Cos Z	τ_{SP}/τ_1	Cos Z	τ_{SP}/τ_1
0.000	0.01	-0.092	0.53	-0.111	3.15	-0.121	9.22	-0.131	29.60
-0.020	0.01	-0.094	0.63	-0.112	3.49	-0.122	10.32	-0.132	33.47
-0.030	0.02	-0.096	0.75	-0.113	3.88	-0.123	11.54	-0.133	37.83
-0.040	0.02	-0.098	0.90	-0.114	4.30	-0.124	12.95	-0.134	42.82
-0.050	0.03	-0.100	1.08	-0.115	4.79	-0.125	14.53	-0.135	48.53
-0.060	0.06	-0.102	1.30	-0.116	5.33	-0.126	16.33	-0.136	55.03
-0.070	0.10	-0.104	1.57	-0.117	5.93	-0.127	18.37	-0.137	62.47
-0.080	0.20	-0.106	1.91	-0.118	6.61	-0.128	20.66	-0.138	70.92
-0.085	0.30	-0.108	2.33	-0.119	7.38	-0.129	23.26		
-0.090	0.45	-0.110	2.84	-0.120	8.25	-0.130	26.23		

z_{17} = 66 km

Cos Z	τ_{SP}/τ_1	Cos Z	τ_{SP}/τ_1	Cos Z	τ_{SP}/τ_1	Cos Z	τ_{SP}/τ_1	Cos Z	τ_{SP}/τ_1
0.000	0.00	-0.094	0.36	-0.112	1.98	-0.125	8.24	-0.134	24.31
-0.010	0.01	-0.096	0.42	-0.114	2.44	-0.126	9.26	-0.135	27.55
-0.040	0.01	-0.098	0.50	-0.116	3.02	-0.127	10.42	-0.136	31.24
-0.050	0.02	-0.100	0.61	-0.118	3.75	-0.128	11.72	-0.137	35.47
-0.060	0.03	-0.102	0.74	-0.120	4.68	-0.129	13.20	-0.138	40.27
-0.070	0.06	-0.104	0.89	-0.121	5.23	-0.130	14.89	-0.139	45.76
-0.080	0.12	-0.106	1.08	-0.122	5.85	-0.131	16.80	-0.140	52.14
-0.090	0.25	-0.108	1.32	-0.123	6.54	-0.132	19.00	-0.141	59.42
-0.092	0.30	-0.110	1.61	-0.124	7.35	-0.133	21.47	-0.142	67.77

$z_{16} = 70$ Km

Cos Z	τ_{SP}/τ_1	Cos Z	τ_{SP}/τ_1	Cos Z	τ_{SP}/τ_1	Cos Z	τ_{SP}/τ_1	Cos Z	τ_{SP}/τ_1
0.000	0.00	-0.096	0.24	-0.116	1.71	-0.128	6.65	-0.138	22.87
-0.020	0.00	-0.098	0.29	-0.118	2.13	-0.129	7.49	-0.139	25.99
-0.030	0.01	-0.100	0.35	-0.120	2.65	-0.130	8.45	-0.140	29.61
-0.050	0.01	-0.102	0.42	-0.121	2.96	-0.131	9.53	-0.141	33.74
-0.060	0.02	-0.104	0.50	-0.122	3.32	-0.132	10.78	-0.142	38.49
-0.070	0.03	-0.106	0.61	-0.123	3.71	-0.133	12.19	-0.143	43.95
-0.080	0.07	-0.108	0.75	-0.124	4.17	-0.134	13.80	-0.144	50.17
-0.090	0.14	-0.110	0.91	-0.125	4.68	-0.135	15.64	-0.145	57.44
-0.092	0.17	-0.112	1.12	-0.126	5.25	-0.136	17.74	-0.146	65.76
-0.094	0.20	-0.114	1.38	-0.127	5.92	-0.137	20.14	-0.147	75.35

SECTION II

VERTICAL DISTRIBUTION OF OZONE

2.1 The problem of distribution of ozone with height in the earth's atmosphere

The ozone content of the atmosphere in different parts of the earth, is found to vary between 0.15 to 0.40 cm at N.T.P. Because of the very high absorption coefficient of ozone in the ultra-violet, this small amount of ozone present in the atmosphere has important effects (1) by causing a rise of temperature with height above 30 Km in the stratosphere and (2) protecting plant and animal life on the surface of the earth against photochemically active radiation. The study of total ozone amount and its distribution with height, is also of importance on account of its variability associated with day-to-day changes in weather. The work done by different workers on different aspects of atmospheric ozone studies has been reviewed by Fabry (1950) in "L' Ozone Atmosphérique", by Götz (1951) in the "Compendium of Meteorology" and by Prof. K.R.Ramanathan (1954) in his Presidential Address to the meeting of the International Meteorological Association.

Laboratory experiments have established several absorption bands of ozone out of which the following ones are important for the study of atmospheric ozone.

1. Hartley Band : Between 2000 Å and 3200 Å with maximum at 2553 Å. This is a very strong absorption band and is independent of temperature.

2. Huggins Band : Weak absorption bands in the region 3200 Å to 3690 Å. The absorption maxima are influenced by temperature.

3. Chappius Band : Weak absorption bands in the region 4500 Å to 7500 Å. Maximum between 5500 Å to 6200 Å. The Chappius bands are not suitable for study of atmospheric ozone because of vapour bands in the solar spectrum in this region. Taking various factors into consideration, it is found that the region 3000 Å to 3400 Å is most suitable for the studies of atmospheric ozone.

Ozone distribution with height has been studied by sending spectrographs with stratospheric balloons by Regener (1934) and recently in V-2 rocket explorations by Johnson, Purcell and Tousey (1951). These direct methods give a good picture of the variation of ozone concentration with height. However, it is practically impossible at present to adopt these methods for routine measurement of vertical distribution of ozone and one has to rely mostly on the indirect methods such as the inversion-effect of the zenith scattered light, discovered by Götz (1931).

With the help of Dobson Spectrophotometer, it is possible to measure the logarithm of the ratio of zenith scattered intensity (I) of lights of two different wave-lengths, say λ = 3112 Å and λ' = 3323 Å. (L = Log (I/I') + Const.). The first one is more strongly absorbed by ozone than the other. With the increase of solar zenith distance (Z), because of rise in the effective height of scattering for wave-length λ , the ratio Log (I/I') decreases. Once the effective height of scattering for λ , goes above the region

of maximum ozone, its intensity (I) decreases at a rate smaller than that of I'. This leads to an inversion in $L - \lambda^4$ curve which is known as Götz umkehr curve. Chapman (1934-35) theoretically derived a number of umkehr curves for different assumed ozone distributions and taking into consideration only primary scattering.

Götz, Meetham and Dobson (1934) put forward two different methods of determing vertical distribution of ozone from the observed umkehr curve. In the analytical method referred to as Method A, the atmosphere is divided in the following layers :

Altitude	Ozone amount
Above 50 Km	0, but scattering not zero
50 - 35 Km	x_1
35 - 20 Km	x_2
20 - 5 Km	$x - (x_1 + x_2 + u)$
5 - 0 Km	u

x is the total ozone amount obtained from direct sun measurements and u is taken as a fixed percentage of x from the knowledge of ozone content in the surface layers. The equation of Log (I/I') can be obtained on the basis of primary scattering for different values of z such as 0°, 80° and 90° in terms of x_1 and x_2. The solution is obtained graphically by plotting x_2 as a function of x_1 and determining the intersection of the curves for $z = 80^\circ$ and 90°.

The synthetic method or the Method B consists of starting with an assumed vertical ozone distribution and

varying it till the calculated and measured umkehr curves are in tolerably good agreement at several points. In the original method, the atmosphere was divided into a number of horizontal sections such that the mass of air in any section was $1/\sqrt{10}$ that of the section below it. The whole of the air and ozone in any section were supposed to be concentrated in a very thin layer at a suitable height above the bottom of the section. This means that in any section, ozone decreases exponentially with height. The Method B was modified by Karandikar and Ramanathan (1949). They divided the atmosphere into 9 Km layers and the center of mass of a layer was assumed to be situated at a height of 3 Km above the base of the layer. It was assumed that no ozone is present above 54 Km and there is uniform ozone distribution within the layer.

The effect of secondary scattering was considered on the experimental basis by Ramanathan, Moorthy and Kulkarni (1952) and on the theoretical grounds by Walton (1953). They showed that the effect of applying correction was to bring down some ozone to the lower part of the atmosphere. Walton (1955) has extended the theory so as to include tertiary scattering.

2.2 "<u>The calculation of vertical distribution of ozone by the data umkehr effect (Method B)</u>" by K.R.Ramanathan and J.V.Dave. Communicated to the International Ozone Commission for publication and regular use during the International Geophysical Year.

NOTE

The values of α, α' and β, β' given in Table 3 have been changed by the International Ozone Commission Circular No. 0.4 dated 5th July, 1957 and the values of α, α' found by Vigroux (1953) have been adopted. It has been decided that all ozone stations should adopt these new values simultaneously from the 1st July 1957. The new values of $(\alpha - \alpha')$ are approximately 1.36 times lower than those adopted previously. Because of the fact that what we measure by the Dobson Spectrophotometer is $(\alpha - \alpha')x$, the effect of adopting the new values of $(\alpha - \frac{\alpha'}{\lambda^4})$ is to increase the total ozone by about 36 %.

It is recommended that the present tables for calculating vertical distribution continue to be used, but if the total ozone amounts are calculated with the new $(\alpha - \alpha')$ values as given in the above Circular, the calculated ozone amount should first be divided by 1.36 before using the tables. At the end of the calculation, all the ozone values, both total as well as the amount in each layer, should be multiplied by 1.36.

THE CALCULATION OF THE VERTICAL DISTRIBUTION OF OZONE BY THE GÖTZ UMKEHR-EFFECT (METHOD B).

By

K.R.RAMANATHAN & J.V.DAVE

Physical Research Laboratory, Ahmedabad 9. India.

The present note gives the details of Method B for calculating the vertical distribution of ozone in the atmosphere from observations on the umkehr-effect. The method was originally due to Götz, Meetham and Dobson[1].

Although the method is not free from objection, it gives information of value about the changes in the vertical distribution of ozone associated with day-to-day changes in weather; it is also comparatively easy to use in clear weather at all stations equipped with a Dobson Spectrophotometer.

The measurements required are the ratios of the intensities of light of two wave-lengths from the clear zenith sky, one of which is much more absorbed by ozone than the other, for zenith distances Z of the sun varying from 40° or 60° to 90°. Considering for example, the light of two wave-lengths 3112 Å and 3323 Å (for which the decimal absorption coefficients of ozone are 1.23 and 0.08 respectively), it is found that the ratio $L = \text{Log}\left[I_{(3112)}/I_{(3323)} \right]$ in the light from the zenith

2...

sky decreases as Z increases until a value of about $86^{\circ}.5$ is reached, and then increases as Z increases to 90°.

Instead of L, one can plot $N = 100(L_o - L)$ where L_o is the value of L extrapolated for a point outside the atmosphere. It is the general practice to plot L or N against Z^4 so as to give an open scale when the sun is near the horizon.

Sample curves of N against Z^4 for $\lambda\lambda$ 3112/3323 and $\lambda\lambda$ 3054/3253 are shown in Fig. 1. (Curves C and A respectively).

The light reaching the observer from the sky in any direction is sunlight scattered by the whole column of atmosphere in that direction. It includes primary as well as multiple scattered light. If only primary scattered light from molecules is considered, it is easy to obtain an expression for the light of any wave-length reaching the observer from the zenith.

In Part I, the method is described of calculating the vertical distribution of ozone, first on the assumption that the light from the zenith sky is only primary scattered light. A short section is added explaining the effect of secondary scattered light and a method of correcting for it. A fully worked out example follows.

In Part II, supplementary tables applicable to stations at or near two higher levels, 912 mb and 810 mb are provided.

3...

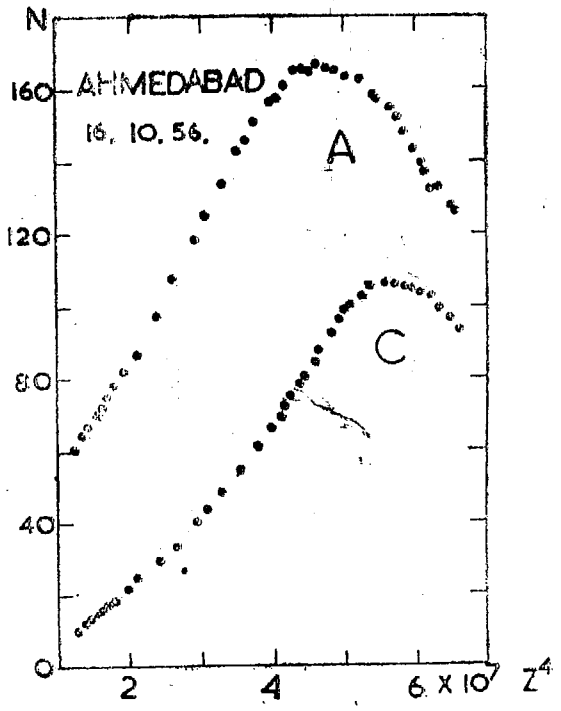

FIG.1. UMKEHR CURVES WITH DOBSON SPECTROPHOTOMETER.

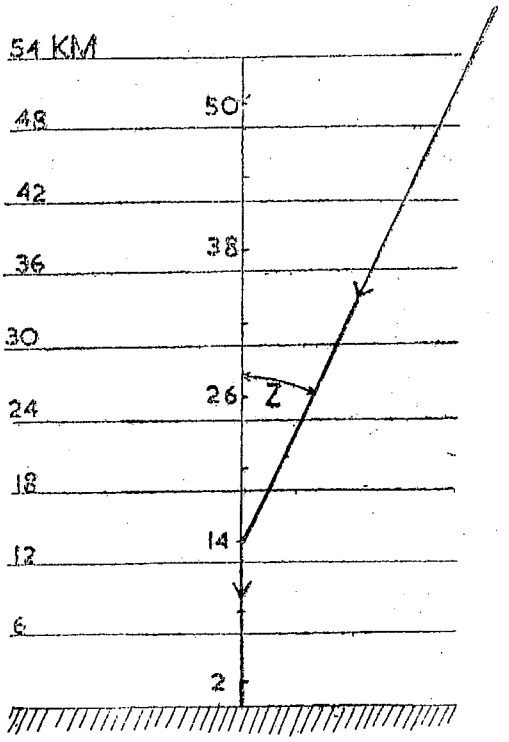

FIG.2. DIVISION OF THE ATMOSPHERE.

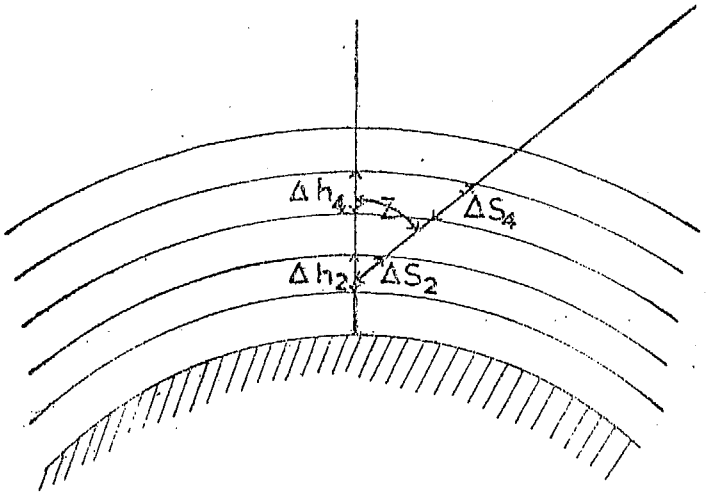

FIG.3. DIAGRAM EXPLAINING ΔS AND Δh.

I. Calculation of primary scattered light received from the zenith sky at the ground.

For calculating the light scattered vertically downward, the atmosphere is divided into layers[2]. The first layer is from the ground (1013 mb level) to 6 km. The second layer is from 6 km to 12 km. The other layers are each 6 km thick up to 54 km, above 54 km the whole atmosphere is treated as one layer.

p_o - 1013 mb.

p - Pressure at height h taken from rocket panel data. (Table 1.)

Δm_n - Mass of air in the n^{th} layer expressed as a fraction of the total mass of air in a standard atmosphere which exerts a pressure of 1013 mb at its base. The air in each 6 km layer is supposed to be concentrated at a height of 2 km above the base of the layer. These assumptions are not free from objection, but are simple and reasonably accurate.

β, β' - Decimal scattering coefficients for light of wave-lengths λ , λ' by a standard atmosphere.

α, α' - Decimal absorption coefficients of ozone for λ , λ' (per cm of ozone at S.T.P.) (Table 3).

4...

The table includes data for all the four pairs of wave-lengths normally used for ozone determination with the Ozone Spectrophotometer.

F_h - Integrated air-path from the top of the atmosphere to h (expressed as multiple of air-mass in one standard atmosphere), and from h vertically downward to the observer. (Table 4). For an observer at pressure-level p_o = 1013 mb,

$F_h = 1 + \frac{p}{p_o}\left[Ch(Z) - 1\right]$ where Ch(Z) is the Chapman function for a spherical atmosphere for zenith angle Z with the vertical through the observer. The values of Ch(Z) have been tabulated by M.V.Wilkes[3]. While considering air-mass in the slant path above a particular height h, it is to be noted that the temperature of the air in the first few kilometers above h exerts a dominant influence. The mean temperatures in the atmosphere as shown by rocket ascents have been taken as a guide in preparing Table 1A.

If the observer is located at a pressure-level kp_o instead of at p_o, the values of F_h in

5...

all rows in Table 4 except the first row (corresponding to 2 km) should be changed to

$k + \frac{p}{p_o} [Ch(Z) - 1]$. Supplementary Table 4X has been prepared for k = 0.9 and 0.8 corresponding to pressure levels 912 and 810 mb respectively. These will hold for stations at 1 km and 2 km respectively above sea level. For the lowest layer, in Table 4X, h has been taken to be 3 km above 1013 mb level. This is sufficiently accurate.

Δs - Total geometrical slant path of light in each layer.

Δh - Corresponding vertical path in the layer.

$\Delta s - \Delta h$ - have been tabulated in Table 6 for all those layers in which there is a slant path. A constant value of the radius a = 6370 km has been used. See Fig. 3. For layers in which there is only a vertical path, $\Delta s - \Delta h = 0$.

y_1, y_2, y_3 etc. upto y_9 are the ozone amounts in 10^{-3}cm/km in successive layers as we go up; it is assumed that the ozone amount above 54 km is negligible so that the total

ozone amount $x = 6y_1 + 6(y_2 + y_3 + " \ " \ " + y_9)$. The factor 6 in the first term on the right will require a small adjustment if the station is above the 1013 mb level.

The total ozone Y in the path of the light when the zenith distance of the sun is Z and the light is scattered from the n^{th} layer is given by the sum of the ozone amounts in the slant path and in the vertical path. In the n^{th} layer, part of the path is vertical and part slant.

$$Y = \sum_{n}^{9} y_r \Delta s_r + \sum_{1}^{n} y_r \Delta h_r$$

$$= \sum_{n}^{9} y_r (\Delta s_r - \Delta h_r) + \sum_{1}^{9} y_r \Delta h_r$$

$$= Y_n + x$$

Tables 6 provide the values of $\Delta s - \Delta h$ for calculating Y_n for the light scattered from each layer and for different zenith distances of the sun ranging from 37° to 90°. An example of the calculation of Y is given in Table 8.

The intensities of the primary scattered light of wave-length λ for the n^{th} layer at the ground is given by $\Delta I_n = K . \beta . \Delta m_n \times 10^{-\beta F - \alpha Y}$ where K is a constant depending on the value of Z. and I the total intensity from all the layers is given by

7...

$$I = \sum \Delta I_n = K.\beta. \sum_{1}^{10} \left[\Delta m_n \times 10^{-\beta F - \alpha Y} \right]$$

The ratio of the intensities of the primary scattered light of two wave-lengths λ and λ' from the zenith sky is given by

$$\frac{I}{I'} = \frac{\beta}{\beta'} \frac{\sum_{1}^{10} \left[\Delta m_n \times 10^{-\beta F - \alpha Y} \right]}{\sum_{1}^{10} \left[\Delta m_n \times 10^{-\beta' F - \alpha' Y} \right]}$$

The values of Log $\Delta m_n - \beta F$ for different layers and Z required in the computation of Log(I'/I) are given in Tables 5A, B, C and D corresponding to different pairs of wave-lengths.

Forms I, II and III are for computing Log(I'/I) for any assumed ozone distribution and for making changes in it corresponding to small changes in the distribution. These are given at the end.

By the method of successive approximation, the ozone amounts in the different layers are so adjusted that the calculated values of Log(I'/I) agree with the calculated values at four or five points of the umkehr curve within the limits of experimental error. In practice, a constant is added to the calculated value of Log(I'/I) so that the calculated and the observed values coincide at some fixed zenith distance like 60°,

8...

where the intensity is determined mainly by the total amount of ozone and not by its distribution. 70°, 75°, 80°, 84°, $86^{\circ}.5$, 88° and 90° are convenient points to choose for fitting the curves.

Correction for Secondary Scattering

In the above, account is taken only of the primary scattered light from the molecules of the atmosphere. But the air is illuminated not only by direct sunlight but also by light scattered once or more by the rest of the atmosphere and by the ground. Neglect of the illumination of the air column by diffused light would be justified if the ratio of the intensities of light of two different wave-lengths (which is the quantity actually measured) gave with sufficient accuracy the ratio of the primary scattered light only of the same two radiations for different zenith distances of the sun.

A little consideration shows that this assumption is not justified. Of the light of two wave-lenths under comparison, one is much more absorbed by ozone than the other, and consequently, the contributions from the different layers of the atmosphere to the total primary-scattered light from the zenith are different, and vary differently with the zenith

9...

distance of the sun. The multiple scattering which is dependent on the distribution in height of the primary scattered light will naturally differ for the two wave-lengths.

Let P, P' be the intensities of primary scattered light of the two wave-lengths λ, λ' from the zenith, and M, M' the intensities of the multiple scattered light.

What we measure with the spectrophotometer is Log I/I' for different solar zenith distances.

Now $$\frac{I}{I'} = \frac{P + M}{P' + M'} = \frac{P\ (\ 1 + M/P\ )}{P'\ (\ 1 + M'/P'\ )}$$

We could correct the I/I' curve to give the P/P' curve if we knew the values of M/P and M'/P' for different zenith distances of the sun.

G.F.Walton[4] has calculated the intensities of primary (P) and secondary (S) scattered light from the zenith sky for different altitudes of the sun. After evaluating S/P for appropriate values of α and β for a few simple distributions of ozone with total ozone amounts of 0.30 and 0.18 cm, he has calculated the corrections to be applied to the observed intensity-ratios to convert them to what they would be if there were only primary scattering. He found that the corrections

10...

varied with the zenith distance of the sun, but were nearly constant when sec Z was between 5 and 20. The effect of correcting for the secondary scattering was to lower the C.C. of the ozone by 2 to 3 km.

Ramanathan, Koorty and Kulkarni[5] obtained similar results by deriving umkehr curves for I(3112)/I(3075) from the observed umkehr curves of I(3112)/I(3323) and I(3075)/I(3278). The object of using the derived curve was to compare the intensities of two wave-lengths both of which are pretty strongly absorbed by ozone; in that case, the assumption $I/I' = P/P'$ would be more nearly correct. They came to the same conclusion as Walton viz., that the effect of taking multiple scattering into account was to increase the ozone amount in the layers below the maximum of ozone and to reduce it at higher levels.

Although there are still a few unsolved questions about the correction required for multiple scattering, it is believed that Table 7 provides for different solar zenith distances, reasonable corrections when the ozone amount is between 0.18 and 0.30 cm.

11...

Table 1

Pressure at different heights above sea-level

(From rocket-panel data)

Height km	Pressure mb	Height km	Pressure mb
0	1013	44	1.90
2	803.5	48	1.15
6	487.5	50	0.902
8	372.4	54	0.547
12	206.5	56	0.426
14	150.7	60	0.254
18	78.5	62	0.194
20	56.9	66	0.111
24	30.5	68	0.082
26	22.5	72	0.045
30	12.5	74	0.033
32	9.31	78	0.017
36	5.32	80	0.012
38	4.07	84	0.007
42	2.43		

12...

Table 1 A

Values of Ch(Z) adopted for different values of h(km) and of Z(degrees). The rocket temperatures at h to h + 10(km) have been taken into consideration in tabulating these.

h \ Z	37	60	70	75	80	84	86.5	88	90
2,3	1.251	1.993	2.90	3.80	5.55	8.73	13.3	18.7	35.5
8	"	"	"	3.81	5.58	8.84	13.6	19.5	38.7
14,20	"	"	"	3.81	5.59	8.87	13.7	19.7	39.7
26,32	"	"	"	3.81	5.57	8.81	13.5	19.2	37.6
38,44,50	"	"	"	3.80	5.55	8.73	13.3	18.7	35.5
56	"	"	"	3.80	5.56	8.77	13.4	19.0	36.6
62	"	"	"	3.81	5.57	8.81	13.5	19.2	37.6
68	"	"	"	3.81	5.59	8.87	13.7	19.7	39.7

13...

Table 2

Logarithm of the mass of air in different layers expressed as fraction of the mass in a vertical column of the std. atmosphere.

Layer	Log Δm_n	Layer	Log Δm_n
0-6	$\bar{1}.715$	42-48	$\bar{3}.100$
6-12	$\bar{1}.443$	48-54	$\bar{4}.778$
12-18	$\bar{1}.101$	54-60	$\bar{4}.461$
18-24	$\bar{2}.676$	60-66	$\bar{4}.149$
24-30	$\bar{2}.250$	66-72	$\bar{5}.820$
30-36	$\bar{3}.848$	72-78	$\bar{5}.431$
36-42	$\bar{3}.455$	78-84	$\bar{5}.000$

Table 3

Decimal absorption coefficients of ozone and scattering coefficients of atmosphere for light of different pairs of wave-lengths.

	λ/λ'	α	α'	β	β'	Log(β/β')
A	3054/3253	2.58	0.16	0.503	0.384	0.1173
B	3085/3291	1.77	0.12	0.481	0.365	0.1198
C	3112/3323	1.23	0.08	0.464	0.350	0.1224
D	3175/3399	0.54	0.02	0.425	0.318	0.1260

α, α' refer to 1 cm of ozone at S.T.P. and β, β' to an atmosphere which exerts a pressure of 1013 mb at its base.

14 ...

Table 4

Values of F_h - Integrated air path (expressed as multiple of one standard atmosphere) from the top of the atmosphere to the level of primary scattering and from that level to the observer at p_o = 1013 mb.

h \ Z	37°	60°	70°	75°	80°	84°	86.5	88°	90°
2	1.199	1.788	2.505	3.221	4.610	7.133	10.748	15.032	28.342
8	1.092	1.365	1.699	2.033	2.684	3.882	5.635	7.786	14.859
14	1.037	1.148	1.283	1.418	1.683	2.171	2.887	3.778	6.751
20	1.014	1.056	1.107	1.158	1.258	1.441	1.713	2.049	3.172
26	1.006	1.022	1.042	1.062	1.101	1.173	1.278	1.404	1.813
32	1.002	1.009	1.017	1.026	1.042	1.072	1.115	1.167	1.337
38	1.001	1.004	1.008	1.011	1.018	1.031	1.049	1.071	1.139
44	1.000	1.002	1.004	1.005	1.009	1.015	1.023	1.033	1.065
50	1.000	1.001	1.002	1.002	1.004	1.007	1.011	1.016	1.031
56	1.000	1.000	1.001	1.001	1.002	1.003	1.005	1.008	1.015
62	1.000	1.000	1.000	1.001	1.001	1.001	1.002	1.003	1.007
68	1.000	1.000	1.000	1.000	1.000	1.001	1.001	1.001	1.003
74	1.000	1.000	1.000	1.000	1.000	1.000	1.000	1.001	1.001
80	1.000	1.000	1.000	1.000	1.000	1.000	1.000	1.000	1.000

$$F_h = 1 + \frac{p}{p_o}\left[Ch\,(Z) - 1\right]$$

Table 5A

$\log \Delta m_n - \beta F$ β (3054) = 0.503

Z \ n	1	2	3	4	5	6	7	8	9	10
37	$\bar{1}.112$	$\bar{2}.894$	$\bar{2}.579$	$\bar{2}.166$	$\bar{3}.744$	$\bar{3}.344$	$\bar{4}.951$	$\bar{4}.597$	$\bar{4}.275$	$\bar{4}.228$
60	$\bar{2}.816$	$\bar{2}.756$	$\bar{2}.524$	$\bar{2}.145$	$\bar{3}.736$	$\bar{3}.340$	$\bar{4}.950$	$\bar{4}.596$	$\bar{4}.274$	$\bar{4}.228$
70	$\bar{2}.455$	$\bar{2}.588$	$\bar{2}.456$	$\bar{2}.119$	$\bar{3}.726$	$\bar{3}.336$	$\bar{4}.948$	$\bar{4}.595$	$\bar{4}.274$	$\bar{4}.228$
75	$\bar{2}.095$	$\bar{2}.420$	$\bar{2}.388$	$\bar{2}.094$	$\bar{3}.716$	$\bar{3}.332$	$\bar{4}.946$	$\bar{4}.594$	$\bar{4}.274$	$\bar{4}.228$
80	$\bar{3}.396$	$\bar{2}.093$	$\bar{2}.254$	$\bar{2}.043$	$\bar{3}.696$	$\bar{3}.324$	$\bar{4}.943$	$\bar{4}.592$	$\bar{4}.273$	$\bar{4}.228$
84	$\bar{4}.127$	$\bar{3}.490$	$\bar{2}.009$	$\bar{3}.951$	$\bar{3}.660$	$\bar{3}.309$	$\bar{4}.936$	$\bar{4}.589$	$\bar{4}.271$	$\bar{4}.225$
86.5	$\bar{6}.309$	$\bar{4}.609$	$\bar{3}.649$	$\bar{3}.814$	$\bar{3}.607$	$\bar{3}.287$	$\bar{4}.927$	$\bar{4}.585$	$\bar{4}.269$	$\bar{4}.225$
88	$\bar{8}.154$	$\bar{5}.527$	$\bar{3}.201$	$\bar{3}.645$	$\bar{3}.544$	$\bar{3}.261$	$\bar{4}.916$	$\bar{4}.580$	$\bar{4}.267$	$\bar{4}.225$
90	$\bar{15}.459$	$\bar{9}.969$	$\bar{5}.705$	$\bar{3}.080$	$\bar{3}.338$	$\bar{3}.175$	$\bar{4}.882$	$\bar{4}.564$	$\bar{4}.259$	$\bar{4}.223$

$\bar{4}.461$

16...

Table 5A (contd)

Log $\Delta m_n - \beta' F$ $\qquad$ $\beta'(3253) = 0.384$

Z \ n	1	2	3	4	5	6	7	8	9	10
37	$\bar{1}.255$	$\bar{1}.024$	$\bar{2}.703$	$\bar{2}.287$	$\bar{3}.864$	$\bar{3}.463$	$\bar{3}.071$	$\bar{4}.716$	$\bar{4}.394$	$\bar{4}.346$
60	$\bar{1}.028$	$\bar{2}.919$	$\bar{2}.660$	$\bar{2}.270$	$\bar{3}.858$	$\bar{3}.461$	$\bar{3}.069$	$\bar{4}.715$	$\bar{4}.394$	$\bar{4}.346$
70	$\bar{2}.753$	$\bar{2}.791$	$\bar{2}.608$	$\bar{2}.251$	$\bar{3}.850$	$\bar{3}.457$	$\bar{3}.068$	$\bar{4}.714$	$\bar{4}.393$	$\bar{4}.346$
75	$\bar{2}.478$	$\bar{2}.662$	$\bar{2}.556$	$\bar{2}.231$	$\bar{3}.842$	$\bar{3}.454$	$\bar{3}.067$	$\bar{4}.714$	$\bar{4}.393$	$\bar{4}.346$
80	$\bar{3}.945$	$\bar{2}.412$	$\bar{2}.455$	$\bar{2}.193$	$\bar{3}.827$	$\bar{3}.448$	$\bar{3}.064$	$\bar{4}.713$	$\bar{4}.392$	$\bar{4}.346$
84	$\bar{4}.976$	$\bar{3}.952$	$\bar{2}.267$	$\bar{2}.123$	$\bar{3}.800$	$\bar{3}.436$	$\bar{3}.059$	$\bar{4}.710$	$\bar{4}.391$	$\bar{4}.346$
86.5	$\bar{5}.588$	$\bar{3}.279$	$\bar{3}.992$	$\bar{2}.018$	$\bar{3}.759$	$\bar{3}.420$	$\bar{3}.052$	$\bar{4}.707$	$\bar{4}.390$	$\bar{4}.346$
88	$\bar{7}.943$	$\bar{4}.453$	$\bar{3}.650$	$\bar{3}.389$	$\bar{3}.711$	$\bar{3}.400$	$\bar{3}.044$	$\bar{4}.703$	$\bar{4}.388$	$\bar{4}.346$
90	$\bar{12}.832$	$\bar{7}.737$	$\bar{4}.509$	$\bar{3}.458$	$\bar{3}.554$	$\bar{3}.335$	$\bar{3}.018$	$\bar{4}.691$	$\bar{4}.382$	$\bar{4}.344$

Table 5B

Log $\Delta m_n - \beta F$ $\qquad$ $\beta(3085) = 0.481$

Z \ n	1	2	3	4	5	6	7	8	9	10
37	$\bar{1}.138$	$\bar{2}.918$	$\bar{2}.602$	$\bar{2}.188$	$\bar{3}.766$	$\bar{3}.366$	$\bar{4}.974$	$\bar{4}.619$	$\bar{4}.297$	$\bar{4}.255$
60	$\bar{2}.855$	$\bar{2}.786$	$\bar{2}.549$	$\bar{2}.168$	$\bar{3}.758$	$\bar{3}.363$	$\bar{4}.972$	$\bar{4}.618$	$\bar{4}.297$	$\bar{4}.255$
70	$\bar{2}.510$	$\bar{2}.626$	$\bar{2}.484$	$\bar{2}.144$	$\bar{3}.749$	$\bar{3}.359$	$\bar{4}.970$	$\bar{4}.617$	$\bar{4}.296$	$\bar{4}.255$
75	$\bar{2}.166$	$\bar{2}.465$	$\bar{2}.419$	$\bar{2}.119$	$\bar{3}.739$	$\bar{3}.354$	$\bar{4}.969$	$\bar{4}.617$	$\bar{4}.296$	$\bar{4}.255$
80	$\bar{3}.498$	$\bar{2}.152$	$\bar{2}.291$	$\bar{2}.071$	$\bar{3}.720$	$\bar{3}.347$	$\bar{4}.965$	$\bar{4}.615$	$\bar{4}.295$	$\bar{4}.253$
84	$\bar{4}.284$	$\bar{3}.576$	$\bar{2}.057$	$\bar{3}.983$	$\bar{3}.686$	$\bar{3}.332$	$\bar{4}.959$	$\bar{4}.612$	$\bar{4}.294$	$\bar{4}.253$
86.5	$\bar{6}.545$	$\bar{4}.733$	$\bar{3}.712$	$\bar{3}.852$	$\bar{3}.635$	$\bar{3}.312$	$\bar{4}.950$	$\bar{4}.608$	$\bar{4}.292$	$\bar{4}.250$
88	$\bar{8}.485$	$\bar{5}.698$	$\bar{3}.284$	$\bar{3}.690$	$\bar{3}.575$	$\bar{3}.287$	$\bar{4}.940$	$\bar{4}.603$	$\bar{4}.289$	$\bar{4}.250$
90	$\bar{14}.082$	$\bar{8}.296$	$\bar{5}.854$	$\bar{3}.150$	$\bar{3}.378$	$\bar{3}.205$	$\bar{4}.907$	$\bar{4}.588$	$\bar{4}.282$	$\bar{4}.248$

Table 5B (contd.)

$\log \Delta m_n - \beta' F$ $\qquad$ $\beta'(3291) = 0.365$

Z \ n	1	2	3	4	5	6	7	8	9	10
37	$\bar{1}.277$	$\bar{1}.044$	$\bar{2}.722$	$\bar{2}.306$	$\bar{3}.883$	$\bar{3}.487$	$\bar{3}.090$	$\bar{4}.735$	$\bar{4}.413$	$\bar{4}.369$
60	$\bar{1}.062$	$\bar{2}.945$	$\bar{2}.682$	$\bar{2}.291$	$\bar{3}.877$	$\bar{3}.480$	$\bar{3}.089$	$\bar{4}.734$	$\bar{4}.413$	$\bar{4}.369$
70	$\bar{2}.801$	$\bar{2}.823$	$\bar{2}.633$	$\bar{2}.272$	$\bar{3}.870$	$\bar{3}.477$	$\bar{3}.087$	$\bar{4}.734$	$\bar{4}.412$	$\bar{4}.369$
75	$\bar{2}.539$	$\bar{2}.701$	$\bar{2}.583$	$\bar{2}.253$	$\bar{3}.862$	$\bar{3}.474$	$\bar{3}.086$	$\bar{4}.733$	$\bar{4}.412$	$\bar{4}.369$
80	$\bar{2}.032$	$\bar{2}.463$	$\bar{2}.487$	$\bar{2}.217$	$\bar{3}.848$	$\bar{3}.468$	$\bar{3}.083$	$\bar{4}.732$	$\bar{4}.412$	$\bar{4}.369$
84	$\bar{3}.111$	$\bar{2}.026$	$\bar{2}.309$	$\bar{2}.150$	$\bar{3}.822$	$\bar{3}.457$	$\bar{3}.079$	$\bar{4}.730$	$\bar{4}.410$	$\bar{4}.369$
86.5	$\bar{5}.792$	$\bar{3}.386$	$\bar{2}.047$	$\bar{2}.051$	$\bar{3}.784$	$\bar{3}.441$	$\bar{3}.072$	$\bar{4}.727$	$\bar{4}.409$	$\bar{4}.367$
88	$\bar{6}.228$	$\bar{4}.601$	$\bar{3}.722$	$\bar{3}.928$	$\bar{3}.738$	$\bar{3}.422$	$\bar{3}.064$	$\bar{4}.723$	$\bar{4}.407$	$\bar{4}.367$
90	$\bar{11}.370$	$\bar{6}.019$	$\bar{4}.637$	$\bar{3}.518$	$\bar{3}.588$	$\bar{3}.360$	$\bar{3}.039$	$\bar{4}.711$	$\bar{4}.402$	$\bar{4}.362$

Table 5C

$\text{Log } \Delta m_n - \beta F$ $\qquad \beta(3112) = 0.464$

Z \ n	1	2	3	4	5	6	7	8	9	10
37	$\bar{1}.159$	$\bar{2}.936$	$\bar{2}.620$	$\bar{2}.206$	$\bar{3}.783$	$\bar{3}.383$	$\bar{4}.991$	$\bar{4}.636$	$\bar{4}.314$	$\bar{4}.267$
60	$\bar{2}.885$	$\bar{2}.810$	$\bar{2}.568$	$\bar{2}.186$	$\bar{3}.776$	$\bar{3}.380$	$\bar{4}.989$	$\bar{4}.635$	$\bar{4}.314$	$\bar{4}.267$
70	$\bar{2}.553$	$\bar{2}.655$	$\bar{2}.506$	$\bar{2}.162$	$\bar{3}.767$	$\bar{3}.376$	$\bar{4}.987$	$\bar{4}.634$	$\bar{4}.313$	$\bar{4}.267$
75	$\bar{2}.220$	$\bar{2}.500$	$\bar{2}.443$	$\bar{2}.139$	$\bar{3}.757$	$\bar{3}.372$	$\bar{4}.986$	$\bar{4}.634$	$\bar{4}.313$	$\bar{4}.267$
80	$\bar{3}.576$	$\bar{2}.198$	$\bar{2}.320$	$\bar{2}.092$	$\bar{3}.739$	$\bar{3}.365$	$\bar{4}.983$	$\bar{4}.632$	$\bar{4}.312$	$\bar{4}.267$
84	$\bar{4}.405$	$\bar{3}.642$	$\bar{2}.094$	$\bar{2}.007$	$\bar{3}.706$	$\bar{3}.351$	$\bar{4}.977$	$\bar{4}.629$	$\bar{4}.311$	$\bar{4}.267$
86.5	$\bar{6}.728$	$\bar{4}.828$	$\bar{3}.761$	$\bar{3}.881$	$\bar{3}.657$	$\bar{3}.331$	$\bar{4}.968$	$\bar{4}.625$	$\bar{4}.309$	$\bar{4}.267$
88	$\bar{8}.740$	$\bar{5}.830$	$\bar{3}.348$	$\bar{3}.725$	$\bar{3}.599$	$\bar{3}.307$	$\bar{4}.958$	$\bar{4}.621$	$\bar{4}.307$	$\bar{4}.265$
90	$\bar{14}.564$	$\bar{8}.548$	$\bar{5}.969$	$\bar{3}.204$	$\bar{3}.409$	$\bar{3}.228$	$\bar{4}.927$	$\bar{4}.606$	$\bar{4}.300$	$\bar{4}.265$

Table 5C (contd.)

Log $\Delta m_n - \beta' F$ $\qquad$ $\beta'(3323) = 0.350$

Z \ n	1	2	3	4	5	6	7	8	9	10
37	$\bar{1}.295$	$\bar{1}.061$	$\bar{2}.738$	$\bar{2}.321$	$\bar{3}.898$	$\bar{3}.497$	$\bar{3}.105$	$\bar{4}.750$	$\bar{4}.428$	$\bar{4}.382$
60	$\bar{1}.089$	$\bar{2}.965$	$\bar{2}.699$	$\bar{2}.306$	$\bar{3}.892$	$\bar{3}.495$	$\bar{3}.104$	$\bar{4}.749$	$\bar{4}.428$	$\bar{4}.382$
70	$\bar{2}.838$	$\bar{2}.848$	$\bar{2}.652$	$\bar{2}.289$	$\bar{3}.885$	$\bar{3}.492$	$\bar{3}.102$	$\bar{4}.749$	$\bar{4}.427$	$\bar{4}.382$
75	$\bar{2}.588$	$\bar{2}.731$	$\bar{2}.605$	$\bar{2}.271$	$\bar{3}.878$	$\bar{3}.489$	$\bar{3}.101$	$\bar{4}.748$	$\bar{4}.427$	$\bar{4}.382$
80	$\bar{2}.101$	$\bar{2}.504$	$\bar{2}.512$	$\bar{2}.236$	$\bar{3}.865$	$\bar{3}.483$	$\bar{3}.099$	$\bar{4}.747$	$\bar{4}.427$	$\bar{4}.382$
84	$\bar{3}.218$	$\bar{2}.084$	$\bar{2}.341$	$\bar{2}.172$	$\bar{3}.839$	$\bar{3}.473$	$\bar{3}.094$	$\bar{4}.745$	$\bar{4}.426$	$\bar{4}.382$
86.5	$\bar{5}.953$	$\bar{3}.471$	$\bar{2}.091$	$\bar{2}.076$	$\bar{3}.803$	$\bar{3}.458$	$\bar{3}.088$	$\bar{4}.742$	$\bar{4}.424$	$\bar{4}.382$
88	$\bar{6}.454$	$\bar{4}.718$	$\bar{3}.779$	$\bar{3}.959$	$\bar{3}.759$	$\bar{3}.440$	$\bar{3}.080$	$\bar{4}.738$	$\bar{4}.422$	$\bar{4}.380$
90	$\bar{11}.795$	$\bar{6}.242$	$\bar{4}.738$	$\bar{3}.566$	$\bar{3}.615$	$\bar{3}.380$	$\bar{3}.056$	$\bar{4}.727$	$\bar{4}.417$	$\bar{4}.378$

Table 5 D

$\log \Delta m_n - \beta F$ $\qquad \beta (3175) = 0.425$

Z \ n	1	2	3	4	5	6	7	8	9	10
37	$\bar{1}.205$	$\bar{2}.979$	$\bar{2}.660$	$\bar{2}.245$	$\bar{3}.822$	$\bar{3}.422$	$\bar{3}.030$	$\bar{4}.675$	$\bar{4}.353$	$\bar{4}.312$
60	$\bar{2}.955$	$\bar{2}.863$	$\bar{2}.613$	$\bar{2}.227$	$\bar{3}.816$	$\bar{3}.419$	$\bar{3}.028$	$\bar{4}.674$	$\bar{4}.353$	$\bar{4}.312$
70	$\bar{2}.650$	$\bar{2}.721$	$\bar{2}.556$	$\bar{2}.206$	$\bar{3}.807$	$\bar{3}.416$	$\bar{3}.027$	$\bar{4}.673$	$\bar{4}.352$	$\bar{4}.312$
75	$\bar{2}.346$	$\bar{2}.579$	$\bar{2}.498$	$\bar{2}.184$	$\bar{3}.799$	$\bar{3}.412$	$\bar{3}.025$	$\bar{4}.673$	$\bar{4}.352$	$\bar{4}.312$
80	$\bar{3}.756$	$\bar{2}.302$	$\bar{2}.386$	$\bar{2}.141$	$\bar{3}.782$	$\bar{3}.405$	$\bar{3}.022$	$\bar{4}.671$	$\bar{4}.351$	$\bar{4}.310$
84	$\bar{4}.683$	$\bar{3}.793$	$\bar{2}.178$	$\bar{2}.064$	$\bar{3}.751$	$\bar{3}.392$	$\bar{3}.017$	$\bar{4}.669$	$\bar{4}.350$	$\bar{4}.310$
86.5	$\bar{5}.147$	$\bar{3}.048$	$\bar{3}.874$	$\bar{3}.948$	$\bar{3}.707$	$\bar{3}.375$	$\bar{3}.009$	$\bar{4}.665$	$\bar{4}.348$	$\bar{4}.310$
88	$\bar{7}.326$	$\bar{4}.134$	$\bar{3}.495$	$\bar{3}.805$	$\bar{3}.653$	$\bar{3}.352$	$\bar{3}.000$	$\bar{4}.661$	$\bar{4}.346$	$\bar{4}.310$
90	$\bar{13}.670$	$\bar{7}.128$	$\bar{4}.232$	$\bar{3}.328$	$\bar{3}.479$	$\bar{3}.280$	$\bar{4}.971$	$\bar{4}.647$	$\bar{4}.340$	$\bar{4}.308$

Table 5D (contd.)

$\log \Delta m_n - \beta' F$ $\qquad$ $\beta'(3399) = 0.318$

Z \ n	1	2	3	4	5	6	7	8	9	10
37	$\bar{1}.334$	$\bar{1}.096$	$\bar{2}.771$	$\bar{2}.354$	$\bar{3}.930$	$\bar{3}.529$	$\bar{3}.137$	$\bar{4}.782$	$\bar{4}.460$	$\bar{4}.417$
60	$\bar{1}.146$	$\bar{1}.009$	$\bar{2}.736$	$\bar{2}.340$	$\bar{3}.925$	$\bar{3}.527$	$\bar{3}.136$	$\bar{4}.781$	$\bar{4}.460$	$\bar{4}.417$
70	$\bar{2}.918$	$\bar{2}.903$	$\bar{2}.693$	$\bar{2}.324$	$\bar{3}.919$	$\bar{3}.525$	$\bar{3}.134$	$\bar{4}.781$	$\bar{4}.459$	$\bar{4}.417$
75	$\bar{2}.691$	$\bar{2}.797$	$\bar{2}.650$	$\bar{2}.308$	$\bar{3}.912$	$\bar{3}.522$	$\bar{3}.134$	$\bar{4}.780$	$\bar{4}.459$	$\bar{4}.417$
80	$\bar{2}.249$	$\bar{2}.589$	$\bar{2}.566$	$\bar{2}.276$	$\bar{3}.900$	$\bar{3}.517$	$\bar{3}.131$	$\bar{4}.779$	$\bar{4}.459$	$\bar{4}.417$
84	$\bar{3}.447$	$\bar{2}.209$	$\bar{2}.411$	$\bar{2}.218$	$\bar{3}.877$	$\bar{3}.507$	$\bar{3}.127$	$\bar{4}.777$	$\bar{4}.458$	$\bar{4}.417$
86.5	$\bar{4}.297$	$\bar{3}.651$	$\bar{2}.183$	$\bar{2}.131$	$\bar{3}.844$	$\bar{3}.493$	$\bar{3}.121$	$\bar{4}.775$	$\bar{4}.457$	$\bar{4}.415$
88	$\bar{6}.935$	$\bar{4}.967$	$\bar{3}.900$	$\bar{2}.024$	$\bar{3}.804$	$\bar{3}.477$	$\bar{3}.114$	$\bar{4}.772$	$\bar{4}.455$	$\bar{4}.415$
90	$\bar{10}.702$	$\bar{6}.718$	$\bar{4}.954$	$\bar{3}.667$	$\bar{3}.673$	$\bar{3}.423$	$\bar{3}.093$	$\bar{4}.761$	$\bar{4}.450$	$\bar{4}.412$

Table 6

$\Delta s - \Delta h$ for different Z and h

$Z = 37^\circ$

Layer \ n	1	2	3	4	5	6	7	8	9	y_n in 10^{-3} cm/km
54-48	1.4	1.4	1.5	1.5	1.5	1.5	1.5	1.5	1.0	y_9 =
48-42	1.4	1.5	1.5	1.5	1.5	1.5	1.5	1.0	-	y_8 =
42-36	1.5	1.5	1.5	1.5	1.5	1.5	1.0	-	-	y_7 =
36-30	1.5	1.5	1.5	1.5	1.5	1.0	-	-	-	y_6 =
30-24	1.5	1.5	1.5	1.5	1.0	-	-	-	-	y_5 =
24-18	1.5	1.5	1.5	1.0	-	-	-	-	-	y_4 =
18-12	1.5	1.5	1.0	-	-	-	-	-	-	y_3 =
12- 6	1.5	1.0	-	-	-	-	-	-	-	y_2 =
6- 0	1.0	-	-	-	-	-	-	-	-	y_1 =

$Z = 60^\circ$

54-48	5.7	5.7	5.7	5.8	5.8	5.9	5.9	5.9	4.0	y_9 =
48-42	5.7	5.7	5.8	5.8	5.9	5.9	5.9	4.0	-	y_8 =
42-36	5.7	5.8	5.8	5.9	5.9	5.9	4.0	-	-	y_7 =
36-30	5.8	5.8	5.9	5.9	5.9	4.0	-	-	-	y_6 =
30-24	5.8	5.9	5.9	5.9	4.0	-	-	-	-	y_5 =
24-18	5.9	5.9	5.9	4.0	-	-	-	-	-	y_4 =
18-12	5.9	5.9	4.0	-	-	-	-	-	-	y_3 =
12- 6	5.9	4.0	-	-	-	-	-	-	-	y_2 =
6- 0	4.0	-	-	-	-	-	-	-	-	y_1 =

24...

Table 6 (contd.)

$Z = 70^{\circ}$

Layer \ n	1	2	3	4	5	6	7	8	9	y_n in 10^{-3} cm/km
54-48	10.5	10.6	10.7	10.9	11.0	11.1	11.3	11.4	7.6	y_9 =
48-42	10.6	10.7	10.9	11.0	11.1	11.3	11.4	7.6	-	y_8 =
42-36	10.7	10.9	11.0	11.1	11.3	11.4	7.6	-	-	y_7 =
36-30	10.9	11.0	11.1	11.3	11.4	7.6	-	-	-	y_6 =
30-24	11.0	11.1	11.3	11.4	7.6	-	-	-	-	y_5 =
24-18	11.1	11.3	11.4	7.6	-	-	-	-	-	y_4 =
18-12	11.3	11.4	7.6	-	-	-	-	-	-	y_3 =
12- 6	11.4	7.6	-	-	-	-	-	-	-	y_2 =
6- 0	7.6	-	-	-	-	-	-	-	-	y_1 =

$Z = 75^{\circ}$

54-48	14.9	15.2	15.4	15.6	16.0	16.2	16.5	16.8	11.4	y_9 =
48-42	15.2	15.4	15.6	16.0	16.2	16.5	16.8	11.4	-	y_8 =
42-36	15.4	15.6	16.0	16.2	16.5	16.8	11.4	-	-	y_7 =
36-30	15.6	16.0	16.2	16.5	16.8	11.4	-	-	-	y_6 =
30-24	16.0	16.2	16.5	16.8	11.4	-	-	-	-	y_5 =
24-18	16.2	16.5	16.8	11.4	-	-	-	-	-	y_4 =
18-12	16.5	16.8	11.4	-	-	-	-	-	-	y_3 =
12- 6	16.8	11.4	-	-	-	-	-	-	-	y_2 =
6- 0	11.4	-	-	-	-	-	-	-	-	y_1 =

Table 6 (contd.)

$Z = 80^{\circ}$

Layer \ n	1	2	3	4	5	6	7	8	9	y_n in 10^{-3} cm/km
5 -40	22.1	22.7	23.4	24.0	24.8	25.6	26.5	27.3	18.8	y_9 =
4 -42	22.7	23.4	24.0	24.8	25.6	26.5	27.3	18.8	-	y_8 =
4 -36	23.4	24.0	24.8	25.6	26.5	27.3	18.8	-	-	y_7 =
3 -30	24.0	24.8	25.6	26.5	27.3	18.8	-	-	-	y_6 =
3 -24	24.8	25.6	26.5	27.3	18.8	-	-	-	-	y_5 =
2 -18	25.6	26.5	27.3	18.8	-	-	-	-	-	y_4 =
1 -12	26.5	27.3	18.8	-	-	-	-	-	-	y_3 =
1 - 6	27.3	18.8	-	-	-	-	-	-	-	y_2 =
0 - 0	18.8	-	-	-	-	-	-	-	-	y_1 =

$Z = 84^{\circ}$

8	31.0	32.4	34.0	35.8	37.8	40.2	43.0	46.4	33.2	y_9 =
2	32.4	34.0	35.8	37.8	40.2	43.0	46.4	33.2	-	y_8 =
6	34.0	35.8	37.8	40.2	43.0	46.4	33.2	-	-	y_7 =
0	35.8	37.8	40.2	43.0	46.4	33.2	-	-	-	y_6 =
4	37.8	40.2	43.0	46.4	33.2	-	-	-	-	y_5 =
8	40.2	43.0	46.4	33.2	-	-	-	-	-	y_4 =
2	43.0	46.4	33.2	-	-	-	-	-	-	y_3 =
6	46.4	33.2	-	-	-	-	-	-	-	y_2 =
0	33.2	-	-	-	-	-	-	-	-	y_1 =

26...

Table 6 (contd.)

$Z = 86^{\circ}.5$

Layer \ n	1	2	3	4	5	6	7	8	9	y_n in 10^{-3} cm/km
54-48	37	40	42	46	50	55	62	72	57	y_9 =
48-42	40	42	46	50	55	62	72	57	-	y_8 =
42-36	42	46	50	55	62	72	57	-	-	y_7 =
36-30	46	50	55	62	72	57	-	-	-	y_6 =
30-24	50	55	62	72	57	-	-	-	-	y_5 =
24-18	55	62	72	57	-	-	-	-	-	y_4 =
18-12	62	72	57	-	-	-	-	-	-	y_3 =
12- 6	72	57	-	-	-	-	-	-	-	y_2 =
6- 0	57	-	-	-	-	-	-	-	-	y_1 =

$Z = 88^{\circ}$

54-48	41	44	47	51	57	65	77	98	91	y_9 =
48-42	44	47	51	57	65	77	98	91	-	y_8 =
42-36	47	51	57	65	77	98	91	-	-	y_7 =
36-30	51	57	65	77	98	91	-	-	-	y_6 =
30-24	57	65	77	98	91	-	-	-	-	y_5 =
24-18	65	77	98	91	-	-	-	-	-	y_4 =
18-12	77	98	91	-	-	-	-	-	-	y_3 =
12- 6	98	91	-	-	-	-	-	-	-	y_2 =
6- 0	91	-	-	-	-	-	-	-	-	y_1 =

27...

Table 6 (contd.)

$Z = 90^{\circ}$

Layer \ n	1	2	3	4	5	6	7	8	9	y_n in 10^{-3} cm/km
54-48	42	46	50	55	62	72	89	125	222	y_9 =
48-42	46	50	55	62	72	89	125	222	-	y_8 =
42-36	50	55	62	72	89	125	222	-	-	y_7 =
36-30	55	62	72	89	125	222	-	-	-	y_6 =
30-24	62	72	89	125	222	-	-	-	-	y_5 =
24-18	72	89	125	222	-	-	-	-	-	y_4 =
18-12	89	125	222	-	-	-	-	-	-	y_3 =
12- 6	125	222	-	-	-	-	-	-	-	y_2 =
6- 0	222	-	-	-	-	-	-	-	-	y_1 =

28...

Table 7

Correction for secondary scattering (Provisional). Amount to be subtracted from values of $N(Z) - N(60^\circ)$ when observations are made with C λ λ'.

Z	60	70	75	80	84	86.5	88	90
Subtract to correct for secondary scattering.	0.0	1.0	2.0	4.5	6.0	6.0	6.0	6.0

Example

An example showing the calculation of Log(I'/I) is given below: It relates to an umkehr curve obtained at Ahmedabad on 16-10-56 with C pair of wave-lengths. The total ozone amount was 0.192 cm. The values of N observed on light scattered from the clear zenith sky are given in Table 9B.

A trial distribution was assumed to start with; this was based on a general knowledge of average distribution corresponding to 0.192 cm. The values of y (in 10^{-3}cm/km) assumed to exist in layers 1 to 9, were

0, 0.5, 0.5, 5.5, 12.0, 8.0, 3.8, 1.4, 0.3.

In Table 8, is shown an example of calculating $Y = Y_n + x$, the total ozone in the path of the light when the zenith distance of the sun was $86^{\circ}.5$.

Using these values of Y and Form I, the values of Log(I'/I)= - L were computed for different values of Z. An example is shown for $Z = 86^{\circ}.5$. As we are interested only in the relative values of L, or of N which is equal to $100(L_o - L)$ when Z changes, the computed value of 100 Log(I'/I) at 60° has a correction added to it so that it becomes identical with the observed values of N at 60°. The same correction term is added

30...

Table 8

Example showing calculation of ozone path Y for $\theta = 86^{\circ}.5$; x = 0.192 cm.

Trial ozone distn.	y_1 0.0	y_2 0.5	y_3 0.5	y_4 5.5	y_5 12.0	y_6 8.0	y_7 3.8	y_8 1.4	y_9 0.3	
Layer	1	2	3	4	5	6	7	8	9	10
9	.0111	.0120	.0126	.0138	.0150	.0165	.0186	.0216	.0171	.0000
8	.0560	.0588	.0644	.0700	.0770	.0868	.1008	.0798	.000	.0000
7	.1596	.1748	.1900	.2090	.2356	.2736	.2166	.0000	.000	.0000
6	.3680	.4000	.4400	.4960	.5760	.4560	.0000	.0000	.000	.0000
5	.6000	.6600	.7440	.8640	.6840	.0000	.0000	.0000	.0000	.0000
4	.3025	.3410	.3960	.3135	.0000	.0000	.0000	.0000	.0000	.0000
3	.0310	.0360	.0285	.0000	.0000	.0000	.0000	.0000	.0000	.0000
2	.0360	.0285	.0000	.0000	.0000	.0000	.0000	.0000	.0000	.0000
1	.0000	.0000	.0000	.0000	.0000	.0000	.0000	.0000	.0000	.0000
Y_n	1.5642	1.7111	1.8755	1.9663	1.5876	0.8329	0.3360	0.101	0.0171	0.0000
$Y = Y_n + x$	1.756	1.903	2.067	2.158	1.780	1.025	0.528	0.293	0.209	0.192

Similar calculations of Y_n and Y are to be made for other values of Z.

Table 9 A.

Trial distribution and changes in trial distribution. The y's are in units of 10^{-3} cm/km.

Layer	1	2	3	4	5	6	7	8	9
Trial distn.	0.0	0.5	0.5	5.5	12.0	8.0	3.8	1.4	0.3
Δ y(a)							-0.1		0.1
Δ y(b)	0.5	0.5	2.0	-2.0	-1.0		-0.1		0.1
Δ y(c)	0.5	1.5	1.0	-2.0	-1.0		-0.1		0.1
Final distn.	0.5	2.0	1.5	3.5	11.0	8.0	3.7	1.4	0.4

Table 9 B.

Observed and calculated values of N for different values of Z and for various ozone distributions.

Z (degrees)	60	70	75	80	84	86.5	88	90
$Z^4 \times 10^{-7}$	1.30	2.40	3.16	4.10	4.98	5.60	6.00	6.56
Observed N	32.0	51.0	67.5	92.2	119.3	126.3	124.5	113.0
N according to trial distn.	32.0	52.7	70.4	96.5	120.6	127.0	123.2	108.9
Δ y(a)	32.0				120.7	127.2	123.8	110.3
Δ y(b)	32.0	51.8	69.0	93.9	118.3	127.0	124.9	112.2
Δ y(c)	32.0	51.8	68.6	93.5	117.9	126.9	124.7	112.4

32...

Table 9 C

Example showing correction due to secondary scattering and its effect.

Layer	1	2	3	4	5	6	7	8	9
y_n	2.0	2.0	3.0	3.7	10.0	7.0	3.2	0.9	0.2
Z	60	70	75	80	84	86.5	88	90	
Observed N corrected for Sec. Scattering	32.0	50.0	65.5	87.7	113.3	120.3	118.5	107.0	
Calculated N	32.0	51.0	66.5	89.0	111.6	120.5	119.2	106.5	

33...

Form I for computing Log(I'/I) for given ozone distribution

Date: 16-10-56 Station: Ahmedabad $Z = 86^{\circ}.5$ $\lambda / \lambda' = C$ $\alpha = 1.23$ $\alpha' = 0.08$ $x = 0.192$ cm.

n	1	2	3	4	5	6	7	8	9	10
y_n	0.0	0.5	0.5	5.5	12.0	8.0	3.8	1.4	0.3	-
Y_n										
x										
$Y = Y_n + x$	1.756	1.903	2.067	2.158	1.780	1.025	0.528	0.293	0.209	0.192
Log $\Delta m_n - \beta F$	$\bar{6}.728$	$\bar{4}.828$	$\bar{3}.761$	$\bar{3}.881$	$\bar{3}.657$	$\bar{3}.331$	$\bar{4}.968$	$\bar{4}.625$	$\bar{4}.309$	$\bar{4}.267$
αY	2.160	2.341	2.543	2.654	2.189	1.261	0.649	0.360	0.257	0.236
D	$\bar{8}.568$	$\bar{6}.487$	$\bar{5}.217$	$\bar{5}.227$	$\bar{5}.468$	$\bar{4}.070$	$\bar{4}.319$	$\bar{4}.265$	$\bar{4}.052$	$\bar{4}.031$
Antilog D	$.0_3000$	$.0_3003$	$.0_3016$	$.0_3017$	$.0_3029$	$.0_3118$	$.0_3208$	$.0_3184$	$.0_3113$	$.0_3107$

$D = \text{Log } \Delta m_n - \beta F - \alpha Y.$ $\qquad I = \sum \Delta I_n = K \beta \sum \text{Antilog } D = 0.0_3795\ K \beta.$

Log $\Delta m_n - \beta' F$	$\bar{5}.953$	$\bar{3}.471$	$\bar{2}.091$	$\bar{2}.076$	$\bar{3}.803$	$\bar{3}.458$	$\bar{3}.088$	$\bar{4}.742$	$\bar{4}.424$	$\bar{4}.382$
$\alpha' Y$	0.140	0.152	0.165	0.173	0.142	0.082	0.042	0.023	0.017	0.015
D'	$\bar{5}.813$	$\bar{3}.319$	$\bar{3}.926$	$\bar{3}.903$	$\bar{3}.661$	$\bar{3}.376$	$\bar{3}.046$	$\bar{4}.719$	$\bar{4}.407$	$\bar{4}.367$
Antilog D'	$.0_2007$	$.0_2208$	$.0_2843$	$.0_2800$	$.0_2458$	$.0_2238$	$.0_2111$	$.0_2052$	$.0_2026$	$.0_2023$

$D' = \text{Log } \Delta m_n - \beta' F - \alpha' Y.$ $\qquad I' = \sum \Delta I'_n = K \beta' \sum \text{Antilog } D' = 0.0277\ K \beta'.$

Log $I = \bar{4}.900 + \text{Log } K\beta$. $\qquad$ Log $I' = \bar{2}.443 + \text{Log } K\beta'$.

Log $(I'/I) = 1.543 - \text{Log } (\beta / \beta') = 1.421$ $\qquad$ 100 Log $(I'/I) = 142.1$

Form II for computing Log(I'/I) for a changed initial distribution

ate: 16-10-56 Station: Ahmedabad Z = 86°.5 $\lambda / \lambda' = C$ $\alpha = 1.23$ $\alpha' = 0.08$ x = 0.192 cm.

n	1	2	3	4	5	6	7	8	9	10
ange in y_n	-	-	-	-	-	-	-0.1	-	+0.1	-
		+0.004	+0.004	+0.005	+0.005	+0.006	+0.006	+0.007	+0.006	0.000
ΔY		-0.005	-0.005	-0.006	-0.006	-0.007	-0.006	-	-	-
		-0.001	-0.001	-0.001	-0.001	-0.001	0.000	+0.007	+0.006	0.000
(from Form I)		$\bar{6}.487$	$\bar{5}.217$	$\bar{5}.227$	$\bar{5}.468$	$\bar{4}.070$	$\bar{4}.319$	$\bar{4}.265$	$\bar{4}.052$	$\bar{4}.031$
$\alpha \Delta Y$		-0.001	-0.001	-0.001	-0.001	-0.001	0.000	+0.009	+0.007	0.000
$- \alpha \Delta Y$		$\bar{6}.488$	$\bar{5}.218$	$\bar{5}.228$	$\bar{5}.469$	$\bar{4}.071$	$\bar{4}.319$	$\bar{4}.256$	$\bar{4}.045$	$\bar{4}.031$
ntilog$(D - \alpha \Delta Y)$	$.0_3000$	$0._3003$	$.0_3017$	$.0_3017$	$.0_3029$	$.0_3118$	$.0_3208$	$.0_3180$	$.0_3111$	$.0_3107$

$= \sum \Delta I_n = K \beta \sum$ Antilog $(D - \alpha \Delta Y) = 0.0_3790\ K \beta$. Log I = $\bar{4}.898$ + Log K β.

' (from Form I)								$\bar{4}.719$		
$\alpha' \Delta Y$	0.000	0.000	0.000	0.000	0.000	0.000	+0.001	0.000	0.000	
$' - \alpha' \Delta Y$								$\bar{4}.718$		
ntilog$(D' - \alpha' \Delta Y)$								$.0_2052$		

$' = \sum \Delta I'_n = K \beta' \sum$ Antilog$(D' - \alpha' \Delta Y) = 0.0277\ K \beta'$. Log I' = $\bar{2}.443$ + Log K β'.

100 Log(I'/I) = 142.3

to the computed values for all other angles also. We thus get a computed (constant-L) or N curve which can be compared with the observed curve. A sample calculation is shown in Tables 9A and 9B and Forms I and II.

The values of N calculated according to the trial distribution and adjusted so that the observed and calculated values coincide at 60°, are entered in row 4 of Table 9B. It will be noticed that the computed values are significantly lower at 90° and significantly higher at 75° and 80°. The first defect can be remedied by adding a small amount of ozone at the top. To remedy the second defect, some ozone has to be brought down from the middle layers to the bottom layers. These changes in distribution are made in successive approximation. Form II is used for computing changed Log(I'/I).

Considering the scatter of values in the observed umkehr curve, it was considered that the values in the last row of Table 9B were sufficiently satisfactory and that the distribution given in the last row of Table 9A accepted as the distribution, provided the zenith skylight was assumed to be due only to primary scattering.

The observed values given in row 3 of Table 9B were corrected for secondary scattering according to Table 7. The

36...

new distribution to fit the corrected observed curve and the corresponding calculated values of N are given in Table 9C.

The following hints may be of some help in making the changes in distribution.

(1) With an assumed trial distribution, calculate Log(I'/I) at Z = 60°. Add an appropriate constant to this so as to make it equal to the observed value of N/100 at 60°.

(2) Calculate Log(I'/I) for 90° and 88°, and apply the same correction. If the calculated value is too high, remove a little ozone from the top layer to layer 6 or 7. If it is too low, add some ozone to the top. A small change at the top will make a large difference in N(90°) and N(88°). Get agreement at 88° and 90° to within 2 units of N.

(3) Calculate Log(I'/I) for 86°.5, 84° and 75° and add the same correction to each. Adjust ozone in the middle and lower layers so as to get satisfactory agreement at all the points.

37...

II Supplementary Tables for use at stations situated at about 912-mb level and at 810-mb level.

The main modifications in the tables for a station at $0.9\ p_o$ (= 912 mb) and at $0.8\ p_o$ (= 810 mb) are given below. It is assumed that the values of $\underline{h}$ in both these cases may be taken to be 3 km instead of 2 km. This is sufficiently accurate for the present purpose. The air mass in the first layer (ground to 6 km) should be changed as given in Table 2X.

If the pressure at the station-level is kp_o, the value of F is given by

$$F = k + \frac{p}{p_o} \left[Ch(Z) - 1 \right]$$

The first row of Table 4 for F_h corresponding to the lowest layer is changed as shown in Table 4X. The values of F_h in all the other rows are decreased by 0.100 when the station is at or near 912 mb, and by 0.200 when it is at or near 810 mb.

For stations at or near 912 mb and 810 mb respectively, the values of Log $\Lambda\ m_n - \beta F$ in the second columns of tables 5A to 5D (corresponding to the lowest layer) require the changes given in Tables 5A (X) to 5D (X). For stations upto a height of 2.5 km, the tables for the nearest pressure-level may be used without appreciable error.

For the succeeding layers 2, 3, 4 etc., the values of Log $\Delta m_n - \beta F$ tabulated in Tables 5A to 5D should be increased by $(1 - k)\beta$ for a station at pressure level kp_o. Thus, for a station at 912 mb level, all the values in the third column of Table 5A should be increased by $0.100\,\beta$, and for a station at the 810 mb level, by $0.200\,\beta$. An example is given in Table 5A(X) for the second and third layers.

The values of $\Delta s - \Delta h$ in the second column of Table 6 corresponding to the first layer requires a small and rather insignificant change, due to the raising of the centre of the layer from 2 to 3 km. These changes for each value of Z are tabulated in Table 6X.

It is recommended that each station should modify tables for regular use at the station.

39...

Table 2X

p_o	Log Δm_n
1013 mb	$\bar{1}.715$
912 mb	$\bar{1}.622$
810 mb	$\bar{1}.503$

The Δm's in the other layers remain the same as in Table 2.

40...

Table 4A

p_o mb	h \ Z	37°	60°	70°	75°	80°	84°	86°5	88°	90°
1013	2	1.199	1.788	2.505	3.221	4.610	7.133	10.748	15.032	28.342
912	3	1.076	1.597	2.232	2.866	4.095	6.329	9.529	13.320	25.101
810	3	0.976	1.497	2.132	2.766	3.995	6.229	9.429	13.220	25.001

Table 5A(X) Log Δm_n - βF for the lowest layer

Z	λ = 3054			λ' = 3253		
	1013 mb	912 mb	810 mb	1013 mb	912 mb	810 mb
37	$\bar{1}$.112	$\bar{1}$.081	$\bar{1}$.012	$\bar{1}$.255	$\bar{1}$.209	$\bar{1}$.128
60	$\bar{2}$.816	$\bar{2}$.819	$\bar{2}$.750	$\bar{1}$.028	$\bar{1}$.009	$\bar{2}$.928
70	$\bar{2}$.455	$\bar{2}$.499	$\bar{2}$.431	$\bar{2}$.753	$\bar{2}$.765	$\bar{2}$.684
75	$\bar{2}$.095	$\bar{2}$.180	$\bar{2}$.112	$\bar{2}$.478	$\bar{2}$.521	$\bar{2}$.441
80	$\bar{3}$.396	$\bar{3}$.562	$\bar{3}$.494	$\bar{3}$.945	$\bar{2}$.050	$\bar{3}$.969
84	$\bar{4}$.127	$\bar{4}$.439	$\bar{4}$.370	$\bar{4}$.976	$\bar{3}$.192	$\bar{3}$.111
86.5	$\bar{6}$.309	$\bar{6}$.829	$\bar{6}$.760	$\bar{5}$.588	$\bar{5}$.963	$\bar{5}$.882
88	$\bar{8}$.154	$\bar{8}$.922	$\bar{8}$.853	$\bar{7}$.943	$\bar{6}$.507	$\bar{6}$.427
90	$\bar{15}$.459	$\bar{14}$.996	$\bar{14}$.927	$\bar{12}$.832	$\bar{11}$.983	$\bar{11}$.903

Table 5B(X) Log Δm_n - βF for the lowest layer

Z	λ = 3085			λ' = 3291		
	1013 mb	912 mb	810 mb	1013 mb	912 mb	810 mb
37	$\bar{1}$.138	$\bar{1}$.104	$\bar{1}$.034	$\bar{1}$.277	$\bar{1}$.229	$\bar{1}$.147
60	$\bar{2}$.855	$\bar{2}$.854	$\bar{2}$.783	$\bar{1}$.062	$\bar{1}$.039	$\bar{2}$.957
70	$\bar{2}$.510	$\bar{2}$.548	$\bar{2}$.478	$\bar{2}$.801	$\bar{2}$.807	$\bar{2}$.725
75	$\bar{2}$.166	$\bar{2}$.243	$\bar{2}$.173	$\bar{2}$.539	$\bar{2}$.576	$\bar{2}$.493
80	$\bar{3}$.498	$\bar{3}$.652	$\bar{3}$.581	$\bar{2}$.032	$\bar{2}$.127	$\bar{2}$.045
84	$\bar{4}$.284	$\bar{4}$.578	$\bar{4}$.507	$\bar{3}$.111	$\bar{3}$.312	$\bar{3}$.229
86.5	$\bar{6}$.545	$\bar{5}$.039	$\bar{6}$.968	$\bar{5}$.792	$\bar{4}$.144	$\bar{4}$.061
88	$\bar{8}$.485	$\bar{7}$.215	$\bar{7}$.144	$\bar{6}$.228	$\bar{6}$.760	$\bar{6}$.678
90	$\bar{14}$.082	$\bar{13}$.548	$\bar{13}$.478	$\bar{11}$.370	$\bar{10}$.460	$\bar{10}$.378

42...

Table 5C(X) Log $\Delta m_n - \beta F$ for the lowest layer

Z	λ = 3112			λ' = 3323		
	1013 mb	912 mb	810 mb	1013 mb	912 mb	810 mb
37	$\bar{1}.159$	$\bar{1}.123$	$\bar{1}.050$	$\bar{1}.295$	$\bar{1}.245$	$\bar{1}.161$
60	$\bar{2}.885$	$\bar{2}.881$	$\bar{2}.808$	$\bar{1}.089$	$\bar{1}.063$	$\bar{2}.979$
70	$\bar{2}.553$	$\bar{2}.586$	$\bar{2}.514$	$\bar{2}.838$	$\bar{2}.841$	$\bar{2}.757$
75	$\bar{2}.220$	$\bar{2}.292$	$\bar{2}.220$	$\bar{2}.588$	$\bar{2}.619$	$\bar{2}.535$
80	$\bar{3}.576$	$\bar{3}.722$	$\bar{3}.649$	$\bar{2}.101$	$\bar{2}.189$	$\bar{2}.105$
84	$\bar{4}.405$	$\bar{4}.685$	$\bar{4}.613$	$\bar{3}.218$	$\bar{3}.407$	$\bar{3}.323$
86.5	$\bar{6}.728$	$\bar{5}.201$	$\bar{5}.128$	$\bar{5}.953$	$\bar{4}.287$	$\bar{4}.203$
88	$\bar{8}.740$	$\bar{7}.442$	$\bar{7}.369$	$\bar{6}.454$	$\bar{6}.960$	$\bar{6}.876$
90	$\bar{14}.564$	$\bar{13}.975$	$\bar{13}.903$	$\bar{11}.795$	$\bar{10}.837$	$\bar{10}.753$

Table 5D(X) Log $\Delta m_n - \beta F$ for the lowest layer

Z	λ = 3175			λ' = 3399		
	1013 mb	912 mb	810 mb	1013 mb	912 mb	810 mb
37	$\bar{1}.205$	$\bar{1}.165$	$\bar{1}.088$	$\bar{1}.334$	$\bar{1}.280$	$\bar{1}.193$
60	$\bar{2}.955$	$\bar{2}.943$	$\bar{2}.867$	$\bar{1}.146$	$\bar{1}.114$	$\bar{1}.027$
70	$\bar{2}.650$	$\bar{2}.673$	$\bar{2}.597$	$\bar{2}.918$	$\bar{2}.912$	$\bar{2}.825$
75	$\bar{2}.346$	$\bar{2}.404$	$\bar{2}.327$	$\bar{2}.691$	$\bar{2}.711$	$\bar{2}.623$
80	$\bar{3}.756$	$\bar{3}.882$	$\bar{3}.805$	$\bar{2}.249$	$\bar{2}.320$	$\bar{2}.233$
84	$\bar{4}.683$	$\bar{4}.932$	$\bar{4}.856$	$\bar{3}.447$	$\bar{3}.609$	$\bar{3}.522$
86.5	$\bar{5}.147$	$\bar{5}.572$	$\bar{5}.496$	$\bar{4}.297$	$\bar{4}.592$	$\bar{4}.505$
88	$\bar{7}.326$	$\bar{7}.961$	$\bar{7}.884$	$\bar{6}.935$	$\bar{5}.386$	$\bar{5}.299$
90	$\bar{13}.670$	$\bar{12}.954$	$\bar{12}.878$	$\bar{10}.702$	$\bar{9}.640$	$\bar{9}.553$

43...

Table 5A(I)

Log $\Delta m_n - \beta F$ for second and higher layers for a station at 810 mb.

	$\lambda = 3054$ $0.200\beta = 0.101$		$\lambda' = 3253$ $0.200\beta' = 0.077$		
n / Z	2	etc..	2	3	etc..
37	$\bar{2}.995$	$\bar{2}.680$	$\bar{1}.101$	$\bar{2}.780$	
60	$\bar{2}.857$	$\bar{2}.625$	$\bar{2}.996$	$\bar{2}.737$	
70	$\bar{2}.689$	$\bar{2}.557$	$\bar{2}.868$	$\bar{2}.685$	
75	$\bar{2}.521$	$\bar{2}.489$	$\bar{2}.739$	$\bar{2}.633$	
80	$\bar{2}.194$	$\bar{2}.355$	$\bar{2}.489$	$\bar{2}.532$	
84	$\bar{3}.591$	$\bar{2}.110$	$\bar{2}.029$	$\bar{2}.344$	
86.5	$\bar{4}.710$	$\bar{3}.750$	$\bar{3}.356$	$\bar{2}.069$	
88	$\bar{5}.628$	$\bar{3}.302$	$\bar{4}.530$	$\bar{3}.727$	
90	$\bar{8}.070$	$\bar{5}.806$	$\bar{7}.814$	$\bar{4}.586$	

44...

Table 6X

$\Delta s - \Delta h$ for the first layer when the centre is at 3 km.

Layer \ Z	37	60	70	75	80	84	86.5	88	90
54-48	1.4	5.7	10.5	14.9	22.1	31.1	37	42	43
48-42	1.4	5.7	10.6	15.2	22.7	32.6	40	45	47
42-36	1.4	5.8	10.7	15.4	23.4	34.2	43	48	51
36-30	1.4	5.8	10.9	15.7	24.2	36.1	46	52	56
30-24	1.5	5.8	11.0	16.0	24.9	38.2	51	58	63
24-18	1.5	5.9	11.1	16.3	25.8	40.6	56	67	74
18-12	1.5	5.9	11.3	16.5	26.6	43.6	63	79	93
12- 6	1.5	5.9	11.5	16.9	27.5	47.0	75	103	137
6- 0	0.8	3.0	5.7	8.5	14.1	25.1	43	71	193

45...

R E F E R E N C E S

1. Götz, F.W.P., Meetham, A.R. and Dobson, G.M.B.,
Proc. Roy. Soc., A, 1934, 145, p. 416.

2. Karandikar, R.V. and Ramanathan, K.R.,
Proc. Ind. Acad. Sci., A, 1949, 29, p. 330.

3. Wilkes, M.V.,
Proc. Phys. Soc., B, 1954, 67, p. 304.

4. Walton, G.F.,
I.U.G.G. General Assembly, Bruxelles - 1953,
Proces-Verbaux IAM, p. 316.

5. Ramanathan, K.R., Moorty, Bh.V.R. and Kulkarni, R.N.,
Quart. Journ. Roy. Met. Soc., 1952, 78, p. 625.

oooOOOOOOooo

2.3 Importance of modified Method B in studying the vertical distribution of ozone in the lower atmosphere

While working out a few vertical distributions of ozone by Method B as described in article 2.2, it was observed that the ozone content of the first four or five layers could be fixed within 0.5 unit (one unit = 10^{-3} cm/km) and that of the upper layers within 0.1 to 0.2 of a unit. Again, it was found necessary to put a smaller ozone amount in 12 - 18 Km layer than in 8 - 12 Km in order to have a tolerable fit at 70°, 75° and 80°. Hence it was considered worthwhile to study this minimum in greater detail for a few instances.

Before taking the vertical distribution obtained by Method B as granted, it is necessary to keep the following points in mind :-

1. A complete observation of the umkehr curve is spread over a period of three to four hours and neither the total ozone nor its vertical distribution can be expected to remain unchanged.

2. The effect of forward scattering by large particles of dust and haze is likely to be more pronounced for solar zenith angles up to 60° or 70°, specially for low level stations and hazy skies.

3. The assumptions involved in Method B.

4. Neglect of the effect of higher orders of scattering and scattering by large particles of dust and haze.

Hence it is desirable to have the vertical distribution of ozone obtained by this indirect method tested by direct measurements in a few instances.

Two sets of observations were selected and analysed to study the variation in the vertical distribution of ozone. (1) during different parts of the year and (2) during the period when there were large changes in total ozone amount.

The first set was selected from the observations taken by Mr. R.M.Kulkarni, M.Sc., during the year 1952. Since Mr. Kulkarni selected 70° as the starting point for analysis, the observed Umkehr curves were extrapolated to 60° in some cases. The second set was selected from the observations taken by Mr. S.S.Degaonkar, M.Sc., during the period 1954-55. All the observations were taken at Mt. Abu with Dobson Spectrophotometer No. 39.

The vertical distributions of ozone for four different months during 1952 as obtained by Mr. Kulkarni using the old 9 Km method, are presented in Table 10 A and those obtained by the modified method are given in Table 10 B. Only the primary scattered radiation is taken into consideration in both the cases.

From Table 10 A, it can be seen that there is no appreciable change in the ozone content of the layers between 0 and 18 Km, and 27 and 54 Km. Any change in the ozone content is due to the changes in the layer 18 - 27 Km. On the other hand, the results given in Table 10 B bring forward the following points :-

Table 10

Vertical distribution of ozone in different months during 1952 (A) as analysed by Mr. Kulkarni - 9 Km steps. (M.Sc. thesis submitted by him to Gujarat University in 1953) and (B) by the modified method B (6 Km steps). Observations by Mr. Kulkarni.

	25-3-52		13-4-52		24-9-52		5-11-52	
x in cm / Layer	0.173		0.183		0.162		0.158	
(A) 9 Km steps								
54-45 Km	0.4	0.017	0.2	0.015	0.4	0.016	0.3	0.015
45-36 Km	1.5		1.5		1.4		1.4	
36-27 Km	7.2	0.147	7.2	0.158	7.4	0.137	7.2	0.134
27-18 Km	9.1		10.3		7.8		7.7	
18- 9 Km	1.0	0.009	1.0	0.009	1.0	0.009	1.0	0.009
9- 0 Km	0.0		0.0		0.0		0.0	
(B) 6 Km steps								
54-48 Km	0.2		0.2		0.2		0.1	
48-42 Km	0.8	0.022	1.0	0.023	0.8	0.019	0.8	0.019
42-36 Km	2.7		2.6		2.2		2.3	
36-30 Km	6.3		5.2		6.3		6.0	
30-24 Km	9.5	0.128	14.2	0.160	9.2	0.129	8.5	0.116
24-18 Km	5.5		7.3		6.0		4.8	
16-12 Km	2.0		0.0		0.5		0.0	
12- 6 Km	1.0	0.023	0.0	0.000	1.0	0.014	2.1	0.023
6- 1 Km	1.0		0.0		1.0		2.1	

1. The ozone content between 36 - 54 Km is slightly higher in the summer months of March and April than that for the months of September and November.

2. The ozone content between 18 - 36 Km and specifically between 24 - 30 Km shows an increase with increase in total ozone amount. This is in confirmity of the results given in Table 10 A.

3. Unlike the results seen in Table 10 A, the ozone amount from the ground to 18 Km, shows large variations from day-to-day. The ozone content of the surface layer (1 to 6 Km) is minimum in April and maximum in November. Again the height distribution of ozone below 18 Km is found to vary considerably. This would be expected if there is occasional transfer of stratospheric ozone into the troposphere followed by turbulent diffusion.

A sudden increase in total ozone amount was observed at Mt. Abu, Ahmedabad and New Delhi on 2nd March 1955. At Mt. Abu, it shot up from 0.180 cm on the 1st to 0.210 cm on 2nd March. Afterwards, it showed a gradual fall and attained a value of 0.175 cm on the 6th March. The umkehr observations at Abu during this period as analysed by Mr. Degaonkar using the old 9 Km method are given in Table 11 A. The distribution as obtained from the modified method, is presented in Table 11 B. The secondary scattering corrections have been applied in both the cases (Walton, Table 7, Section II).

Table 11

Vertical distribution of ozone at Mt. Abu during the period 2 to 6th March 1955. (A) analysed by Mr. Deganonkar with 9 Km steps. (M.Sc. thesis submitted by him to the Gujarat University in 1955) and (B) by the modified method (6 Km steps). Observations by Mr. Deganonkar.

Layer \ x in cm.	2-3-55	3-3-55	4-3-55	6-3-55
	0.210	0.194	0.184	0.175
(A) 9 Km steps				
54-45 Km	0.2	0.4	0.2	0.2
45-36 Km	1.0 — 0.011	1.0 — 0.013	1.1 — 0.012	1.0 — 0.011
36-27 Km	5.7	6.4	6.0	6.2
27-18 Km	9.4 — 0.136	8.8 — 0.137	8.2 — 0.128	8.0 — 0.128
18- 9 Km	3.5	3.0	3.5	2.5
9- 0 Km	3.5 — 0.063	2.0 — 0.045	1.5 — 0.045	1.5 — 0.036
(B) 6 Km steps				
54-48 Km	0.1	0.2	0.3	0.2
48-42 Km	0.8 — 0.018	0.7 — 0.019	0.6 — 0.017	0.7 — 0.016
42-36 Km	2.1	2.2	1.9	1.7
36-30 Km	4.1	6.1	4.4	4.9
30-24 Km	9.5 — 0.124	8.5 — 0.126	10.0 — 0.122	9.6 — 0.126
24-18 Km	7.0	6.5	6.0	6.5
18-12 Km	5.0 →	3.5 →	2.0 →	1.0
12- 6 Km	3.5 — 0.009	3.0 — 0.049	3.0 — 0.045	2.0 — 0.033
6- 1 Km	3.5	2.0	3.0	3.0

The results of computation presented in Tables 11 A and B are in good agreement for heights above 18 Km. The sudden increase of the total ozone amount on 2nd March, can be attributed to a large influx of ozone into the troposphere. The gradual decrease observed on the following days, is presumably due to destruction of ozone at ground and downward transport from upper troposphere. A gradual decrease of ozone in 12 - 18 Km layer can be seen clearly from Table 11 B. A gradual increase in the afternoon surface ozone at Ahmedabad was observed during this period (Please see Section III).

2.4 Secondary and multiple scattered light corrections to the observed umkehr curve

Secondary scattering corrections to be applied to the observed umkehr curve given in Table 7 (Section II) were calculated by Walton for a plane-parallel infinite atmosphere of finite optical thickness and on the assumption that ozone is concentrated in one or two thin layers. Since a good part of the umkehr curve is related to very low altitudes of the sun, it was considered desirable to study the effect of the curvature of the atmosphere and of the actual distribution of ozone, on the ratio R_2/R_1 of secondary and primary scattered radiations.

2.41 Effect of the curvature of the atmosphere

The method of computing secondary scattered radiation for a curved atmosphere has been described in article 1.2 while treating the problem of the intensity and polarisation of the sky during twilight. For computing the secondary scattered

radiation E_2 (i.e. $E_{2n} + E_{2t}$) received by an observer at the ground, it is necessary to compute the secondary emission B_2 (i.e. $B_{2n} + B_{2t}$) at different points in the direction of observation. Neglecting the anisotropy of the molecules, the equation of B_2 can be written down from Eqs. 10 to 16 (article 1.2) as follows :-

$$B_2 = \frac{3\sigma}{16\pi} \iint \left\{ \left(\cos^2 \chi_{nn'} + \cos^2 \chi_{tn'} \right) + \cos^2 \psi' \left(\cos^2 \chi_{nt'} + \cos^2 \chi_{tt'} \right) \right\} \times R_{1n'} \times \sin\vartheta' \, d\vartheta' \, d\phi'$$

for a given solar zenith angle z_0 and the height (b_n) of the point Q above the observer for which B_2 is to be calculated.

For the curved earth, the variation of $R_{1n'}$ with Cos ϕ' (shown in Fig. 5, article 1.2) will be much more pronounced and non-linear for shorter wave-lengths and in the presence of a strong absorbing layer. On the other hand, for a plane-parallel atmosphere, $R_{1n'}$ is constant and its value may be taken as that for $\phi' = 90^0$ (plane perpendicular to the principal plane through the sun). The integral

$$\int_0^{2\pi} \left\{ \left(\cos^2 \chi_{nn'} + \cos^2 \chi_{tn'} \right) + \cos^2 \psi' \left(\cos^2 \chi_{nt'} + \cos^2 \chi_{tt'} \right) \right\} R_{1n'} \, d\phi'$$

was calculated (A) by taking into consideration the variation of $R_{1n'}$ with ϕ', corresponding to the case of the actual earth and (B) taking $R_{1n'}$ as constant over ϕ' and taking its value as that for $\phi' = 90^0$ which corresponds to the case of a plane-parallel earth. The method of computation used was similar to that adopted for twilight work, but in this case the atmosphere was divided into 9 Km layers and the centre of gravity of the layer taken at a height of 3 Km above the

base of the layer.

The results of computation by both the methods are presented in Table 12, for $\lambda = 3112$ Å and $Z_0 = 88^0$. The effect of a thin layer of ozone containing 0.180 cm of ozone at N.T.P. and situated at a height of 27 Km above sea-level, was also considered. Proper allowances were made for reduction in intensity whenever the direct or the scattered light travelled through the ozone layer. The decimal scattering coefficient (σ) of the atmosphere was taken as 0.455 and the decimal absorption coefficient (α) of one cm of ozone at N.T.P. was taken as 1.23.

From Table 12, it can be seen that when the point of secondary emission Q, is situated at the ground, no appreciable error is introduced even if variation of B_{1n}, with ϕ is neglected. This is because in this case, most of the contribution to the integral comes from a cone having a semi-angle less than 75^0.

On the other hand, if the point is situated at 18 Km, there is a little over estimation. But as can be seen from Table 13, most of the secondary scattered radiation is obtained from the first 9 Km and hence no appreciable error is introduced even if a plane-parallel earth is assumed.

Table 12

$$\int_0^{2\pi} \left\{ (\cos^2 \chi_{nn'} + \cos^2 \chi_{tn'}) + \cos^2 \psi' (\cos^2 \chi_{nt'} + \cos^2 \chi_{tt'}) \right\} R_{n'} \, d\phi'$$

$\lambda = 3112$ Å $\quad \theta_0 = 88^0$ $\quad \beta = 0.455$ $\quad \alpha = 1.23$

For Q situated at 0 Km

θ' in degrees	No ozone		0.18 cm of O_3 at 27 Km	
	A	B	A	B
30	1.38×10^{-2}	1.39×10^{-2}	2.91×10^{-3}	2.92×10^{-3}
60	0.75	0.77	1.07	1.03
75	0.18	0.18	0.07	0.07
80	0.04	0.04	0.00	0.00
85	0.00	0.00	0.00	0.00

For Q situated at 18 Km

30, 150	4.04×10^{-2}	4.07×10^{-2}	0.89×10^{-2}	0.89×10^{-2}
60, 120	4.88	5.00	0.68	0.70
75, 105	6.57	6.80	0.35	0.36
80, 100	8.09	8.38	0.18	0.18
85, 95	11.12	11.52	0.02	0.03
90	5.00	5.56	0.00	0.00

Table 13

Distribution of secondary scattered light in the atmosphere

$I_\infty = 1$, $\lambda = 3112$ Å $\quad Z_0 = 88^0$ $\quad \beta = 0.455$ $\quad \alpha = 1.23$

Layer	No ozone	0.18 cm of O_3 at 27 Km
0- 9 Km	0.52×10^{-3}	0.77×10^{-4}
9-18 Km	0.24	0.27
18-27 Km	0.09	0.09
27-36 Km	0.03	0.07
36-45 Km	0.01	0.02
45-54 Km	0.00	0.01
R_2	0.89×10^{-3}	1.23×10^{-4}

2.42 Effect of distributing total ozone content of the atmosphere into three thin layers

In the previous sub-section, 0.18 cm of ozone was assumed to be concentrated in one thin layer situated at a height of 27 Km. However, ozone is actually distributed from the ground to 54 Km, the maximum being at about 25 Km. The distribution of secondary scattered radiation as shown by Table 13 (Section II) for $Z_0 = 88^0$ suggests that if ozone amount be divided in more than one thin layer, keeping in mind its vertical distribution, the ratio R_2/R_1 is likely to be affected. For this purpose, computations were carried out by assuming total ozone content of the atmosphere distributed in three thin layers:

(A) 0.02 cm at 9 Km

(B) 0.05 cm at 18 Km

and (C) 0.11 cm at 27 Km.

The calculations were carried out for two different wave-lengths 3112 Å and 3323 Å having α = 1.23 and 0.07, and β = 0.462 and 0.350 respectively. The following changes were made in the method described in article 1.2.

1. Keeping in mind the results of article 2.41, variation of $k_{1n'}$ with ϕ' was neglected. $k_{1n'}$ was assumed to be constant over ϕ' and its value taken as that for $\phi' = 90^0$.

2. Wilkes tables were used to compute equivalent air-paths for different Z and θ' corresponding to H = 7 Km and the radius of the earth 6400 Km.

3. The atmosphere was divided into 3 Km layers and the centre of a layer was taken at a height of 1 Km above the base of the layer.

4. Actual air-mass in a layer was taken instead of the term $\rho' dh$ where ρ' is the density at the centre of the layer.

5. Proper allowances were made for the reduction in intensity whenever the direct or the scattered light crossed any one of the ozone layers.

The ratio i_2/i_1 for different values of Z and two different distributions of ozone is given in Table 14 along with Walton's results for an ozone amount of 0.16 cm situated

at 24 Km. It can be seen that the effect of distributing ozone in three thin layers is to reduce R_2/R_1 by a small amount in the range 0^0 to 75^0 and to increase by a small amount in the range 75^0 to 90^0. The ratios obtained by Walton are slightly higher than ours.

Table 14

R_2/R_1 for 3112 and 3323 Å for different values of Z

Z in degrees	No ozone	0.18 cm at 24 Km	0.18 cm in three layers	Walton 0.18 cm at 24 Km
	3112 Å			
0	0.49	0.47	0.46	0.52
60	0.59	0.56	0.54	0.59
75	0.66	0.59	0.57	0.60
80	0.70	0.52	0.54	0.52
90	0.67	0.44	0.44	0.45
	3323 Å			
0	0.43	0.42	0.42	0.48
60	0.50	0.50	0.50	0.54
75	0.56	0.56	0.55	0.61
80	0.58	0.58	0.57	0.63
90	0.58	0.54	0.55	0.60

The secondary scattering corrections to be applied to the observed umkehr curve are given in Table 15. It can be seen that there is no appreciable difference in corrections obtained by different methods.

Table 15

Secondary scattering corrections to be applied to the observed umkehr curve

Z in degrees	0.18 cm at 24 Km	0.18 cm in three layers	Walton 0.18 cm at 24 Km	
0	0.00	0.00	0.00	
60	0.00	0.00	0.00	
75	0.01	0.01	0.02	
80	0.03	0.02	0.04	
90	0.05	0.05	0.06	

2.43 Effect of multiple scattering

The problem of scattering of light by the atmosphere taking into account all the orders of scattering was solved by Chandrasekhar. The functions necessary for calculating the intensity and polarisation of any part of the sunlit sky have been tabulated by Chandrasekhar and Elbert for a number of values of τ_1. (For details, please refer to Section IV). The theory is still to be extended to the case when one or more absorbing layers are present.

A general idea about the effect of multiple scattered light on the observed umkehr curve can be obtained in the following manner. In column 3 of Table 16, are given the ratios of multiple scattered light (M) to the primary scattered light (P) for $\tau_1 = 1.0$ for different values of $\mu_0 = \cos Z$ calculated from the tables supplied by Chandrasekhar and Elbert. These

are the ratios when no absorption layer is present. For obtaining the ratio M/P when an absorbing layer is present, we shall make the following assumptions which may be considered as correct to the first approximation.

1. The ratios given in column 3 stand for 3323 when ozone is present and for 3112 when it is absent. The ratios R_2/R_1 (or M/P) for 3112 and 3323 without ozone differ by a small amount as can be seen from Table 14, column 2. However, this difference can be neglected because while calculating the corrections to the observed umkehr curve, it becomes trivial.

2. Since most of the secondary scattered radiation is obtained from the space below the ozone layer, it has not to travel through the ozone layer while giving rise to third and higher orders of scattering. It can be expected that the ratios M/P or S/P are affected by the same amount by ozone.

The ratio S/P without and with 0.16 cm of ozone at 24 Km as obtained by Dalton, are given in columns 4 and 5 respectively (Table 16). The amounts by which the ratio S/P decreases due to ozone are given in column 6. The column 7 gives M/P for 3112 as expected from the assumptions stated above. The corrections given by

$$-\text{Log}\ \frac{1 + (M/P)_{3112}}{1 + (M/P)_{3323}}$$

are shown in column 8. It can be seen that the correction is appreciably affected when all the orders of scattering are taken

Table 14

Corrections to be applied to the observed umkehr curve when multiple scattering is taken into consideration

Z	μ_o	$(M/P)_{3323}$	(S/P) without ozone	(S/P) with 0.18 cm at 24 Km	Effect of O_3 on S/P	$(M/P)_{3112}$	correction
11.5	0.98	1.24	0.56	0.55	0.982	1.22	0.00
48.7	0.66	1.49	0.60	0.571	0.952	1.42	0.01
60.0	0.50	1.65	0.652	0.591	0.906	1.49	0.03
71.3	0.32	1.86	0.710	0.608	0.856	1.59	0.04
76.1	0.24	1.95	0.734	0.573	0.781	1.52	0.07
79.6	0.18	2.01	0.745	0.522	0.701	1.41	0.10
81.9	0.14	2.04	0.749	0.488	0.652	1.33	0.12
84.2	0.10	2.03	0.748	0.466	0.615	1.25	0.13
86.5	0.06	2.09	0.733	0.455	0.621	1.30	0.13
87.7	0.04	1.95	0.715	0.455	0.636	1.24	0.12

2.5 Conclusion

The method B for calculating the vertical distribution of ozone as used in India uptil now is modified in the following manner :- (1) Division of the atmosphere into 6 Km layers instead of 9 Km ones and (2) fitting of the curve at eight different places. With the help of this modified method, it has become possible to follow the day-to-day changes in distribution of ozone with height in the entire atmosphere.

It has been shown that the effects of the curvature of the earth and of the actual distribution of ozone, on the

secondary scattering corrections, are quite negligible. On the other hand, the effect of higher orders of scattering on the observed umkehr curve is quite considerable. A more satisfactory theory and calculations are essential to obtain an idea of the proper corrections to be applied to the observed umkehr curve, when all the orders of scattering are taken into consideration. It would be sufficient to treat the problem for a plane-parallel atmosphere having only one absorption layer of ozone at a proper height.

2.6 References

1	Chapman, S.	1934-35	Phil. Trans. Roy. Soc. London 234 A, P. 205
2	Fabry, C.	1950	"L'ozone Atmosphérique" National Centre of Scientific Research, Paris.
3	Götz, F.W.P.	1931	Gerl. Beitr. 31 P. 119
4	Götz, F.W.P., Meetham, A.R. & Dobson, G.M.B.	1934	Proc. Roy. Soc. A 145 P. 416
5	Götz, F.W.P.	1951	"Ozone in the Atmosphere" Compendium of Meteorology, Amer. Met. Soc. Boston, Mass. P. 275

6	Johnson, F.S., Purcell, J.D. & Tousey, R.	1951	Journ. Geophys. Res. 56 P. 583
7	Karandikar, R.V. & Ramanathan, K.R.	1949	Proc. Ind. Acad. Sci. 29 Sec. A, P. 330
8	Ramanathan, K.R.	1954	Presidential Address, Rome Assembly of the International Association of Meteorology, Sept. 1954. Butterworths Scientific Publications, London.
9	Ramanathan, K.R., Koorthy, Sh. V.R. & Kulkarni, R.N.	1952	Quart. Journ. Roy. Met. Soc. 78, P. 625
10	Regener, E. & Regener, V.H.	1934	Phys. R. 35, P. 788
11	Salton, G.F.	1953	I.U.G.G. General Assembly, Bruxelles, Proces-Verbaux, I.A.M., P. 316
12	Salton, G.F.	1955	Phil. Mag. 46, P. 281
13	Silkes, M.W.	1954	Proc. Phy. Soc. 67, B, P. 304

SECTION III

MEASUREMENT OF SURFACE OZONE

3.1 Introduction

The ozone content of the surface layers of the atmosphere, though small, is of great interest because of its physiological and biological importance and of its usefulness to meteorology as an indicator of air masses and their movements. Recently, it has been suggested that ozone is also formed in the lower atmosphere by the action of solar radiation on petroleum "smog" and that ozone has a deleterious effect on rubber products. Systematic measurements of surface ozone are however few, perhaps because simple methods for the reliable measurements of small concentrations of ozone have only been recently developed. Two different methods are available for direct determination of surface ozone :- (1) Spectroscopic method and (2) Chemical method. In this section, the results of one year's measurements of ozone in air near the ground level at Ahmedabad together with a brief discussion, are presented.

The spectroscopic method is based on the measurement of the absorption by a long column of air of a narrow band of wave-lengths in the ultra-violet region of the Hartley band. The determination of the intensity of light from a source at a known distance on two or three wave-lengths with a proper allowance for scattering by the molecules of air and for absorption and scattering by large particles of dust and haze, can give the total ozone amount along the path traversed by the radiation. The accurate measurement of feeble intensities in the ultra-violet part of the spectrum is

however difficult and the method has been used mainly for special studies. Stair, Bagg and Johnston[1].

The chemical method is based on the well known oxidation reaction of ozone on potassium iodide

$$O_3 + 2KI + H_2O \rightarrow O_2 + 2KOH + I_2 \qquad \ldots 1$$

As the atmospheric air contains in addition to ozone, other oxidising agents such as H_2O and reducing agents like SO_2, what we can measure is the net equivalent of all these substances. The method used has to be specific for ozone, and since the ozone content of atmospheric air is small, method of titrating the ozone has to be more accurate than the standard starch indicator method. There is also the problem of the evaporation of free iodine from the solution when a large volume of air is passed through the solution.

The method of electro-chemical titration developed by Faneth and others[2] and later successfully applied by Ehmert[3] has been found to be quick and accurate and is applied now-a-days for the measurement of surface ozone. Bowen and Regener[4] and Carbenay and Vassy[5] have developed instruments for the automatic determination of ozone based on this principle.

The method of electro-chemical titration of ozone as improved by Ehmert[6,7] is as follows : A 2 % solution of potassium iodide is made in double distilled water with a few micrograms of sodium thiosulphate. A few cubic centimeters of this is taken in a small bottle which is fitted to a

bubbling apparatus. A known volume of air is drawn through a sintered glass diaphram and a solution. At this concentration of potassium iodide, the reaction of ozone with potassium iodide is complete while that of N_2O is only 5 % as effective. It has been established that the concentration of N_2O in the atmospheric air near the ground is not more than that of ozone. The presence of $Na_2S_2O_3$ removes the free iodide

$$2\ Na_2S_2O_3 + I_2 \rightarrow 2\ NaI + Na_2S_4O_6 \qquad \ldots 2$$

and there is therefore no change of free iodide escaping with the air.

For determining the sodium thiosulphate in the solution through which air has been passed, the electro-chemical method is used. Two pairs of platinum electrodes are inserted in the bottle containing the solution and this is mounted on a stand which can be rotated with uniform speed. Between one pair of electrodes, a constant small difference of potential of a few millivolts is applied. The electrodes get polarised, the cathode with hydrogen and the anode with oxygen and there is no current in the circuit. The second pair of electrodes is used to liberate iodine at a constant rate by electrolysis from the solution. This liberated iodine reacts with the $Na_2S_2O_3$ present in the solution, and its concentration gradually decreases as the electrolysis proceeds. When all the $Na_2S_2O_3$ present in the solution is used up, the iodine starts depolarising the first pair of

electrodes and a current starts in the circuit and steadily increases. The exact time of electrolysis for completing the reaction with $Na_2S_2O_3$ is obtained from the current-time graph. The quantity of electricity passed through the solution is a measure of the amount of iodine required for the reaction. If J_0 is the amount of iodine required to be liberated to neutralise the $Na_2S_2O_3$ present in a given amount of stock solution through which air has not been passed and J_1 the iodine to be liberated in the same amount of solution through which N litres of air has been passed, then $J_0 - J_1$ is the iodine equivalent to the ozone present in the volume of air which has been passed through the solution. The amount of ozone in microgram per cubic metre of air is then given by

$$[O_3] \quad \gamma/m^3 = \frac{189\ (J_0 - J_1)}{N} \qquad \ldots 3$$

Manual or automatic observations of ozone by the chemical method have been carried out at a number of places in Europe and America. However, there have been no systematic surface ozone measurements made in India or other tropical countries. The Physical Research Laboratory, Ahmedabad, obtained an Ehsert surface ozone instrument through the International Ozone Commission and systematic observations were carried out at Ahmedabad (Lat. 23°N, Long. 72½°E) for a period of one year from June 1954 to May 1955. Part of the data was presented by Professor Ramanathan[8] at the Rome meeting of the International Union of Geodesy and Geophysics in September 1954 and appeared later in I.U.G.G. News Letter. Dave[9].

3.2 Presentation of the observed data and discussion

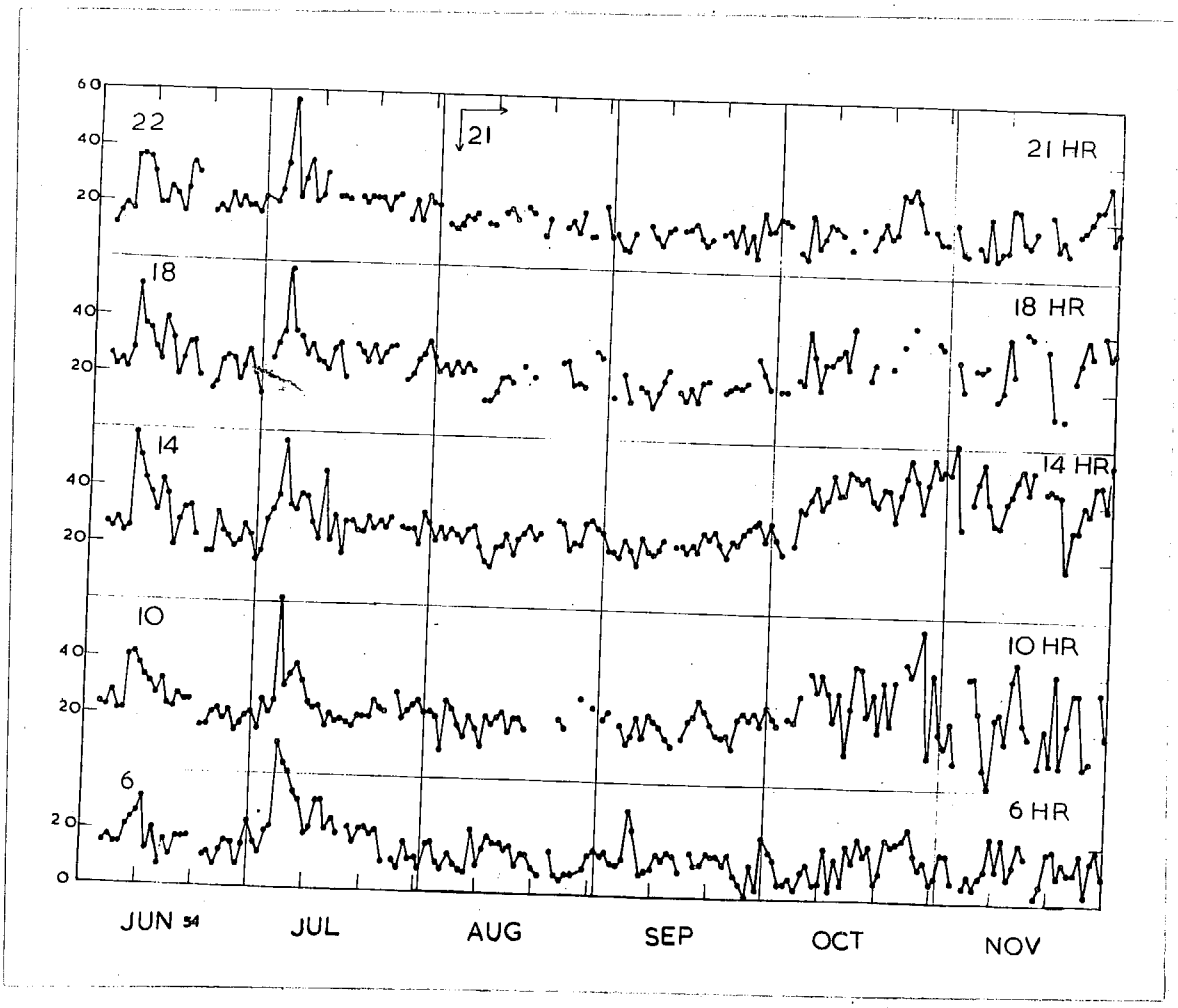

Fig. 1. Day-to-day surface ozone values at Ahmedabad. 6, 10, 14, 18 and 21 hrs. Surface ozone values in micrograms/m3. From June 54-Nov. 54.

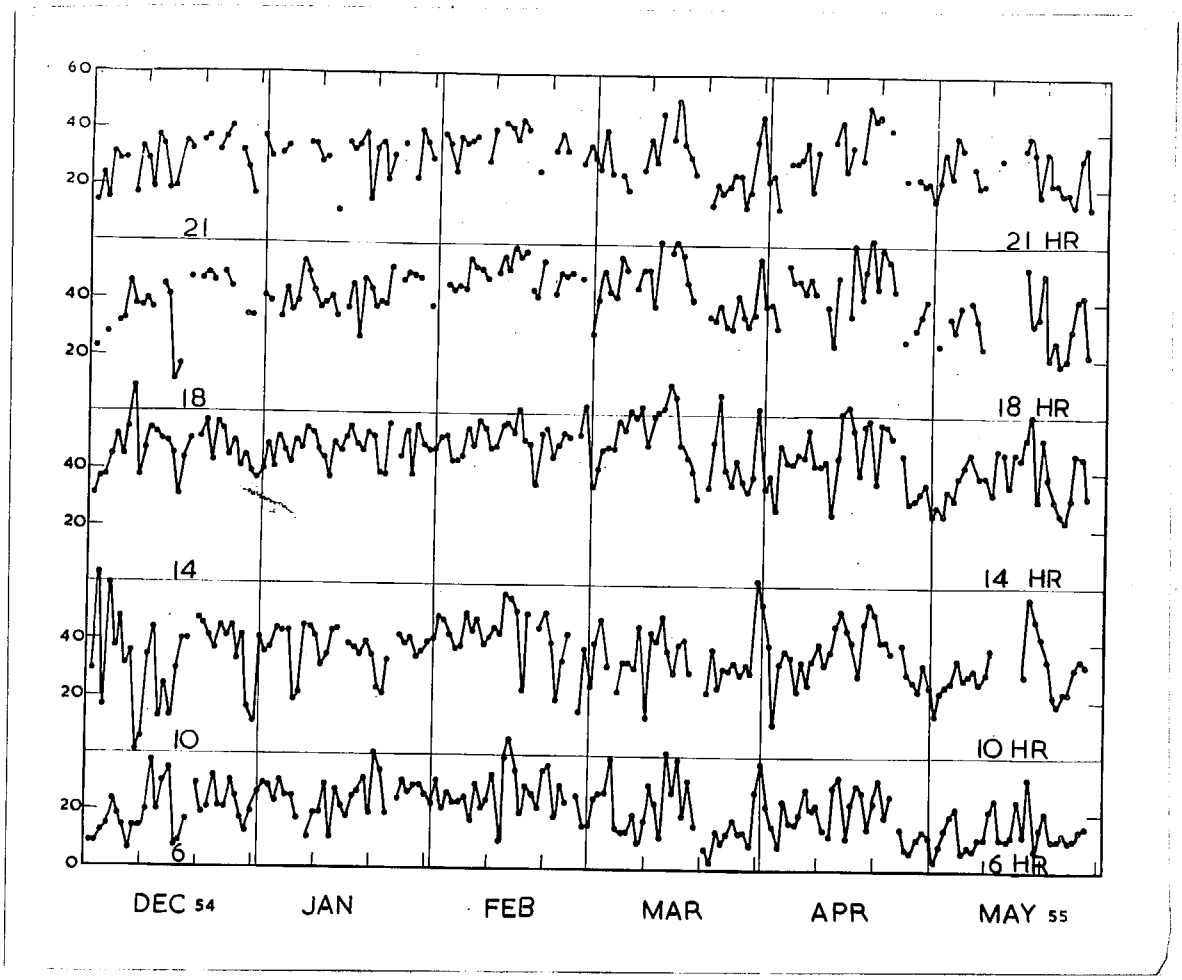

Fig. 1. Day-to-day surface ozone values at Ahmedabad. 6, 10, 14, 18 and 21 hrs. Surface ozone values in micrograms/m^3. From Dec. 54-May 55.

The observations were made throughout the year in a well-ventilated room on the ground floor of the Physical Research Laboratory, Ahmedabad. Generally five observations were taken in a day : at 6 Hr, 10 Hr, 14 Hr, 18 Hr and 21 Hr. In June and July only, the night observations were made at 22 Hr. They are plotted in Fig. 1 separately for each hour. The hourly observed values for different months are given

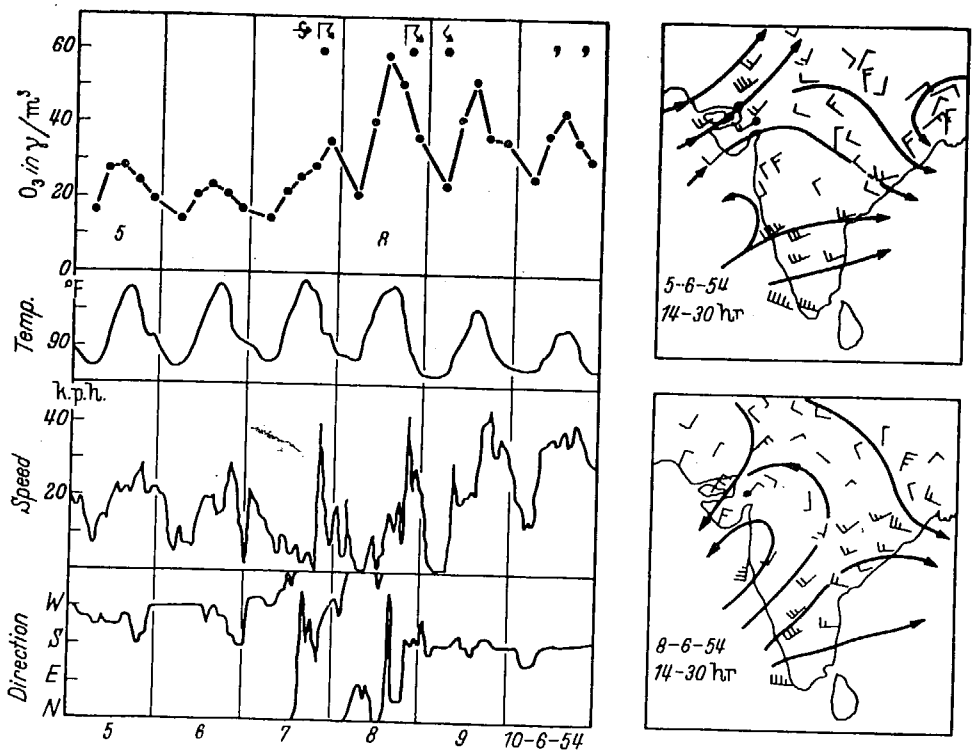

Fig. 2. Surface ozone, temperature and winds at Ahmedabad during the period 5 to 10 June 1954. Also upper winds at 5000 ft. on 5 and 8 June 1954

Fig. 2. Surface ozone, temperature and winds at Ahmedabad during the period 5 to 10 June 1954. Also upper winds at 5000 ft on 5 and 8 June 1954.

This was accompanied by decrease of minimum temperatures and of evening dew points, clearing of skies and the establishment of North-Westerly winds in the lower atmosphere.

The large fluctuations observed at 10 hr during November and December can be attributed to very weak winds and late heating of the ground and consequent lack of mixing in the lower atmosphere on some of the days.

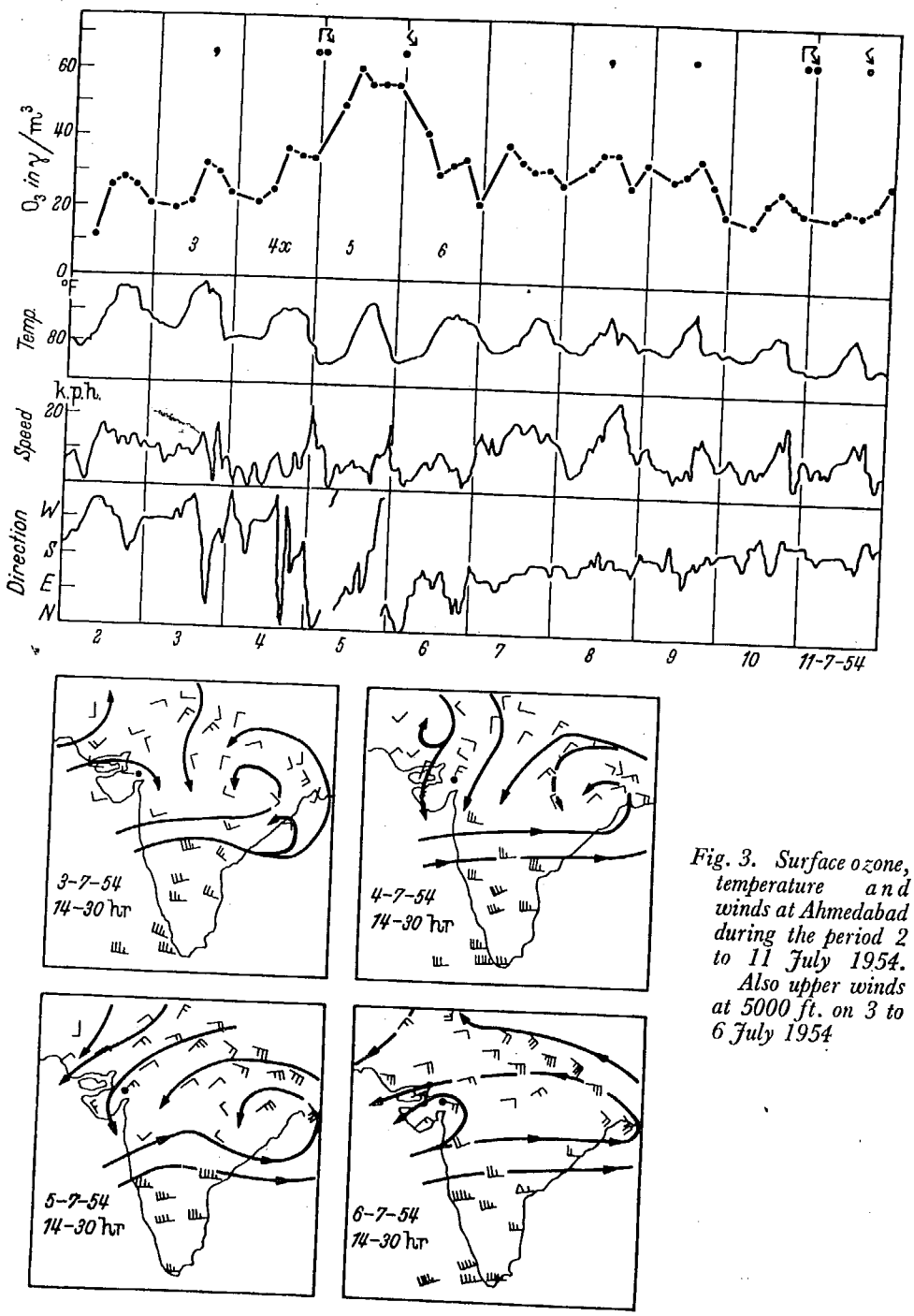

Fig. 3. Surface ozone, temperature and winds at Ahmedabad during the period 2 to 11 July 1954. Also upper winds at 5000 ft. on 3 to 6 July 1954

Fig. 3. Surface ozone, temperature and winds at Ahmedabad during the period 2 to 11 July 1954. Also upper winds at 5000 ft on 3 to 6 July 1954.

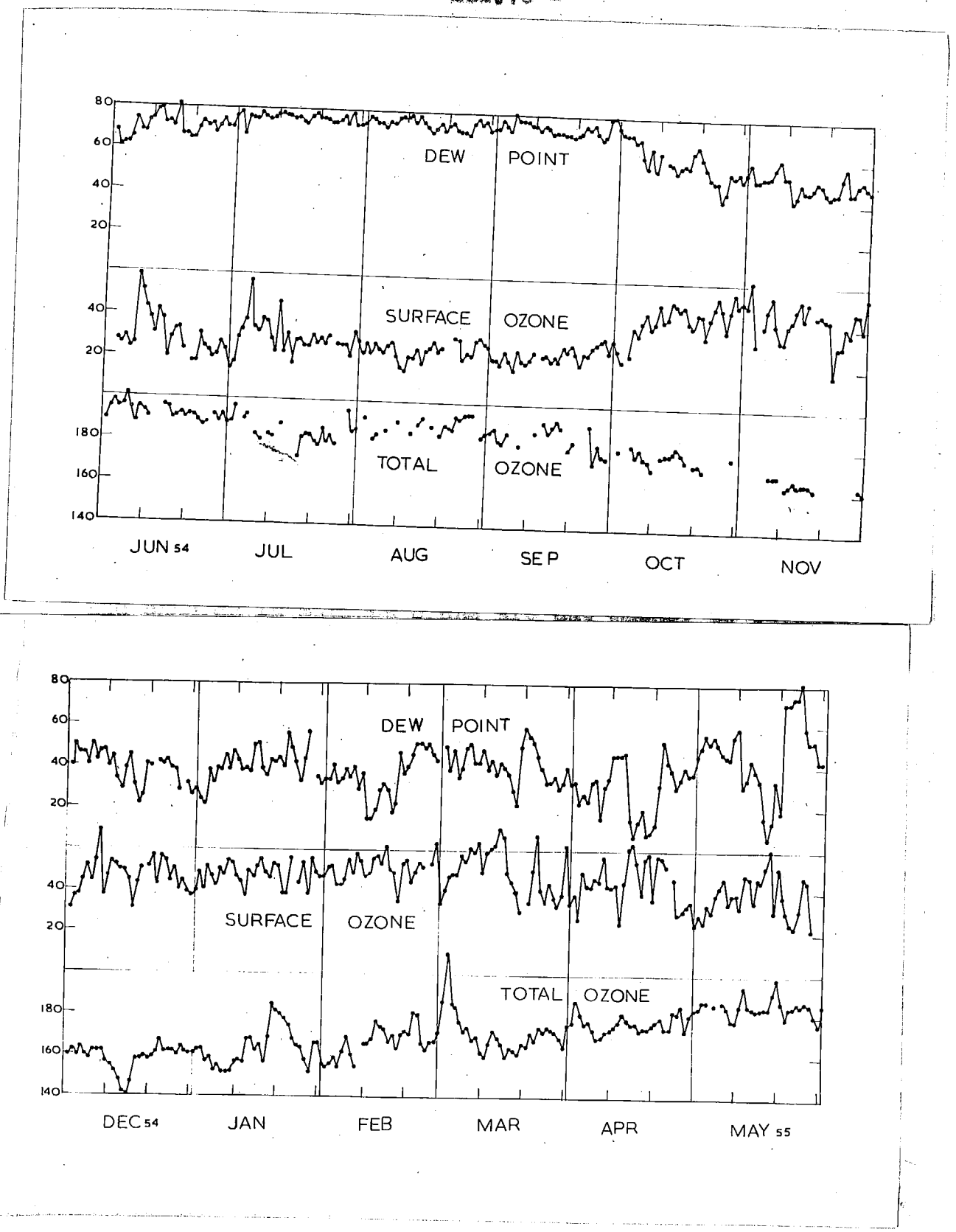

Fig. 4. 1730 hr dew point in °F, 14 hr surface ozone (micrograms/m³) value at Ahmedabad and afternoon total ozone (10^3 cm) at Mt. Abu.

The marked decrease in afternoon surface ozone values can be connected with the setting in of regular sea-breeze in April.

In Fig. 4 are plotted the surface ozone values at 14 Hr at Ahmedabad along with the dew point at 1730 Hr at Ahmedabad and afternoon total ozone amount at Mt. Abu. Mt. Abu is situated about 100 miles north of Ahmedabad and the total ozone at Ahmedabad and Mt. Abu have been found to run very nearly parallel. There is practically no correlation between the changes in total ozone amount at Abu and the concentration of surface ozone, suggesting that the changes in surface ozone are due mainly to changes in the lower part of the atmosphere, while the day-to-day changes of total ozone take place mainly in the upper atmosphere.

Some correlation was found (1) between surface ozone and minimum surface temperatures and (2) surface ozone and evening dew point; in the latter case, the correlation was found to be rather good. The correlation coefficient between 14 Hr surface ozone and 1730 Hr dew point is specially significant in the period when the air masses are getting replaced. Thus, in October 1954 at the time of the withdrawal of the monsoon, the correlation coefficient was - 0.67. Again, in April and May 1955, when sea-breeze comes more or less regularly in the afternoon or evening, the coefficient was - 0.42 and - 0.65 respectively. There is no significant correlation in the other months.

Month	Correlation coefficient between 14 Hr surface ozone and 1730 Hr dew point at Ahmedabad.
June 54	0.03
July	- 0.11
August	- 0.31
September	- 0.27
October	- 0.67
November	0.02
December	0.19
January 55	0.17
February	- 0.10
March	0.24
April	- 0.42
May	- 0.65

In Fig. 5 are plotted the monthly mean diurnal variations for each month. The monthly mean maximum (X) and minimum (N) temperatures and dew points at Ahmedabad and total ozone at Mt. Abu are also given. It will be seen that in the monsoon period June - September, the range of the diurnal variation is small; the monthly mean concentration is the lowest in the monsoon months of August and September. The withdrawal of monsoon in the beginning of October is shown by large range of diurnal variation of surface ozone, decrease in minimum temperature and 1730 Hr dew point and increase in difference between maximum and minimum temperature (X - N) of the day.

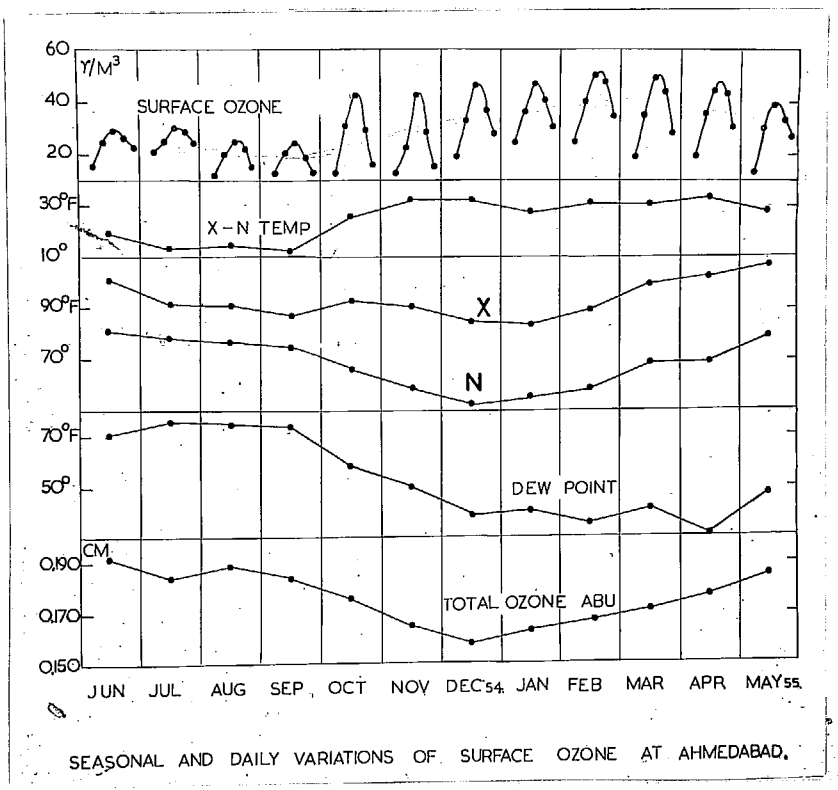

SEASONAL AND DAILY VARIATIONS OF SURFACE OZONE AT AHMEDABAD.

Fig. 5. Seasonal and daily variation of surface ozone at Ahmedabad. Also difference of maximum and minimum temperature (X - N), monthly mean maximum temperature (X), minimum temperature (N), dew point and total ozone.

In Fig. 6 are given the monthly mean values of surface ozone as observed at four different stations in the world for comparison.

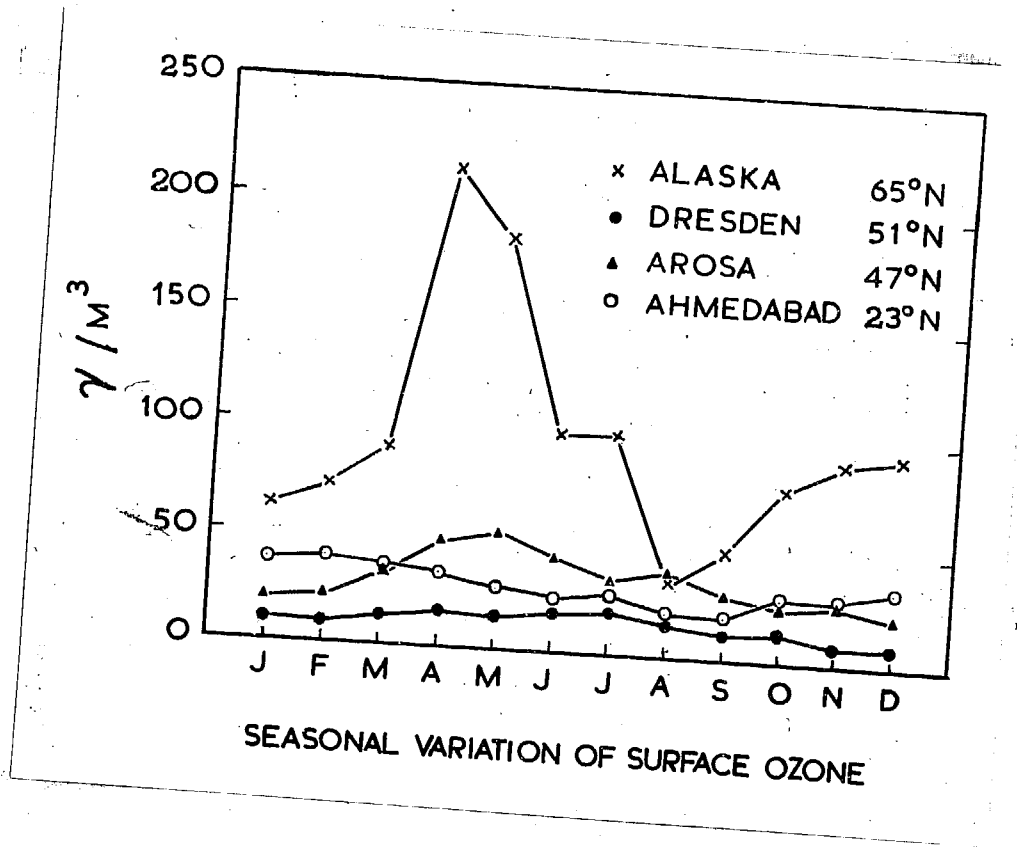

Fig. 6. Seasonal variation of surface ozone at Alaska, Dresden, Arosa and Ahmedabad.

Station	Name of the observer	Period of observation
Alaska	Wilson, Guenther, Lowrey, and Cain(10)	1950
Dresden	Teichert and Warnbt(11)	1952
Arosa	Götz and Volz(12)	April 1950 - March 1951
Ahmedabad	Dave	June 1954 - May 1955

The sharp increase in the Alaska values in the period September - December has been explained as being due to the fact that Alaska is snow-covered after September and ozone undergoes comparative little decomposition by coming in

June 1954

Date	6 Hr	10 Hr	14 Hr	18 Hr	22 Hr
1	-	-	-	-	-
2	-	-	-	-	-
3	-	23.6	26.9	26.0	12.1
4	15.1	22.5	25.5	21.9	16.3
5	16.8	27.9	28.4	24.6	19.1
6	14.2	20.8	23.9	21.3	17.3
7	14.6	21.5	25.8	28.1	35.9
8	20.8	40.2	58.6	51.0	36.3
9	23.6	41.6	51.6	36.9	35.9
10	25.5	37.3	43.0	35.4	30.4
11	30.5	33.5	37.8	28.6	19.8
12	12.3	31.7	30.4	24.6	19.8
13	19.8	26.5	42.1	39.5	25.8
14	7.1	32.1	37.8	32.1	23.2
15	15.6	23.6	19.7	19.4	17.0
16	10.2	22.5	28.4	25.0	24.6
17	17.0	26.9	32.9	31.0	34.0
18	17.0	25.0	33.5	31.7	30.2
19	17.0	25.5	23.2	19.1	-
20	-	-	-	-	-
21	-	16.5	17.0	14.6	17.0
22	10.4	16.5	17.3	16.7	19.8
23	11.8	20.6	31.0	24.6	17.0
24	7.6	22.2	24.4	26.3	23.4
25	12.1	18.9	22.7	25.5	18.4
26	15.6	22.0	19.4	18.0	21.9
27	14.6	14.2	20.3	22.7	18.9
28	7.8	17.0	26.5	28.8	19.7
29	14.5	19.8	23.7	20.3	17.0
30	22.7	21.3	14.8	13.4	22.0
Mean	15.8	24.9	29.1	26.2	22.8

July 1954

Date	6 hr	10 hr	14 hr	18 hr	22 hr
1	15.6	15.8	17.5	-	-
2	11.8	26.0	28.8	26.5	20.8
3	19.8	21.7	32.4	30.7	24.6
4	21.3	25.3	37.8	35.0	34.3
5	50.6	61.4	56.7	56.7	56.7
6	43.8	30.6	34.0	35.9	22.2
7	40.2	35.0	32.3	33.5	28.6
8	33.8	38.1	38.0	27.7	35.7
9	30.2	32.6	37.5	30.1	21.3
10	18.9	25.0	28.4	24.8	22.9 *
11	21.0	23.2	22.2	24.9	31.2
12	30.4	23.6	46.5	22.2	-
13	30.2	16.3	22.2	29.6	23.6
14	20.3	21.7	31.0	31.2	23.6
15	24.1	18.6	17.5	19.8	22.2
16	19.4	19.4	28.4	-	-
17	-	18.0	29.0	31.5	23.0
18	21.5	16.5	26.0	28.4	21.5
19	16.5	20.3	25.7	25.3	23.6
20	21.3	20.3	30.2	30.9	23.3
21	21.3	20.3	26.9	25.7	23.4
22	19.4	26.0	29.8	28.4	19.4
23	20.3	23.8	26.6	30.5	23.8
24	9.9	22.2	30.7	30.7	24.3
25	-	-	-	-	-
26	10.1	29.0	26.9	19.8	15.9
27	7.4	20.1	26.5	21.3	22.2
28	16.5	23.3	26.5	26.6	15.6
29	10.7	24.9	21.7	28.2	24.1
30	11.8	26.6	33.1	33.1	21.9
31	8.0	22.5	28.8	27.9	20.8
Mean	21.6	24.9	30.0	29.2	24.8

* at 2030 hr.

August 1954

Date	6 Hr	10 Hr	14 Hr	18 Hr	21 Hr
1	16.1	23.2	23.2	22.7	-
2	17.0	21.7	27.4	25.0	14.2 *
3	9.9	9.5	23.6	21.5	12.3 **
4	7.8	26.7	27.7	26.0	14.6
5	12.8	24.1	25.0	22.5	17.5
6	9.6	18.1	23.4	25.3	16.5
7	7.6	14.2	26.6	23.2	18.1
8	6.8	21.7	28.1	-	-
9	20.6	17.0	21.3	12.5 ***	14.9
10	9.7	11.8	16.1	12.8	14.6
11	14.2	21.3	14.6	15.9	-
12	18.9	18.4	21.3	20.8	18.4
13	17.0	21.7	21.5	22.0	20.3
14	17.2	23.0	25.5	19.4	17.0
15	14.9	16.1	18.4	-	-
16	16.1	21.3	24.1	25.0	20.8
17	9.6	20.3	26.0	-	18.4
18	13.7	17.7	26.4	21.7	-
19	13.5	-	24.1	-	11.3
20	9.0	-	26.0	-	17.5
21	6.1	-	-	-	-
22	-	-	-	-	-
23	14.6	-	30.7	26.6	14.2
24	6.1	20.8	30.0	26.9	16.3
25	4.7	18.0	20.8	19.1	12.0
26	6.8	-	23.6	19.4	19.8
27	6.6	-	22.7	18.2	10.9
28	-	28.4	30.0	-	11.1
29	8.7	-	31.7	30.4	-
30	13.7	25.7	28.8	28.2	22.2
31	15.6	-	27.4	-	11.3
Mean	11.9	20.0	24.8	22.1	15.8

* 2200 Hr

** 2145 Hr

*** 1730 Hr.

September 1954

Date	6 Hr	10 Hr	14 Hr	18 Hr	21 Hr
1	13.7	21.7	21.1	14.5	12.3
2	15.1	23.9	20.5	-	7.6
3	11.3	-	18.4	23.6	6.6
4	10.6	19.4	24.8	13.7	13.2
5	12.3	13.0	20.8	-	-
6	29.8	16.1	16.1	18.9	-
7	23.3	22.2	25.5	17.0	15.9
8	7.8	15.6	20.3	11.8	11.8
9	9.2	23.2	19.4	17.0	9.0
10	9.9	21.3	21.3	20.8	14.2
11	14.6	19.4	25.0	24.6	15.4
12	12.6	15.6	-	-	-
13	15.8	12.8	22.9	17.3	14.2
14	14.6	-	23.8	14.2	14.6
15	8.8	15.6	20.8	18.4	16.5
16	-	21.5	23.3	14.0	11.8
17	15.6	23.6	21.5	21.1	9.9
18	11.8	28.4	27.9	21.5	11.6
19	11.8	25.5	26.0	-	-
20	15.3	20.8	28.4	-	13.7
21	14.2	17.0	24.6	17.7	14.2
22	14.6	16.1	19.7	18.6	9.9
23	11.8	16.5	25.0	19.8	16.5
24	15.1	12.3	24.1	19.4	7.6
25	7.6	22.7	27.9	21.3	13.7
26	4.3	25.0	29.8	-	5.7
27	0.5	22.7	30.9	29.3	21.3
28	11.8	25.0	32.3	24.4	14.4
29	3.3	20.3	25.5	19.4	15.1
30	21.3	26.9	31.7	-	18.9
Mean	12.7	20.1	24.1	19.1	12.9

October 1954

Date	6 hr	10 hr	14 hr	18 hr	21 hr
1	16.1	23.3	26.5	18.4	18.6
2	13.7	20.8	21.7	18.4	16.8
3	5.5	-	-	-	-
4	5.4	23.6	24.3	22.2	7.6
5	7.6	22.2	37.8	21.1	5.2
6	3.8	31.5	36.5	39.4	20.8
7	9.9	-	40.4	31.2	9.6
8	12.3	39.7	44.9	19.7	12.3
9	5.4	33.5	37.8	28.6	17.5
10	5.7	39.0	40.2	28.2	16.5
11	18.1	32.9	49.9	31.5	14.0
12	3.3	22.7	41.3	33.4	-
13	14.0	33.1	42.8	27.1	8.5
14	5.7	11.8	50.6	40.9	-
15	18.7	27.7	49.6	-	16.1
16	13.7	42.5	47.3	-	-
17	21.3	41.6	48.9	23.0	9.9
18	15.3	24.8	41.6	28.6	14.0
19	19.2	32.6	39.2	-	18.4
20	6.1	19.4	45.5	-	13.7
21	9.5	37.1	44.9	27.7	14.6
22	21.5	22.0	34.0	-	28.4
23	18.9	36.9	43.2	35.6	27.1
24	20.0	-	49.1	-	30.7
25	21.3	43.9	53.4	41.4	26.5
26	25.8	39.7	48.0	-	16.1
27	16.3	-	37.3	-	-
28	11.3	55.3	46.8	-	16.1
29	14.2	11.1	55.9	37.1	11.8
30	6.4	39.9	49.8	35.0	11.8
31	8.5	19.4	51.8	-	-
Mean	12.7	30.7	42.7	29.4	16.1

November 1954

Date	6 Hr	10 Hr	14 Hr	18 Hr	21 Hr
1	16.7	15.1	50.1	-	18.4
2	16.5	22.7	61.1	30.4	8.7
3	6.8	9.6	31.7	20.1	8.0
4	-	-	-	-	-
5	5.5	38.7	40.0	27.9	11.3
6	9.5	39.2	48.0	27.7	7.7
7	5.2	27.6	54.3	28.8	21.3
8	9.0	7.3	40.9	-	6.6
9	11.8	0.9	33.4	16.8	9.5
10	23.3	24.3	32.8	20.5	9.7
11	11.8	26.7	40.6	38.7	24.6
12	22.7	16.5	43.8	26.0	23.9
13	9.0	38.7	48.2	-	12.9
14	12.8	45.1	52.7	40.6	11.8
15	21.3	23.4	44.4	39.5	16.7
16	16.1	18.4	52.0	-	-
17	-	-	-	-	-
18	2.8	9.0	45.4	35.9	22.7
19	6.6	21.5	46.1	11.6	10.6
20	18.0	9.9	44.6	-	14.0
21	19.2	40.4	43.9	10.7	8.3
22	9.9	9.0	17.5	-	-
23	14.5	23.8	31.2	24.4	16.1
24	10.9	34.5	31.7	30.1	17.7
25	11.1	34.5	40.0	38.3	20.6
26	18.0	8.5	37.6	32.8	24.6
27	3.5	10.4	47.4	-	24.8
28	15.8	-	47.7	40.4	33.1
29	19.8	35.2	39.7	32.6	13.4
30	9.9	18.9	54.3	34.2	17.0
Mean	12.8	22.6	42.9	29.0	15.9

December 1954

Date	6 hr	10 hr	14 hr	18 hr	21 hr
1	9.0	29.3	30.7	23.0	14.2
2	9.0	62.8	36.7	-	23.8
3	12.3	16.5	37.3	27.9	14.9
4	14.5	59.3	44.6	-	31.2
5	23.4	37.6	51.7	31.7	28.4
6	18.4	47.3	44.7	32.4	29.1
7	14.6	31.0	54.3	45.8	-
8	6.6	35.4	68.5	37.8	17.2
9	14.8	0.9	37.3	36.9	33.1
10	14.2	5.7	46.8	39.9	29.1
11	19.8	34.3	53.9	36.4	18.9
12	36.9	43.9	52.2	-	37.3
13	20.0	13.0	50.1	45.2	34.0
14	30.2	24.3	49.8	41.4	18.4
15	35.0	12.8	44.9	11.8	19.8
16	7.6	29.8	30.7	17.0	15.1
17	9.0	40.2	43.9	-	35.4
18	16.5	40.6	50.1	47.5	32.9
19	-	-	-	-	-
20	29.5	47.3	51.8	47.0	35.9
21	19.4	45.8	56.7	48.9	37.6
22	21.2	41.6	43.0	46.3	-
23	32.1	36.9	56.7	-	32.6
24	21.9	44.4	54.3	49.8	36.9
25	20.8	41.6	45.1	44.1	41.1
26	30.7	44.9	50.1	-	-
27	25.0	33.1	40.9	-	31.9
28	17.3	41.4	44.4	34.5	26.5
29	12.3	16.1	39.7	34.0	17.3
30	19.7	11.3	36.9	-	-
31	26.5	40.6	40.0	41.4	37.8
Mean	19.6	33.7	46.3	37.3	28.1

January 1955

Date	6 Hr	10 Hr	14 Hr	18 Hr	21 Hr
1	29.5	35.9	48.5	39.7	30.7
2	28.8	37.3	41.1	-	-
3	23.4	44.1	51.3	34.0	31.5
4	30.5	43.3	46.8	43.5	34.2
5	25.5	43.5	42.5	36.6	-
6	25.0	18.9	50.1	39.7	-
7	17.0	21.3	47.7	53.2	-
8	-	45.2	54.3	49.6	35.4
9	11.3	44.2	53.2	43.0	35.0
10	19.4	41.6	46.8	36.7	28.6
11	19.2	31.2	44.2	38.3	30.2
12	29.3	35.4	37.8	40.8	-
13	10.4	43.5	49.3	34.3	11.8
14	27.7	43.9	46.3	-	-
15	21.5	-	51.5	36.9	35.9
16	18.0	39.2	55.8	45.8	33.1
17	25.0	37.6	49.0	27.1	35.0
18	26.5	35.0	46.5	47.7	38.7
19	31.7	39.7	52.9	43.5	15.6
20	18.9	35.0	51.5	37.8	33.7
21	40.6	23.8	38.7	39.4	35.9
22	34.2	21.7	38.1	38.5	22.5
23	19.7	32.6	56.0	51.5	31.2
24	-	-	-	-	-
25	24.1	41.9	44.4	46.8	35.0
26	30.2	39.2	53.4	49.3	-
27	27.1	40.6	38.3	48.5	22.7
28	28.8	34.0	55.3	47.3	40.0
29	29.1	35.9	49.1	-	35.4
30	26.0	39.7	46.8	37.8	29.8
31	22.7	40.2	47.0	-	-
Mean	24.9	36.7	47.8	41.8	31.0

February 1955

Date	6 Hr	10 Hr	14 Hr	18 Hr	21 Hr
1	31.2	48.2	51.3	-	38.3
2	21.7	47.1	52.0	45.4	34.8
3	26.3	42.1	42.8	43.0	25.5
4	23.6	37.3	43.2	44.7	37.8
5	23.6	37.8	45.4	43.9	35.6
6	25.0	49.6	54.6	54.2	36.4
7	16.7	43.5	48.7	51.5	37.8
8	29.8	47.4	57.4	51.0	-
9	21.3	38.7	54.5	47.4	28.8
10	24.1	40.6	47.3	-	40.2
11	33.1	44.4	48.7	49.9	-
12	9.5	42.2	55.8	55.3	42.5
13	38.7	56.2	56.7	51.0	40.6
14	45.8	54.3	53.2	58.6	36.6
15	34.2	50.6	61.4	55.3	43.8
16	19.8	22.5	50.8	57.0	40.2
17	28.8	49.9	49.1	43.9	-
18	26.0	-	35.0	41.6	25.5
19	21.7	44.4	52.9	53.4	-
20	34.0	50.1	54.3	-	-
21	36.1	39.7	44.4	42.1	33.4
22	18.2	19.6	49.4	49.6	39.0
23	29.6	33.1	53.7	48.7	32.9
24	23.4	42.1	51.5	49.8	-
25	-	-	-	-	-
26	25.8	15.6	53.2	47.7	28.5
27	15.1	37.3	62.7	-	34.8
28	15.4	24.1	34.5	28.2	30.2
Mean	25.9	40.7	50.5	48.4	35.4

March 1955

Date	6 Hr	10 Hr	14 Hr	18 Hr	21 Hr
1	24.6	39.7	40.9	40.0	26.9
2	26.3	47.3	47.3	50.1	40.2
3	26.9	31.7	48.7	43.5	25.5
4	38.6	-	48.2	41.3	-
5	14.2	22.7	57.5	55.6	25.0
6	12.8	32.6	54.3	51.3	19.1
7	13.2	32.3	60.5	-	-
8	18.6	30.2	59.1	44.2	-
9	9.6	44.9	63.1	51.0	26.2
10	17.0	13.7	49.6	50.6	37.1
11	29.6	43.2	59.1	38.0	28.8
12	23.2	40.2	60.8	60.3	46.1
13	10.7	48.2	62.4	-	-
14	40.6	37.1	70.6	57.2	37.8
15	26.9	28.8	66.4	61.0	51.2
16	38.7	39.2	49.1	56.5	35.9
17	18.4	41.1	44.9	46.3	31.2
18	31.2	29.8	40.2	40.6	25.5
19	15.6	-	30.7	-	-
20	-	-	-	-	-
21	6.8	22.4	34.5	34.5	14.2
22	2.4	37.8	50.1	33.5	21.3
23	13.7	24.1	66.9	38.1	18.4
24	9.5	31.2	40.4	31.7	21.1
25	12.1	30.5	35.4	30.1	24.3
26	17.5	33.1	43.9	42.1	24.6
27	12.8	28.4	36.9	35.0	13.2
28	13.2	32.1	33.3	31.8	18.6
29	8.0	29.8	38.3	35.9	36.7
30	27.7	61.9	62.1	55.3	45.5
31	37.0	53.9	34.0	38.3	23.2
Mean	19.9	35.3	49.6	44.2	28.7

April 1955

Date	6 Hr	10 Hr	14 Hr	18 Hr	21 Hr
1	22.2	39.4	38.3	39.7	25.0
2	15.4	11.8	27.2	31.0	13.2
3	8.0	32.8	49.6	-	-
4	24.6	37.8	43.7	52.6	29.6
5	16.8	35.0	42.7	47.3	29.3
6	16.1	23.3	46.6	47.3	30.9
7	19.8	33.5	45.4	43.2	37.0
8	28.5	25.8	57.0	48.2	19.6
9	21.7	34.0	42.5	43.8	33.7
10	23.2	39.9	42.1	-	-
11	14.6	32.6	43.9	38.3	-
12	12.3	37.8	25.8	25.0	37.0
13	29.8	46.3	45.2	49.0	43.9
14	32.3	51.5	61.0	-	26.5
15	11.3	44.9	63.6	35.4	35.0
16	23.6	40.6	54.8	60.5	-
17	40.2	28.8	39.5	41.1	30.2
18	27.9	47.4	56.4	51.7	49.3
19	14.2	54.1	58.6	62.4	44.4
20	24.1	51.2	36.2	45.4	45.4
21	31.8	40.4	57.6	58.8	-
22	18.7	41.1	56.7	54.8	41.1
23	26.0	36.9	52.3	44.4	-
24	-	-	-	-	-
25	14.9	39.7	46.3	26.3	23.9
26	7.4	29.3	29.6	-	-
27	6.6	26.9	30.4	31.2	24.1
28	11.1	23.6	33.1	35.4	21.7
29	14.0	33.1	35.9	40.8	22.5
30	12.1	25.0	24.4	-	16.5
Mean	19.6	36.0	44.4	43.9	30.9

May 1955

Date	6 Hr	10 Hr	14 Hr	18 Hr	21 Hr
1	3.3	14.8	28.4	25.2	23.6
2	6.8	23.4	25.7	-	33.1
3	15.1	24.8	34.0	34.7	24.6
4	9.5	26.5	30.7	30.0	39.2
5	12.3	34.5	38.6	38.7	35.2
6	6.1	27.9	42.2	-	-
7	8.5	29.3	46.8	40.2	27.9
8	7.8	30.5	34.7	34.2	21.7
9	11.3	26.0	38.7	24.6	21.9
10	11.5	29.8	38.7	-	-
11	21.3	38.0	33.3	-	-
12	25.5	-	48.2	-	31.2
13	11.8	-	47.3	-	-
14	10.4	-	35.6	-	-
15	12.1	-	47.1	-	-
16	24.6	-	45.5	-	34.8
17	12.6	28.8	52.4	52.3	39.2
18	32.1	56.7	60.5	33.1	33.4
19	7.1	48.4	31.2	35.6	18.4
20	15.1	42.2	52.0	50.4	33.5
21	20.3	34.7	38.5	21.0	22.7
22	10.9	21.5	30.7	27.1	22.5
23	10.7	18.6	25.8	19.1	18.9
24	12.8	23.2	23.8	20.6	18.6
25	10.9	22.7	31.5	30.5	14.5
26	10.7	31.7	47.4	41.6	30.7
27	14.6	34.8	45.8	43.2	35.0
28	15.3	32.6	22.2	22.2	14.0
29	-	-	-	-	-
30	-	-	-	-	-
31	-	-	-	-	-
Mean	13.3	30.5	38.5	32.9	27.0

3.5 References

1. Stair, R., Bagg, T.C. & Johnston, R.G. — J. Res. Nat. Bur. Std. 1954, 52, P. 133

2. Gluckauf, E., Heal, H.G., Martin, G.A. & Paneth, F.A. — J. Chem. Soc. 1944, Part I, P. 1

3. Ehmert, A. — Zs. Naturf. 1949, 4b, P. 321

4. Bowen, I.S. & Regener, V.H. — Journ. Geophys. Res. 1951, 56, P. 307

5. Carbonay, J. & Vassy, A. — Annal. Geophys. 1953, 9, P. 300

6. Ehmert, A. — Met. Rdsch. 1951, 4, P. 64

7. Ehmert, A. — Journ. Atmos. Terr. Phys. 1952, 2, P. 189

8. Ramanathan, K.R. — Presidential Address, Rome Assembly of the International Association of Meteorology, September 1954. Butterworths Scientific Publications, London.

9. Dave, J.V. — I.U.G.G. News Letter 1955, No.9, P. 12

10. Milnon, W.S., Guenther, W.B., Lowrey, R.D. & Cain, J.C. — Trans. Amer. Geophys. Union 1952, 33, P. 361

11. Teichert, F. & Warnbt, M. — Abhandlungen des Meteor. und Hydro. 1955, 5, No. 34

12. Götz, F.W.P. & Volz, F. — Z. Naturforsch. 1951, 6a, P. 634

SECTION IV

A REVIEW OF WORK ON SCATTERING OF LIGHT BY THE EARTH'S ATMOSPHERE

4.1 Effect of curvature of the earth on the equivalent optical path

A beam of light travelling through the earth's atmosphere from the sun (S) to a point (P) in the atmosphere, suffers a loss of intensity due to scattering by the molecules in the path SP. The intensity of the beam at P is given by

$$I = I_0 e^{-\tau_{sp}} \qquad \ldots 1$$

where

I_0 = intensity of the incident radiation on the top of the atmosphere

and τ_{sp} = equivalent optical path from the sun to the point P.

τ_{sp} depends upon the zenith angle of the sun (χ) i.e. the angle which SP makes with the vertical through P. It also depends on the curvature of the earth, the distribution of air density in the earth's atmosphere and the wave-length of light. For a plane-parallel infinite atmosphere of finite optical thickness, τ_{sp} is sec χ times the vertical optical path above P. For $\chi = 90^0$, $\tau_{sp} = \infty$.

Chapman in 1931 derived an integral expression for the equivalent optical path for different scale heights taking into account the curvature of the earth. The function which was originally denoted by the symbol $f(x, \chi)$ is now generally referred to as Chapman Function $Ch(x, \chi)$ in the literature. x stands for $(a + h)/H$ where a is the radius of the earth and h, height of the point under consideration. χ is the zenith distance of the sun. For x = 600 which corresponds to H = 8 Km

and $Z = 90^0$, $Ch(x, \chi)$ has a value of 35.46. In a later paper, Chapman (1953) expressed $Ch(x, \chi)$ in the form $\sec(\chi - \Delta\chi)$ and tabulated the values of $\Delta\chi$ for different values of x and χ. For $x = 600$ and $\chi = 90^0$, $\Delta\chi = 1^0\ 37'$. Recently, Wilkes (1954) has tabulated the Chapman Function for values of x between 50 and 1000 Km in steps of 50 Km up to 500 Km and steps of 100 Km between 500 and 1000 Km and for χ varying from 20^0 to 100^0 in steps of 1^0 when $Ch(x, \chi)$ does not exceed 100. The values given are correct to three decimal places. These tables are of great help in computing air paths for different temperature distributions and angles of incidence. A simple but less accurate formula for the optical path was used by the present author (1956) in his calculations on the intensity and polarisation of the sky during twilight.

When Bemperod made his calculations in 1907, he assumed a temperature distribution with height in the atmosphere as it was then known. The values adopted by him cannot be accepted today. However, as it is the temperature of the air in the first few kilometers above the point P that exerts a dominant influence on the optical path τ_{gp}, the Bemperod functions may still be taken as reasonably accurate when the point is situated at heights up to 10 Km above ground.

Link and Sekera (1940) have considered the effect of atmospheric refraction and calculated the equivalent optical paths for two different temperature distributions (1) corresponding to winter and (2) summer. The density data used were based on the results of sounding balloon ascents and other atmospheric

data available at that time. The values of equivalent optical paths as given by different workers are summarised in Table 1.

Table 1

Equivalent optical path from the sun to the point P situated at the ground as given by different workers

z	Sec z	Chapman. x = 700	800	900	1000	Calculated H = 7	Bw	Link & Sakera Winter	Summer
0	1.000	1.000	1.000	1.000	1.000	1.00	1.00	1.00	1.00
60	2.000	1.992	1.993	1.993	1.994	1.99	2.00	-	-
75	3.864	3.791	3.800	3.807	3.812	3.80	3.82	3.83	3.84
80	5.759	5.525	5.551	5.572	5.590	5.56	5.60	5.60	5.60
85	11.474	10.008	10.144	10.257	10.352	10.28	10.39	10.36	10.34
88	28.65	18.087	18.685	19.209	19.670	19.22	19.79	19.71	19.48
90	∞	33.177	35.466	37.615	39.648	37.81	39.65	39.68	38.83

Bw Bemporad.

4.2 Scattering of light by a plane-parallel atmosphere

4.21 Work of Rayleigh, King and Tichanowsky

Lord Rayleigh worked out the effect of small dielectric spheres in scattering electromagnetic radiation. When the linear dimensions of the particle are small compared to the wave-length (λ) of the incident radiation, the secondary radiation is proportional to λ^{-4}. It was recognised by Lord Rayleigh that the blue colour of the sky and its polarisation could be explained by the scattering of sunlight by the molecules in air.

According to Rayleigh's law of scattering, when the incident light is unpolarised natural light, the intensity of light scattered at an angle θ to the incident radiation and confined in a small cone of solid angle $d\omega$, is proportional to

$$(1 + \cos^2 \theta)\, d\omega$$

when this is integrated over all directions of ω, and since

$$(1 + \cos^2 \theta)\, d\omega = 16\pi/3 \qquad \ldots 2$$

We have, the fraction of total incident radiation scattered in the cone $d\omega$, given by

$$\frac{3\sigma}{16\pi}(1 + \cos^2 \theta)\, d\omega \qquad \ldots 3$$

where σ is the scattering coefficient of the particle and is proportional to λ^{-4}.

If we take only primary scattering into account, the light scattered at right angles to an incident beam of unpolarised radiation would be completely polarised. Experiments show that there is a residual polarisation at right angles to the incident radiation. Lord Rayleigh explained this as being due to the anisotropy of the molecules. For pure air, laboratory experiments show a value of 0.042 for the depolarisation factor. The values of maximum polarisation observed on clear days are however significantly lower than those calculated on the basis of primary scattering by anisotropic molecules. Hence higher orders of scattering have to be taken into account as was realised by Lord Rayleigh himself.

L.V.King (1913) formulated the integral equations for the scattered radiation on the following assumptions:-

1. Owing to the random motions of the molecules in a gas, contributions to the total intensity of the scattered radiation by different molecules in an element of volume may be obtained by adding the intensities of light scattered by individual molecules.

2. Instead of considering the height of a point in the plane-parallel infinite atmosphere, its position is defined in terms of air density at that point. If the atmosphere is assumed to be isothermal with density decreasing exponentially with height, the formulae developed can be applied to any height distribution of mass.

3. Instead of treating the distribution of scattered radiation according to Rayleigh's phase law, an average value over a spherical surface was taken.

4. Anisotropy of the molecules, reflection by ground and refraction in the atmosphere were neglected.

The integral equation given by King consists of two parts (1) contribution to the intensity of sky light due to the sun's radiation which had been scattered once by the atmosphere and (2) contribution to "self-illumination" by higher orders of scattering. King found it difficult to evaluate the second part.

The complete solution of the problem of polarisation of sky radiation requires the solution of two simultaneous integral equations in three variables and as this was considered to be an almost impossible task at that time, King tried to calculate the polarisation on the assumption that primary scattered light was polarised according to Rayleigh's law and that "self-illumination" was unpolarised.

Tichanowsky (1927, 1928) formulated the equations for primary, secondary and tertiary scattered radiations in a plane-parallel stratified atmosphere taking into account the anisotropy of the molecules. The effect of loss of intensity due to scattering was neglected and hence the treatment can be assumed to apply only to weakly attenuated radiations in the red and infra-red region of the spectrum.

4.22 Theory of Chapman and Hammad

The equations for calculating the primary and secondary scattered radiations from the sky for any zenith angle of the sun above the horison, were formulated by Chapman and Hammad (1939). The method is true for a plane-parallel atmosphere of finite optical thickness, scattering according to Rayleigh's law. The necessary functions for computing the primary and secondary scattered radiations were discussed fully in the original paper and their values were tabulated for some special cases by Hammad (1945, 1947 and 1948). The method is described in brief in this sub-section.

The height of a point is specified in terms of the

fraction m of total air mass (m) of the atmosphere below it (level), or $\bar{m}$ the fraction of the total mass above it (depth). $m + \bar{m} = 1$. A beam of incident radiation of intensity I_∞, falling on the top of the atmosphere in a direction $\underline{s}$, suffers attenuation as it comes down the atmosphere. Its intensity at P (level m' and depth $\bar{m}'$) is given by

$$I_\infty \, e^{-c\bar{m}' \sec Z} \qquad \ldots 4$$

where

$c = \sigma M$ = scattering coefficient of the atmosphere

σ = scattering coefficient per unit mass of air

M = total air mass of the atmosphere

and Z = angle which $\underline{s}$ makes with the vertical.

At P, direct sunlight gets scattered along the direction $\underline{k}'$ making an angle Ψ' with $\underline{s}$. The amount of energy scattered in a small cone of solid angle $d\underline{k}'$ is given by

$$\frac{3}{16\pi}\sigma I_\infty (1 + \cos^2 \Psi') \, e^{-c\bar{m}' \sec Z} \, d\underline{k}' \qquad \ldots 5$$

In travelling from P to another point Q (level m, depth $\bar{m}$), the primary scattered radiation undergoes a further attenuation given by

$$e^{-c(\bar{m} \sim \bar{m}') \sec \theta'}$$

where θ' is the angle which $\underline{k}'$ makes with the vertical. The contribution to the intensity of primary scattered radiation passing from P through a surface normal to $\underline{k}'$ at Q is proportional to

$$\frac{3\sigma}{16\pi} I_\infty (1 + \cos^2 \psi') e^{-c\bar{m}' \sec Z} e^{-c(\bar{m} \sim \bar{m}') \sec\theta'} \quad \ldots 6$$

At Q, let the primary scattered radiation given by (6) undergo a second scattering process in the direction of observation $\underline{k}$ such that the angle between $\underline{k}'$ and $\underline{k}$ is χ. The secondary emission at Q in the direction $\underline{k}$ is proportional to

$$\frac{9\sigma^2}{256\pi^2} I_\infty (1 + \cos^2 \psi') (1 + \cos^2 \chi) e^{-c\bar{m}' \sec Z} \times$$

$$\times e^{-c(\bar{m} \sim \bar{m}') \sec\theta'} \quad \ldots 7$$

Integrating over all directions around Q and the air mass of the entire atmosphere, the total secondary emission E_2 at Q in the direction $\underline{k}$ is given by

$$E_2 = \frac{9\sigma^2 M}{256\pi^2} I_\infty \int_0^{2\pi}\int_0^{\frac{\pi}{2}}\int_0^{1} e^{-c\bar{m}' \sec Z} e^{-c(\bar{m} \sim \bar{m}') \sec\theta'} \times$$

$$\times (1 + \cos^2 \psi') (1 + \cos^2 \chi) \sec\theta' \sin\theta' \, dm' \, d\theta' \, d\phi' \quad \ldots 8$$

ϕ' is the azimuth with respect to the vertical plane through the sun and the observer. Since the exponential terms are independent of ϕ', the integration over ϕ' can be easily carried out taking θ' and m' as constant. The solution of the integral

$$\frac{1}{\pi} \int_0^{2\pi} (1 + \cos^2 \psi') (1 + \cos^2 \chi) \, d\phi'$$

can be written in the form

$$A_0 + A_1 \cos^2 \theta' + A_2 \cos^4 \theta' \qquad \ldots 9$$

where A_0, A_1 and A_2 are the functions of direction of incident radiation $(Z, 0)$ and the direction of secondary scattered radiation (θ, ϕ). Please see Table 2. Substituting this in eq. (6),

$$K_2 = \frac{9}{256} \frac{\sigma^2 M}{\pi} I_\infty \int_0^{\frac{\pi}{2}} \int_0^{1} e^{-\sigma \bar{m}' \sec Z} e^{-\sigma (\bar{m} \sim \bar{m}') \sec \theta'} \times$$

$$\times \left\{ A_0 + A_1 \cos^2 \theta' + A_2 \cos^4 \theta' \right\} \sec \theta' \sin \theta' \, dm' \, d\theta'$$

$$\ldots 10$$

changing the variable from θ' to $\sec \theta'$ and as

$$d \sec \theta' = \sec \theta' \tan \theta' \, d\theta'$$

we have,

$$K_2 = \frac{9}{256} \frac{\sigma^2 M}{\pi} I_\infty \int_1^{\infty} \int_0^{1} e^{-\sigma \bar{m}' \sec Z} e^{-\sigma (\bar{m} \sim \bar{m}') \sec \theta'} \times$$

$$\times \left\{ A_0 (\sec \theta')^{-1} + A_1 (\sec \theta')^{-3} + A_2 (\sec \theta')^{-5} \right\} \times$$

$$\times \, dm' \, d \sec \theta' \qquad \ldots 11$$

Integration in eq. (11) is replaced by L_n functions (n = 1, 3 and 5) which depend upon the scattering coefficient of the atmosphere, solar zenith angle and the position of Q. Three consecutive odd values of n occur, because of the consecutive negative odd powers of sec θ'.

$$E_2 = \frac{9\sigma^2 s_n}{256\pi} \; I_\infty \; (A_0 L_1 + A_1 L_3 + A_2 L_5) \qquad \ldots 12$$

L_n can be expressed in the form

$$L_n (c, Z, m) = \frac{1}{c} \; e^{-c\bar{m}} \sec Z \; x$$

$$x \left\{ E_{kn} (cm, -\sec Z) + E_{kn} (c\bar{m}, \sec Z) \right\} \qquad \ldots 13$$

where the first term in the bracket represents the contribution to E_2 at Q from the part of the atmosphere below level n and the second term corresponds to the contribution from the part of the atmosphere above level n.

$$E_{kn} (\tau, b) = \int_0^\tau e^{bt} \; E_{jn} (t) \; dt \qquad \ldots 14$$

where

$$E_{jn} (t) = \int_1^\infty e^{-tx} \; x^{-n} \; dx \qquad \ldots 15$$

shows that the contribution E_{kn} is obtained by two steps : (1) integrating over sec θ' from 1 to ∞ keeping m' constant and (2) then summing up for different levels above or below

n as the case may be. E_{jn} functions have been tabulated by

1. Gold (1908) n = 1 to 3 and several values of t from 0 to 6

2. Hammad (1947) n = 1 to 5 and t = 0.00 to 1.00 at an interval of 0.01

3. Placzek (1947) n = 1 to 20, and t = 0.00 to 2.00 at an interval of 0.01, and t = 2.0 to 10.0 at an interval of 0.1.

Total secondary scattered radiation (R_2) received by the observer at ground level, can be obtained by integrating E_2 over dm. We have,

$$R_2 = \frac{\sigma_s^2}{2\pi} I_\alpha \sec\theta \left\{ A_0 Ld_1 + A_1 Ld_3 + A_2 Ld_5 \right\}$$

...16

where

$$Ld_n = e^{-c \sec\theta} \int_0^{\bar{m}} e^{-c\bar{m} \sec\theta} L_n(c, z, m)\, d\bar{m}$$

...17

In practice, Ld_n functions are calculated starting from the values of E_{jn} and dividing the atmosphere into a number of layers containing equal air masses.

The functions A_0, A_1 and A_2 occuring in the above formulae as originally given by Chapman and Hammad (1939)

assume that the primary scattered radiation is unpolarised. Eq. (7). This is not correct. This was corrected by Hamnad (1948) while considering the polarisation of secondary scattered radiation and also independently by Sakuhara (1951). Their values are given in Table 2 in terms of z for the direction of observation along the zenith ($\theta = 0^0$, $\phi = 0^0$).

Table 2

Functions A_0, A_1 and A_2 for $\theta = 0^0$, $\phi = 0^0$

	Chapman and Hamnad (1939)	Hamnad (1948)		Sakuhara (1951)
		Normal	Transverse	
A_0	$2 + \sin^2 z$	$2 - \frac{1}{2}\sin^2 z$	$2 - \frac{1}{2}\sin^2 z$	$4 - 2\sin^2 z$
A_1	$4 - 2\sin^2 z$	$3\sin^2 z$	$\sin^2 z$	$4\sin^2 z$
A_2	$2 - 3\sin^2 z$	$2 - \frac{5}{2}\sin^2 z$	$2 - \frac{7}{2}\sin^2 z$	$4 - 6\sin^2 z$

Hamnad (1948) modified the original theory so as to include the polarisation of the scattered light and the anisotropy of the molecules. This modified theory is given briefly in the paper presented in article 1.2 of Section I. Hamnad (1953) showed that the values of polarisation and the positions of neutral points calculated on the basis of his theory, were in close agreement with the values observed on clear skies.

4.22 Chandrasekhar's theory of radiative equilibrium

The problem of sky illumination taking into consideration all orders of scattering and reflection by ground according to a definite Law, has been solved by Chandrasekhar. The necessary corrections for molecular anisotropy have also been dealt with. The theory is described fully by Chandrasekhar in his book on "Radiative Transfer" (1950). The theoretical values of polarisation, and positions of neutral points and neutral lines are presented by Chandrasekhar and Elbert (1951) for $\tau_1 = 0.15$. A brief summary with the necessary tables to compute the intensity and polarisation of the sunlit sky at any point for visible and near ultra-violet parts of the spectrum, have been given by Chandrasekhar and Elbert (1954). Coulson (1954) has computed the positions of neutral points for different values of τ_1 such as 0.02, 0.15, 0.25 and 1.00. He has shown the existence of double Arago point for large optical thicknesses. The effect of ground reflection on the positions of neutral points, has also been considered. In this sub-section, the summary of the theory is given keeping in view the problem of sky illumination.

4.23a Stokes parameters

A beam of unpolarised natural light on scattering, gets polarised and for complete representation of the radiation scattered in any direction, it is essential to know its intensity, direction of polarisation and degree of

polarisation. These quantities are different in nature and two or more independently polarised beams cannot be combined together by simple addition. This necessitates a search for a new representation and it has been observed by Chandrasekhar that the Stokes parameters satisfy all the required conditions. An elliptically polarised beam of light can be fully represented by four parameters and a partially polarised beam of light by three. Let l and r be two directions at right angles to each other and I_l and I_r represent the intensity along these two directions. $I(\Psi)$, the intensity in a direction at an angle Ψ to l (measured clockwise) is given by

$$I(\Psi) = I_l \cos^2\Psi + I_r \sin^2\Psi + \tfrac{1}{2} U \sin 2\Psi \qquad \ldots 18$$

The coefficients I_l, I_r and U are called the Stokes parameters. In terms of these, the angle χ which the direction of polarisation makes with l is given by

$$\tan 2\chi = \frac{U}{I_l - I_r} \qquad \ldots 19$$

and the degree of polarisation by

$$\delta = \frac{I_l - I_r}{I_l + I_r} \sec 2\chi \qquad \ldots 20$$

A law of transformation of Stokes parameters for a rotation of the axis through an angle ϕ can be easily derived and is given below in its final form. If

$\underline{I} = (I_l, I_r, U)$ denote the components of a partially polarised beam of light, then the effect of rotation of the axis through an angle ϕ in a clockwise direction is to subject $\underline{I}$ to the linear transformation

$$\underline{L}(\phi) = \begin{pmatrix} \cos^2\phi & \sin^2\phi & \frac{1}{2}\sin 2\phi \\ \sin^2\phi & \cos^2\phi & -\frac{1}{2}\sin 2\phi \\ -\sin 2\phi & \sin 2\phi & \cos 2\phi \end{pmatrix} \qquad \ldots 21$$

e.g. $U_\phi = -I_l \sin 2\phi + I_r \sin 2\phi + U \cos 2\phi$

4.23b Rayleigh's law in terms of phase matrix

In order to relate the Stokes parameters of the scattered light to those of the incident radiation, Rayleigh's law of scattering can be enunciated as follows :-

If $\underline{I}$ (I_l, I_r, U) represent the incident light, the scattered intensity in the direction θ is given by

$$\sigma \frac{d\omega'}{4\pi} \underline{R}\,\underline{I}\, d\omega$$

where

$$\underline{R} = \frac{3}{2} \begin{pmatrix} \cos^2\theta & 0 & 0 \\ 0 & 1 & 0 \\ 0 & 0 & \cos\theta \end{pmatrix} \qquad \ldots 22$$

$\underline{R}$ is called the phase matrix for Rayleigh's scattering and σ the scattering coefficient per particle.

4.23c Absorption coefficient

A pencil of radiation of intensity I_ν after traversing a distance ds in a medium will be weakened by

$$dI_\nu = - K_\nu \rho I_\nu ds \qquad \ldots 23$$

where ρ is the density of the medium and K_ν the mass absorption coefficient for radiation of frequency ν. The loss dI_ν may reappear partly or fully in other directions as scattered light.

Considering the case of scattering, a material is said to have a mass scattering coefficient K_ν, if from a pencil of radiation incident on an element of mass of cross-section $d\sigma$ and height ds, energy scattered from it at the rate of

$$K_\nu . \rho . ds . I_\nu . \cos\theta . d\nu . d\sigma . d\omega .$$

in all the directions. But $dm = \rho . \cos\theta . d\sigma . ds$, therefore, energy is scattered at the rate of

$$K_\nu . I_\nu . dm . d\nu . d\omega$$

On considering the angular distribution of the scattered radiation according to a phase function P (Cos θ),

$$K_\nu . I_\nu . P(\cos\theta) . \frac{d\omega'}{4\pi} dm . d\nu . d\omega \qquad \ldots 24$$

gives the rate at which energy is being scattered into an element of solid angle $d\omega'$ and in a direction at an angle θ

to the direction of radiation incident on an element of mass dm.

Total loss of energy in all the directions, from the incident beam is given by

$$K_\nu \cdot I_\nu \cdot dm \cdot d\nu \cdot d\omega \int P(\cos\theta) \frac{d\omega'}{4\pi} \qquad \ldots 25$$

For scattering according to Rayleigh's law,

$$P(\cos\theta) = \frac{3}{4}(1 + \cos^2\theta) \qquad \ldots 26$$

4.23d Emission coefficient

The emission coefficient j_ν is defined in such a way that an element of mass dm emits in the directions confined to solid angle $d\omega$, in the frequency interval $(\nu, \nu + d\nu)$ and in time dt, an amount of radient energy given by

$$j_\nu \cdot dm \cdot d\omega \cdot d\nu \cdot dt.$$

In the case of a medium which scatters radiation, there will be a contribution to the emission coefficient from the scattering of radiation from all the other directions into the pencil of direction considered. Thus it follows from (24) that the scattering of a pencil of radiation from the direction (θ', ϕ') contributes to a pencil in the direction (θ, ϕ') energy at the rate of

$$K_\nu \cdot dm \cdot d\nu \cdot d\omega \cdot \underline{P}(\theta, \phi\ ;\ \theta', \phi')\ \underline{I}(\theta', \phi')\ \times$$

$$\times\ \frac{\sin\theta' \cdot d\theta' \cdot d\phi'}{4\pi}$$

where $\underline{P}(\theta, \phi\ ;\ \theta', \phi')$ denotes the phase function for the angle between the directions (θ, ϕ) and (θ', ϕ'). Hence the contribution $j_\nu^{(s)}$ to the emission coefficient by scattering alone is

$$j_\nu^{(s)} = K_\nu \frac{1}{4\pi}\int_0^{\pi}\int_0^{2\pi} \underline{P}(\theta, \phi\ ;\ \theta', \phi')\ \times$$

$$\times\ \underline{I}(\theta', \phi')\ \sin\theta' \cdot d\theta' \cdot d\phi' \qquad \ldots 27$$

For a scattering atmosphere,

$$j_\nu = j_\nu^{(s)}$$

4.23e Source function

The ratio of emission to the absorption coefficient which plays an important part in the theory of radiative transfer is called the source function $\underline{J}_\nu$. For a scattering atmosphere,

$$\underline{J}_\nu(\theta, \phi) = \frac{1}{4\pi}\int_0^{\pi}\int_0^{2\pi} \underline{P}(\theta, \phi\ ;\ \theta', \phi')\ \times$$

$$\times\ \underline{I}_\nu(\theta', \phi')\ \sin\theta' \cdot d\theta' \cdot d\phi' \qquad \ldots 28$$

4.23f Equation of transfer

With these definitions, the equation of transfer can be written down as follows : In an element of cross-section

$d\sigma$ and height ds, the difference in radiant energy in the frequency interval $(\nu, \nu + d\nu)$ crossing the two faces normally, in a given time dt, and confined to an element of solid angle, is given by

$$\frac{dI_\nu}{ds}\, ds.\, d\nu\, .\, d\sigma.\, d\omega.\, dt.$$

This difference in energy must arise from the excess of emission over absorption. The amount of energy absorbed is

$$K_\nu . \rho .\, ds.\, I_\nu .\, d\nu .\, d\sigma .\, d\omega .\, dt$$

while the amount of energy emitted is

$$j_\nu . \rho .\, d\sigma .\, ds.\, d\nu .\, d\omega .\, dt.$$

Therefore,

$$\frac{dI_\nu}{ds} = - K_\nu . \rho . I_\nu + j_\nu . \rho$$

or in the terms of source function J_ν (article 4.23e)

$$- \frac{dI_\nu}{K_\nu . \rho .\, ds} = I_\nu - J_\nu \qquad \ldots 29$$

This is the equation of transfer.

For a plane-parallel atmosphere, it is convenient to measure linear distances normal to the plane of stratification. If z is this vertical distance, the equation of transfer becomes, on suppressing the suffix ν,

$$\frac{-\cos\theta \cdot d\underline{I}(z,\theta,\phi)}{K.\rho.dz} = \underline{I}(z,\theta,\phi) - \underline{J}(z,\theta,\phi)$$

where θ denotes the inclination to the outward normal and ϕ the azimuth referred to suitably chosen axes. Introducing

$$\int_z^\infty K.\rho.dz = \tau$$

and $$\mu = \cos\theta$$

the equation of transfer for a plane-parallel atmosphere can be written as

$$\frac{\mu\, d\underline{I}(\tau,\mu,\phi)}{d\tau} = \underline{I}(\tau,\mu,\phi) - \underline{J}(\tau,\mu,\phi) \quad \ldots 30$$

The evaluation of the source function $\underline{J}(\theta,\phi)$ can be carried out with the help of Eqs. 21 and 22. The contribution $d\underline{J}(\theta,\phi;\theta',\phi')$ to the source function arising from the scattering of a pencil of radiation of solid angle $d\omega'$ in the direction (θ',ϕ') will be given by

$$\underline{R}.\underline{I}\frac{d\omega'}{4\pi}$$

if $\underline{I}(\theta',\phi')$ is referred to the direction parallel and perpendicular to the plane of scattering, but for a plane-parallel atmosphere, $\underline{I}(\theta',\phi')$ refers to a vertical axis and a plane, therefore it becomes necessary to multiply by appropriate phase matrices for the rotation of axes at two places. The resultant source function $\underline{P}(\mu,\phi;\mu',\phi')$

can be expressed in the form

$$\underline{P}(\mu,\phi;\mu',\phi') = \frac{1}{4\pi}\left[\underline{P}^{(0)}(\mu,\mu') + (1-\mu^2)^{k}(1-\mu'^2)^{k}\,\underline{P}^{(1)}(\mu,\phi;\mu',\phi') + \underline{P}^{(2)}(\mu,\phi;\mu',\phi')\right] \quad \ldots 31$$

where

$$\underline{k} = \begin{bmatrix} 1 & 0 & 0 \\ 0 & 1 & 0 \\ 0 & 0 & 2 \end{bmatrix} \quad \ldots 32$$

$$\underline{P}^{(0)}(\mu,\mu') = \frac{3}{4}\begin{bmatrix} 2(1-\mu^2)(1-\mu'^2)+\mu^2\mu'^2 & \mu^2 & 0 \\ \mu'^2 & 1 & 0 \\ 0 & 0 & 0 \end{bmatrix} \quad \ldots 33$$

$$\underline{P}^{(1)}(\mu,\phi;\mu',\phi') = \frac{3}{4}\begin{bmatrix} 4\mu\mu'\cos(\phi'-\phi) & 0 & 2\mu\sin(\phi'-\phi) \\ 0 & 0 & 0 \\ -2\mu'\sin(\phi'-\phi) & 0 & \cos(\phi'-\phi) \end{bmatrix} \quad \ldots 34$$

and

$$\underline{P}^{(2)}(\mu,\phi;\mu',\phi') =$$

$$\frac{3}{4}\begin{bmatrix} \mu^2\mu'^2\cos 2(\phi'-\phi) & -\mu^2\cos 2(\phi'-\phi) & \mu^2\mu'\sin 2(\phi'-\phi) \\ -\mu'^2\cos 2(\phi'-\phi) & \cos 2(\phi'-\phi) & -\mu'\sin 2(\phi'-\phi) \\ -\mu\mu'^2\sin 2(\phi'-\phi) & \mu\sin 2(\phi'-\phi) & \mu\mu'\cos 2(\phi'-\phi) \end{bmatrix}$$

...35

and the equation of transfer eq. (30) for a plane-parallel atmosphere can be written in the form

$$\mu\frac{d\underline{I}(\tau;\mu,\phi)}{d\tau} = \underline{I}(\tau;\mu,\phi) - \frac{1}{4\pi}\int_{-1}^{+1}\int_{0}^{2\pi}\underline{P}(\mu,\phi;\mu',\phi')\,\underline{I}(\tau;\mu',\phi')\,d\mu'.\,d\phi'$$

...36

It should be noted that $\underline{I}(\tau;\mu',\phi')$ characterises the diffused radiation but in addition there is a reduced incident flux $\pi\underline{F}\,e^{-\tau/\mu_0}$ at the level τ, in the direction $(-\mu_0,\phi_0)$ and hence the equation of transfer appropriate for the problem of diffused reflection and transmission has the form

$$\mu\frac{d\underline{I}(\tau;\mu,\phi)}{d\tau} = \underline{I}(\tau;\mu,\phi) - \frac{1}{4\pi}\int_{-1}^{+1}\int_{0}^{2\pi}\underline{P}(\mu,\phi;\mu',\phi')\,\underline{I}(\tau;\mu',\phi')\,d\mu'.\,d\phi' - \frac{1}{4}\underline{F}\,e^{-\tau/\mu_0}\,\underline{P}(\mu,\phi;-\mu_0,\phi_0).$$

...37

The boundary conditions for solving this equation are

$$\left.\begin{aligned} \underline{I}\ (0;\ -\mu,\ \phi) &= 0 \\ \underline{I}\ (\tau_1;\ \mu,\ \phi) &= 0 \end{aligned}\right\} \quad (0 < \mu \leq 1,\ 0 \leq \phi \leq 2\pi) \qquad \ldots 38$$

i.e. there is no diffused radiation falling on the top or from below the bottom of the atmosphere. The case of reflection by ground will be taken up in article 4.23i.

4.23g Modification for the molecular anisotropy

The scattering of a partially plane polarised beam of light by an anisotropic particle may be regarded as equivalent to a super position of Rayleigh's scattering with a weight $(1-\gamma)/(1+2\gamma)$ and isotropic scattering of each of the components I_l and I_r with a weight $3\gamma/2(1+2\gamma)$ where γ is given by $d = 2\gamma/(1+\gamma)$. This means that the following phase matrix should be used in the Eq. (37) for $\underline{I} = (I_l,\ I_r,\ U)$.

$$\frac{1-\gamma}{1+2\gamma}\ \underline{P}\ (\mu, \phi; \mu', \phi') + \frac{3\gamma}{2(1+2\gamma)} \begin{pmatrix} 1 & 1 & 0 \\ 1 & 1 & 0 \\ 0 & 0 & 0 \end{pmatrix} \qquad \ldots 39$$

4.23h Solution of the equation of transfer

It has been found convenient to express the intensity reflected at the top of the atmosphere in the direction (μ, ϕ) by

$$\underline{I}(0;\mu,\phi) = \frac{1}{4\mu}\ \underline{S}(\mu,\phi;\mu_0,\phi_0)\ \underline{F} \qquad \ldots 40$$

and the intensity transmitted below the layer τ_1 by

$$\underline{I}(\tau_1;-\mu,\phi) = \frac{1}{4\mu}\ \underline{T}(\mu,\phi;\mu_0,\phi_0)\ \underline{F} \qquad \ldots 41$$

where $\underline{S}$ and $\underline{T}$ are called scattering and transmitting matrices respectively. They are functions of μ, Φ, and μ_0, ϕ_0. τ_1 is taken as a parameter. In terms of these matrices, and with the boundary conditions given in Eq. (38), the solution of equation of transfer (37) becomes easy.

The nature of $\underline{F}(\mu,\phi;\mu',\phi')$ suggests that $\underline{I}(\tau;\mu,\phi)$ should have three components : (1) $\underline{I}^{(0)}(\tau;\mu)$ independent of azimuth, (2) $\underline{I}^{(1)}(\tau;\mu,\phi)$ has a period of 2π in $(\phi_0-\phi)$ and (3) $\underline{I}^{(2)}(\tau;\mu,\phi)$ having a period of π in $(\phi_0-\phi)$. Thus

$$\underline{I}(\tau;\mu,\phi) = \underline{I}^{(0)}(\tau;\mu) + (1-\mu^2)^{\frac{1}{2}}(1-\mu_0^2)^{\frac{1}{2}}\,\underline{I}^{(1)}(\tau;\mu,\phi) + \underline{I}^{(2)}(\tau;\mu,\phi) \qquad \ldots 42$$

The solutions of $\underline{I}^{(1)}$ and $\underline{I}^{(2)}$ suggest that if transmitting function is expressed in the form

$$I(\mu,\phi;\mu_0,\phi_0) = \frac{1}{4}\left[\frac{1}{2} I^{(0)}(\mu;\mu_0) + (1-\mu^2)^{\frac{1}{2}}(1-\mu_0^2)^{\frac{1}{2}} I^{(1)}(\mu,\phi;\mu_0,\phi_0) + I^{(2)}(\mu,\phi;\mu_0,\phi_0)\right] \quad \ldots 43$$

$I^{(1)}$ is expressible in the form

$$\left(\frac{1}{\mu_0}-\frac{1}{\mu}\right) I^{(i)} = \Gamma^{(i)}(-\mu,\phi;-\mu_0,\phi_0) \times \left[Y^{(i)}(\mu) X^{(i)}(\mu_0) - X^{(i)}(\mu) Y^{(i)}(\mu_0)\right] \quad (i = 1, 2) \quad \ldots 44$$

where $X^{(1)}$, $Y^{(1)}$ and $X^{(2)}$, $Y^{(2)}$ are defined in terms of characteristic functions

$$\left.\begin{aligned} \psi^{(1)}(\mu) &= \frac{3}{8}(1-\mu^2)(1+2\mu^2) \\ \text{and} \quad \psi^{(2)}(\mu) &= \frac{3}{16}(1+\mu^2)^2 \end{aligned}\right\} \quad \ldots 45$$

X and Y functions are solved in Chapter VIII of "Radiative Transfer".

On the other hand, the solution of azimuth independent term $I^{(0)}$ is much more complicated and is given by

$$\left(\frac{1}{\mu_0}-\frac{1}{\mu}\right) I^{(0)}(\mu,\mu_0) =$$

$$\begin{pmatrix} \xi(\mu) & 2^{\frac{1}{2}}\eta(\mu) & 0 \\ \sigma(\mu) & 2^{\frac{1}{2}}\theta(\mu) & 0 \\ 0 & 0 & 0 \end{pmatrix} \begin{pmatrix} \Psi(\mu_0) & \chi(\mu_0) & 0 \\ 2^{\frac{1}{2}}\phi(\mu_0) & 2^{\frac{1}{2}}\zeta(\mu_0) & 0 \\ 0 & 0 & 0 \end{pmatrix}$$

$$= \begin{pmatrix} \Psi(\mu) & 2^{\frac{1}{2}}\phi(\mu) & 0 \\ \chi(\mu) & 2^{\frac{1}{2}}\zeta(\mu) & 0 \\ 0 & 0 & 0 \end{pmatrix} \begin{pmatrix} \xi(\mu_0) & \sigma(\mu_0) & 0 \\ 2^{\frac{1}{2}}\eta(\mu_0) & 2^{\frac{1}{2}}\theta(\mu_0) & 0 \\ 0 & 0 & 0 \end{pmatrix}$$

...46

where the eight functions $\Psi, \xi, \phi, \eta, \chi, \sigma, \zeta$ and θ are defined in terms of X_1, Y_1 and X_r, Y_r and the constants $\nu_1, \nu_2, \nu_3, \nu_4, u_3, u_4$ and Q whose values can be obtained in terms of the moments of X_1, Y_1 and X_r, Y_r functions. These are defined in terms of the characteristic functions

$$\Psi_1(\mu) = \frac{3}{4}(1-\mu^2) \text{ and } \Psi_r(\mu) = \frac{3}{8}(1-\mu^2)$$

...47

Substituting $\underline{F} = (F_1, F_r, U) = (\frac{1}{2}F, \frac{1}{2}F, 0)$ in Eq. (41) because the incident light is natural, the equations of I_1 etc. corresponding to $(\tau_1; -\mu, \phi; \mu_0, \phi_0)$ can be written down from the Eqs. (43, 44 and 46). Using notations of Coulson (1954),

$$I_1 = C\left\{ K\xi_1(\mu) + L\eta(\mu) - M\chi(\mu) - N\phi(\mu) + \mu(1-\mu^2)^{\frac{1}{2}}\, G\, \cos(\phi_0 - \phi) - \mu^2 H \cos 2(\phi_0 - \phi)\right\}$$

$$I_r = C\left\{ K\sigma(\mu) + L\Theta(\mu) - M\lambda(\mu) - N\gamma(\mu) + H\cos 2(\phi_0 - \phi)\right\}$$

and

$$U = C\left\{(1-\mu^2)^{\frac{1}{2}}\, G\, \sin(\phi_0 - \phi) - 2\mu H \sin 2(\phi_0 - \phi)\right\} \quad \ldots 48$$

where

$$C = \frac{3}{32}\,\frac{\mu_0 F}{\mu - \mu_0}$$

$$G = 4\mu_0(1-\mu_0^2)^{\frac{1}{2}}\left\{ x^{(1)}(\mu_0)\, y^{(1)}(\mu) - y^{(1)}(\mu_0)\, x^{(1)}(\mu)\right\}$$

$$H = (1-\mu_0^2)\left\{ x^{(2)}(\mu_0)\, y^{(2)}(\mu) - y^{(2)}(\mu_0)\, x^{(2)}(\mu)\right\}$$

$$K = \psi(\mu_0) + \chi(\mu_0)$$

$$M = \xi(\mu_0) + \sigma(\mu_0)$$

$$L = 2\left\{\phi(\mu_0) + \gamma(\mu_0)\right\}$$

$$N = 2\left\{\Theta(\mu_0) + \eta(\mu_0)\right\} \quad \ldots 49$$

4.231 <u>The effect of reflection by ground</u>

The equations of I_1, I_r and U given by Eq. (48) are derived on the assumption that the ground is a perfect absorber Eq. (38). In practice, however, the ground always

reflects a part of the total radiation falling on it. It can be assumed that ground reflects according to Lambert's law, i.e., the light reflected by ground is unpolarised and uniform in the outward direction independently of the state of incident flux. Further, the outward flux of the reflected light is always a certain fixed fraction λ_0 (albedo) of the total inward flux of radiation falling on the surface of the earth.

The total inward flux of radiation falling on the ground consists of three parts :

1. Directly transmitted light $\pi F e^{-\tau_1/\mu_0}$

2. Diffusely transmitted light $\underline{I}(\tau_1; -\mu, \phi)$

3. The flux of radiation re-reflected by the atmosphere towards the ground.

It has been shown that the effect of ground reflection is to increase $\underline{I}(\tau_1; -\mu, \phi; \mu_0, \phi_0)$ by an amount $\underline{I}^*(\tau_1; -\mu, \phi; \mu_0, \phi_0)$ where

$$I_1^* = C^* \left\{1 - \gamma_1(\mu)\right\}$$

$$I_2^* = C^* \left\{1 - \gamma_2(\mu)\right\}$$

$$Q^* = 0 \qquad \ldots 50$$

where

$$C^* = \frac{\lambda_0 F}{\pi(1 - \lambda_0 \bar{a})} \mu_0 \left\{\gamma_1(\mu_0) + \gamma_2(\mu_0)\right\} \qquad \ldots 51$$

4.3 References

1. Bemperod, A. 1907 Met. Zeit. P. 306

2. Chandrasekhar, S. 1950 "Radiative Transfer" Clarendon Press, Oxford

3. Chandrasekhar, S. & Elbert, D. 1951 Nature 167, P. 51

4. Chandrasekhar, S. & Elbert, D.D. 1954 Trans. Amer. Phil. Soc. New Series, 44, Part VI, P. 643

5. Chapman, S. 1931 Proc. Phy. Soc. 43, P. 483

6. Chapman, S. & Hammad, A. 1939 Phil. Mag. Ser. 7, 28, P. 99

7. Chapman, S. 1953 Proc. Phy. Soc. 66 B, P. 710

8. Coulson, K.L. 1954 Investigation of polarisation of sky light, Contract No. AF 19 (122) - 239. Report 7

9. Dave, J.V. & Ramanathan, K.R. 1956 Proc. Ind. Acad. Sci. 43, Sec. A, P. 67

10. Dave, J.V. 1956 Proc. Ind. Acad. Sci. 43, Sec.A, P. 336

11. Gold, E. 1908 Proc. Roy. Soc. 82, P. 62

12. Hammad, A. 1945 Phil. Mag. Ser. 7, 36, P. 434

13. Hammad, A. 1947 Phil. Mag. Ser. 7, 38, P. 515

14. Hammad, A. 1948 Phil. Mag. Ser. 7, 39, P. 956

15. Hammad, A. 1948 Astrophys. Journ. 108, P. 338

16. Hammad, A. 1953 Journ. Opt. Soc. Amer. 43, P. 184

17. King, L.V. 1913 Phil. Trans. Roy. Soc. London 212, A, P. 375

18. Link, F. & Sekera, Z. 1940 Publ. Obs. Nat. Prague. 14, P. 1

19. Placzek, G. 1947 National Research Council of Canada, Division of Atomic Energy, Ontario. No. 1547.

20. Sakihara, F. 1951 Papers Met. Geophys. 2, P. 158

21. Tichanowsky, J.J. 1927 Phys. Zeits. 28, P. 680

22. Tichanowsky, J.J. 1928 Phys. Zeits. 29, P. 442

23. Wilkes, M.W. 1954 Proc. Phy. Soc. 67 B, P. 304

ooo000ooo